

A little goes a long way: how circulating *Bacillus anthracis* lethal toxin prevents the neutrophil response to infection

Zachary Patrick Weiner
Greensboro, NC

M.S. Biological and Physical Sciences, University of Virginia 2010
B.S. Microbiology, North Carolina State University 2008
B.S. Food Science, North Carolina State University 2008
B.S. Science Technology & Society, North Carolina State University 2008

A Dissertation presented to the Graduate Faculty
of the University of Virginia in Candidacy for the Degree of
Doctor of Philosophy

Department of Microbiology, Immunology, and Cancer Biology

University of Virginia
August, 2013

Abstract

Bacillus anthracis is a Gram-positive spore-forming bacterium that is the causative agent of the disease anthrax, which is traditionally a disease of grazing livestock and a zoonosis of humans that work closely with infected animals. *B. anthracis* has become of more interest in modern times due to the ease by which it is weaponized for biological warfare or terrorism. Anthrax can be contracted through several routes of exposure: by inhalation, cutaneously through breaks in the skin, and by ingestion. Of the exposure routes, inhalation anthrax elicits the highest mortality rate, while cutaneous infection has the lowest. The cause of *B. anthracis* high mortality rates is attributed to two main virulence factors, a tripartite exotoxin and a gamma-linked poly-glutamic acid capsule. The tripartite AB exotoxin consists of a receptor-binding translocase subunit, protective antigen (PA), and two enzymatic subunits, lethal factor (LF) and edema factor (EF). When PA is bound to LF or EF the complex becomes lethal toxin (LT) or edema toxin (ET), respectively.

A great deal of research has been devoted to discovering how the exotoxins produced by *B. anthracis* manipulate macrophages and dendritic cells to the benefit of the bacterium. This is because in the inhalational model of infection it is thought that the exotoxins manipulate phagocytes to act as a “Trojan horse” which transports ungerminated spores to the regional draining lymph node from where germination and dissemination originates. However, recent data suggests that *B. anthracis* spore germination and dissemination originates at sites outside of the regional draining lymph node. Additionally it has

been suggested that LT intoxication of polymorphonuclear leukocytes (PMNs aka neutrophils) is necessary for bacterial dissemination.

The goal of the following research was to examine areas of knowledge not covered in the literature, and to determine how and where *B. anthracis* disseminates from as well as how LT is used to circumvent the innate immune response. The research summarized hereafter demonstrates that, 1) dissemination of *B. anthracis* originates at the initial site of spore deposit and not from spores which have trafficked to the draining lymph node, 2) low levels of circulating LT are capable of attenuating PMNs ability to both kill vegetative bacilli and accumulate at sites of inflammation, and 3) circulating LT prevents PMNs ability to kill by preventing generation of the oxidative burst.

Acknowledgements

My PhD would not be possible without the help and support of many people. I would first like to thank the one most directly responsible for my training at UVA, my mentor Dr. Ian Glomski. Not only did he provide excellent guidance, he also exhibited an inordinate amount of patience in the face of my many questions and growing pains during my time in lab. However, Ian was not the only one in lab. I made great use out of the encyclopedic knowledge of literature and techniques possessed by my fellow graduate student, David Lowe. And nothing would have gotten done without the hard work of our technicians Christine Zito, Kelly Smucker, Stephen Ernst, and Amanda House. Finally, our post doc, Heath Damron, who joined the lab late but still managed to have a big impact, and provided valuable insights in how to take the next step of my career. All of the aforementioned people provided a lab environment that will be hard to beat, and has led to many strong friendships.

Many others in at UVA contributed positively to my scientific and personal development. My committee consisting of Erik Hewlett, Alison Criss, Ulrike Lorenz, and Mehrad Borna deserve a lot of gratitude, without their vital input and tough love I would not have had nearly the success that I have had. I would especially like to thank Criss lab members Brittany Johnson and Louise Ball for letting me borrow their knowhow and reagents to complete my PMN based experiments. Likewise, Mehrad lab member Marie Burdick provided lab space, equipment and expertise to help me get vital pieces of data. Finally, I would like

to thank our collaborators at the Centers for Disease Control, Drs Anne Boyer and John Barr, for all their help and use of their wonderful LF detection assay.

Of course, no list of acknowledgements would be complete without my support network starting with my wife, Melissa Ivey, for moving to Charlottesville to be with me while in school, and putting up with me during the many stressful and frustrating times. I would also like to thank my parents Patrick and Ellen Weiner for encouraging my scholastic pursuits from a very early age, from taking me to the Greensboro Science Center for summer classes to paying for my undergraduate education at NCSU. Also my little sister Natalie Weiner for always having my back, and making me feel like my degree is useful when calling to ask whether various foods are okay to eat or not, and is this bacteria bad or okay. In addition, much thanks to my extended family for humoring me when I try to explain to them what exactly it is that I study.

Table of Contents

Abstract	i
Acknowledgements	iii
Table of Contents	v
List of figures and tables	viii
List of abbreviations	xi
Chapter 1: General Introduction	1
<i>Bacillus anthracis</i>	2
Virulence factors.....	2
Initiation of infection.....	4
Dissemination factors.....	5
Trojan horse hypothesis of dissemination controversy.....	7
Introducing the jail break hypothesis of dissemination.....	18
Summary.....	19
Research objectives.....	21
Chapter 2: Debridement Increases Survival in a Mouse Model of	
Subcutaneous Anthrax.....	23
Introduction.....	24
Results.....	26
Discussion.....	39
Materials and methods.....	44
Chapter 3: Circulating lethal toxin decreases the ability of neutrophils to kill	
vegetative <i>Bacillus anthracis</i> by preventing oxidative burst.....	49

Introduction.....	50
Results.....	52
Discussion.....	73
Materials and methods.....	79
Chapter 4: Circulating lethal toxin decreases the ability of neutrophils to accumulate at sites of PMA induced inflammation.....	86
Introduction.....	87
Results.....	89
Discussion.....	97
Materials and methods.....	100
Chapter 5: Examining circulating <i>B. anthracis</i> edema toxin effects on PMN function.....	105
Introduction.....	106
Results.....	107
Discussion.....	113
Materials and methods.....	117
Chapter 6: Summary, discussion, and future directions.....	122
Summary.....	123
Discussion.....	128
Future directions.....	132
Appendix I: Development of an <i>in vivo</i> PMN accumulation assay using adoptive transfer.....	138
Introduction.....	139

Results.....	136
Discussion.....	148
Appendix II: Establishment of a luminol chemiluminescence assay to access the effects of LT on murine PMN oxidative burst.....	151
Introduction.....	152
Results.....	152
Discussion.....	154
References.....	158

List of Figures and Tables

Chapter 1

Figure 1.1: The Trojan horse hypothesis of infection.....12

Figure 1.2: The Jailbreak hypothesis of infection.....20

Chapter 2

Figure 2.1: Debridement significantly increases mouse survival from
subcutaneous *B. anthracis* infection.....29

Figure 2.2: *B. anthracis* spores are found in the draining cervical lymph node
early in infection.....32

Figure 2.3: Presence of lethal factor in cervical draining lymph node does not
alter cellular activation.....37

Table 2.1: Lethal Factor is measurable in the ear, draining cervical lymph nodes
and serum at the time of debridement 12 hours after spore inoculation...35

Chapter 3

Figure 3.1: Three defined stages of *B. anthracis* infection.....54

Figure 3.2: Mouse PMNs kill vegetative *B. anthracis*.....58

Figure 3.3: Injected LT is enzymatically active in PMNs isolated from mouse
bone marrow.....61

Figure 3.4: Circulating LT attenuates PMN killing of vegetative *B. anthracis*.....63

Figure 3.5: Circulating LT does not decrease viability of bone marrow PMNs...65

Figure 3.6: Human and mouse PMNs kill vegetative TKO to a similar degree....68

Figure 3.7: Oxidative burst is required for mouse PMNs to kill vegetative TKO..69

Figure 3.8: Circulating LT causes a decrease in oxidative burst in response to

TKO but not PMA.....	71
Figure 3.9: Phagocytosis is necessary for PMN killing of vegetative TKO.....	74
Table 3.1: LF levels increase in all major organs over time during <i>B. anthracis</i> Infection.....	56
Table 3.2: LF concentration after injection of purified toxin components are consistent with levels found during active infection.....	60
Chapter 4	
Figure 4.1: PMN accumulation at sites of inflammation can be measured in real-time.....	91
Figure 4.2: PMN accumulation at sites of inflammation can be measured in real-time.....	92
Figure 4.3: Circulating LT attenuates PMN accumulation at sites of PMA induced Inflammation.....	94
Figure 4.4: Circulating LT does not affect circulating PMN levels.....	95
Figure 4.5: Circulating LT causes a decrease in PMN migration.....	96
Figure 4.6: NECre luc mice demonstrate less susceptibility to circulating LT than C57Bl/6 mice.....	98
Chapter 5	
Figure 5.1: Ability of <i>B. anthracis</i> to produce ET does not alter PMN ability to kill vegetative bacilli.....	108
Figure 5.2: i.p. injected ET does not attenuate the ability of PMNs to kill vegetative <i>B. anthracis</i>	110
Figure 5.3: ET does not affect PMNs ability to kill vegetative TKO at earlier	

time points.....	111
Figure 5.4: Retro-orbital injection of ET does not lead to alteration in PMNs ability to kill vegetative TKO.....	112
Figure 5.5: ET and EF attenuate PMN accumulation at sites of PMA induced inflammation.....	114
Chapter 6	
Figure 6.1: Flow chart summary of dissertation research.....	129
Figure 6.2: Model of early events during <i>B. anthracis</i> infection.....	137
Appendix I	
Figure 7.1: adoptively transferred luc+ WBCs accumulate at site of PMA induced inflammation.....	141
Figure 7.2: PMN accumulation in response to inflammatory stimuli in AJ and FVB mice.....	144
Figure 7.3: PMN migration to TKO spore versus vegetative challenge.....	145
Figure 7.4: Luminescence per PMN and WBC Standard curves.....	147
Figure 7.5: Quantification of PMNs at site of inflammation <i>in vivo</i>	150
Appendix II	
Figure 8.1: Presence of heat-inactivated serum is necessary for TKO induced oxidative burst.....	155
Figure 8.2: Presence of heat-inactivated serum inhibits PMA-induced oxidative burst.....	156
Figure 8.3: HBSS +Ca +Mg causes oxidative burst in control unstimulated PMNs.....	157

List of Abbreviations

BLI = Bio-luminescent imaging

BSL2 = Bio-safety level 2

CAMs = Cell adhesion molecules

cLN = cervical lymph node

CXCL2 = Chemokine (C-X-C motif) ligand 2

DPI = Diphenylene iodonium

EF = Edema factor

ET = Edema toxin

fMLP = N-Formyl-Met-Leu-Phe

GALT = Gut-associated lymphoid tissue

HBSS = Hanks balanced salt solution

i.p. = intra-peritoneal

i.v. = intra-venous

KO = knockout

KC = Chemokine (C-X-C motif) ligand 1 (CXCL1)

LF = Lethal factor

LN = lymph node

LT = Lethal toxin

Luc⁻ = Firefly luciferase negative

Luc⁺ = Firefly luciferase positive

Lux = Luciferase genes from *Photobacterium luminescens*

NALT = Nasal-associated lymphoid tissue

NECre luc = transgenic mice expressing Cre recombinase under a neutrophil elastase promoter (129-Elane^{tm1(cre)Roes}/H mice) with floxed stop luciferase mice (FVB.129S6(B6)-Gt(ROSA)26Sor^{tm1(luc)kael}/J mice)

MIP-2 = macrophage inflammatory protein 2

PA = Protective antigen

PAMPs = Pathogen-associated molecular patterns

PI3K = phosphatidylinositol 3 kinase

PMA = phorbol-12-myristate-13-acetate

PMNs = Polymorphonuclear cells (aka neutrophils)

r.o. = retro-orbital

ROS = Reactive oxygen species

TKO = Triple toxin knockout Sterne strain

WT = Wild type

Chapter 1: Introduction

Elements of this chapter published as: Updating perspectives on the initiation of

Bacillus anthracis growth and dissemination through its host

Zachary P. Weiner and Ian J. Glomski

Infection and Immunity 2012 May; 80(5):1626-33. doi: 10.1128/IAI.06061-11.

Epub 2012 Feb 21.

Bacillus anthracis

Bacillus anthracis is a Gram-positive spore-forming bacterium that is the causative agent of the disease anthrax (81). Most commonly associated with grazing livestock and game, anthrax is a zoonotic disease for humans who associate with them, such as herders and wool processors (153). Classically, anthrax can be contracted through several routes of exposure: by inhalation, cutaneously through breaks in the skin, and by ingestion (2, 70, 104). In addition, it should be noted that recently a new form of anthrax has been recognized and deemed “injection anthrax”, because of its association with the injection of *B. anthracis*-contaminated illicit drugs, such as heroin (115). Cutaneous anthrax is the most common form of infection in humans, accounting for 95% of all cases (153). The cutaneous form has the lowest mortality rate at 1% with antibiotic treatment and 20% without. Inhalational anthrax has the highest mortality rate at 45% with antibiotic treatment and upwards of 97% without (15). Gastrointestinal anthrax has roughly the same mortality rate as the inhalational form of infection but likely goes underreported due to difficulties in diagnosis and its prevalence in less developed countries (6).

Virulence Factors

B. anthracis has multiple virulence factors. The most important of these are exotoxins and capsule, which are encoded on two different virulence plasmids, pXO1 and pXO2, respectively (71). The tripartite AB exotoxin consists of a receptor-binding translocase subunit, protective antigen (PA), and two enzymatic subunits, lethal factor (LF) and edema factor (EF). When PA is bound

to LF or EF the complex becomes lethal toxin (LT) or edema toxin (ET), respectively, but it should be noted that oligomerized PA has been modeled to bind multiple subunits at the same time and thus a single exotoxin complex may contain PA, LF, and EF simultaneously (80). LF is a metalloprotease that cleaves most mitogen-activated protein kinase kinases (MAPKK's), or MEKs, when delivered to the cytosol by PA (3, 38, 55, 103). LT can cause the death of cells and experimental animals (103). EF is a calmodulin-activated adenylate cyclase that converts ATP to cAMP and induces edema in host tissues when introduced into the cytosol by PA (5, 83). *B. anthracis* capsule biosynthetic machinery is encoded on pXO2 and is responsible for producing a capsule that consists of gamma-linked poly-glutamic acid that is covalently bound to the cell wall (16, 117). Capsule serves to protect *B. anthracis* from phagocytosis and complement deposition (93, 94, 127).

While the vegetative form of the bacterium is capable of causing infection in the laboratory (143), the spore is the infectious particle in nature, presumably because of the spores are capable of persisting in the environment as viable entities for decades (96). For this reason, the spore can itself be considered vital in causing infection. Spores are metabolically inactive and resistant to environmental stresses such as extreme heat, cold, and radiation. These properties also make spores resistant to killing by the host immune system. Spores are generally 1-2 microns in length and are composed of a core, a thick peptidoglycan layer called the cortex, a proteinaceous coat, and an exosporium, which is a loose-fitting sac-like structure on the exterior of the spore (17, 51). The

size of aerosol particles in which spores are contained plays a large role in the efficacy of the establishment of inhalational infections. Particles greater than 12 μ m containing spores are much less infective in guinea pigs and rhesus monkeys than spores less than 5 μ m (36).

Initiation of infection

Most of what is known about initiation of anthrax has been derived from animal models of infection. While caveats are inherent when comparing animal infections with human infections, animals are the only means to study anthrax in a complete host system (57). While anthrax infection in non-human primates is arguably the most similar to human infections, often the cost of primates is prohibitory. Likewise non-human primates have relatively few molecular, genetic, and immunological tools with which to study the infection when compared to the diversity of genetic tools and reagents available for mice, and to a lesser degree rabbits and guinea pigs. These tools permit for specialized analysis of the dissemination of bacteria within the host, the host response, and disease that could not be done previously. Many, but not all, of the key characteristics of anthrax are recapitulated in mouse models of infection (57). Information gleaned from studies using genetic tools in mice improves the design and implementation of infection studies performed in non-human primates and other less experimentally tractable animals.

The manner by which *B. anthracis* infection initiates has been a focus of research by a number of laboratories. In 2002 Guidi-Rontani coined the name “Trojan horse” for her proposed hypothesis of dissemination based on long

accumulating data, with particular emphasis on that of Joan Ross, and is described in greater detail below. This Trojan horse model has become the most widely cited model for inhalation anthrax. Of late, however, data derived from animal models of infection have necessitated a reassessment of the Trojan horse concept. The following will describe the observations that gave birth to the Trojan horse and summarize recent research that modifies the Trojan horse hypothesis as proposed in 2002, and review research that questions the necessity for a Trojan horse to cause infection. Lastly, a new hypothesis describing the establishment and dissemination of *B. anthracis* infections is proposed.

Dissemination factors

B. anthracis is non-motile, thus dissemination beyond the initial site of contact necessitates the active participation of the host (141, 153). Accordingly, determining the means by which *B. anthracis* virulence factors influence host function are essential for understanding dissemination. Exotoxins play a significant role in dissemination and influence many aspects of host function. Knockouts of LT and ET in unencapsulated pXO2-deficient *B. anthracis* are incapable of progressing beyond the draining lymph node during inhalational and subcutaneous infection in A/J mice (90). This may reflect the exotoxins' ability to break down epithelial and endothelial cell barriers and cause hemorrhaging in animal models (45, 103, 146). Effects on endothelial barrier function can be seen even with low exotoxin (100ng ET and 1 μ g LT) concentrations *in vitro*. At these low doses, ET and LT alter the transendothelial electrical resistance of endothelial cell monolayers (136, 146). Likewise, capsule plays an important role

in dissemination. It has been shown that encapsulated *B. anthracis* is able to disseminate from initial sites of infection to blood quicker than their non-encapsulated counterparts, although the mechanism behind this phenomenon is currently ill defined (2, 37, 56).

In addition to the major virulence factors, *B. anthracis* produces at least four separate proteases that promote host tissue degradation to eliminate physical barriers of bacterial dissemination (113). These proteases break down gelatin, casein, fibronectin, laminin and collagen. In mice, exposure to supernates containing *B. anthracis* proteases led to hemorrhaging or death within two to three days when introduced intratracheally (21, 113). Thus, factors beyond the classical major virulence determinants should be considered when investigating *B. anthracis* dissemination through a host.

While the mortality rates of the four types of *B. anthracis* infection differ, the majority of reported lethal anthrax cases in animals and humans exhibit bacteremia and toxemia at the time of death, independent of the route of spore entry. Autopsies reveal *B. anthracis*-containing lesions associated with edema and hemorrhaging throughout the body (2, 48, 50, 56). While investigating *B. anthracis* dissemination in Rhesus monkeys, Lincoln *et al.* reported that *B. anthracis* appears in the mediastinal lymph nodes after aerosol challenge, and the thoracic duct after intradermal infection (87). This was the first direct evidence to suggest that *B. anthracis* first spread via the lymphatics before entering the blood stream in a manner that was not dependent on the original route of exposure, although previous experiments had implied this to be the

case. These observations were later supported with bioluminescent imaging (BLI) studies utilizing light-producing bacteria to infect BALB/c and A/J mice. These studies demonstrated that after initiation of infection, bacteria were next detected in the regional draining lymph nodes before appearance in the blood stream in all three major forms of anthrax (39, 54, 56, 90). While it is generally accepted that *B. anthracis* must escape the lymphatic system before infection can spread hematogenously, disagreement remains regarding whether the lymphatic system is where spores germinate to initiate vegetative outgrowth.

The Trojan horse hypothesis of dissemination

The Trojan horse hypothesis posits that during inhalational anthrax, spores do not germinate in the lungs and must be transported by alveolar macrophages past the lung epithelial barrier to lymph nodes in order to germinate and initiate the production of virulence factors (60). This idea has its roots in very early *B. anthracis* research. Initial research on inhalational anthrax involved infecting small and large animals, however in all cases very few vegetative bacteria were found in the lumen of the lungs at any stage of infection (119, 158). Lack of vegetative bacilli in the lungs has also been observed in recent studies (2, 15, 23, 29, 49, 66). Because vegetative bacilli are rarely seen in the lumen of the lung, it is thought that the lung itself is refractory to spore germination. If spores cannot germinate in the lung it was hypothesized that spores would need to traverse from the lumen of the lungs into deeper tissue in order to germinate and cause disseminated disease. A mechanism for the movement of spores out of the lumen of the lung was proposed in 1957 by Joan

Ross, who observed a macrophage containing a phagocytosed spore in transit to the draining tracheo-bronchial lymph node (119). Lincoln's 1965 study built upon Ross's observations by demonstrating that *B. anthracis* infection progressed from the lung lymphatically and not hematogenously in Rhesus monkeys (87). Later research determined that phagocytosed spores were capable of germinating and escaping from phagocytes (34, 61, 123). A germination operon, gerX, was found to be linked with germination of *B. anthracis* within macrophages (62). These observations led to Guidi-Rontani's 2002 opinion article focusing on *B. anthracis* dissemination. She hypothesized that alveolar macrophages are responsible for transportation of *B. anthracis* spores from the lumen of the lungs to the mediastinal lymph nodes (60). Because of this, she named alveolar macrophages as the "Trojan horse" for *B. anthracis* dissemination. This hypothesis also proposed that differences in lethality between animal species and different routes of infection could be due to the presence or absence of germinants within macrophages from different species.

Another important aspect of the Trojan horse model revolves around exotoxin's effects on macrophages, specifically whether exotoxins prevent the destruction of *B. anthracis*. Exotoxins have been reported to modulate the oxidative burst in both macrophages and neutrophils (30, 64). The idea that exotoxins are selectively targeting the innate immune system is supported by a study which showed that the elimination of cellular toxin receptor CMG2 in myeloid cells leads to complete protection of mice from subcutaneous and intravenous infection (88). Likewise, exotoxins have been shown to modify

multiple behaviors of innate immune cells including chemotaxis, cytokine secretion, and activation (3, 95, 139).

Elements of the Trojan horse hypothesis have been in place since the 1950's and once the hypothesis was formally defined it became the only well defined model of inhalational *B. anthracis* dissemination. Since 2002 the Trojan horse hypothesis has been the most cited model of inhalational *B. anthracis* infection. Over time, this hypothesis has been incrementally modified after it was demonstrated in mice that lung dendritic cells are capable of phagocytosing spores and transporting them into the lymphatic system more effectively than alveolar macrophages (14, 23).

Because the Trojan horse hypothesis is highly cited, a significant body of research has focused on refining its mechanistic details. These studies have presented data that calls for a reassessment of a number of the Trojan horse's central tenets as they were originally defined. *In vitro* epithelial cells, endothelial cells, and fibroblasts have been shown to engulf and transcytose spores and vegetative bacilli through cell monolayers without disrupting barrier integrity (121, 122, 143). These data raised questions as to whether phagocytes are the sole cell type that can act as Trojan horses and thus whether phagocytes are an absolute necessity for spores to transit from the lumen of the lung. However, transport through non-phagocytes occurs less frequently than spore uptake by phagocytes, and the ability of spores to cross-epithelial barriers has been difficult to demonstrate definitively with *in vivo* models.

Two studies by Cote *et al.* demonstrated an increase in the lethality of inhalational *B. anthracis* infections with the depletion of alveolar macrophages, and thus spores do not require alveolar macrophages to bypass epithelial barriers (28, 29). However it must be noted that these studies used chlodronate liposomes as an alveolar macrophage-depleting agent, which have multiple non specific effects, may deplete cell types other than macrophages, or incompletely eliminate resident macrophages (135). Relatedly, Wu *et al* found that human alveolar macrophages are more resistant to intoxication than murine macrophages, and do not express significant amounts of anthrax toxin receptors (155). Human alveolar macrophages are less susceptible to *B. anthracis* exotoxins compared to those in mice, and their presence increases survival in inhalational infections. Alveolar macrophages may be better than other phagocytes at clearing *B. anthracis* infection from the lungs (155). Because interactions with alveolar macrophages would often lead to death of the bacteria, the implication is that it would be advantageous for spores to avoid phagocytosis (69, 77). The killing ability of aveolar macrophages may explain why autopsy of humans and animals reveal few spores and vegetative bacteria within the alveolar spaces (4, 23, 29, 59). Depletion of other innate immune cells implicated to be Trojan horses has demonstrated that monocytes, macrophages, and neutrophils are protective against *B. anthracis* rather than acting to promote infection, as would have been predicted by the Trojan horse model (29, 88).

Because potential Trojan horse phagocytes are protective against *B. anthracis* infection, spores may not be dependent on phagocytes for transport

from the lumen of the lungs beyond the epithelial barrier. While phagocytes may not act as a Trojan horse, spores in the draining lymph node may still act as the founding population of disseminated disease. The idea that *B. anthracis* could use multiple mechanisms to transverse epithelial barriers to arrive at a draining lymph node should not be discounted. Many other pathogens, including *Salmonellae*, *Shigellae*, and *Listeria* utilize multiple distinct methods for crossing epithelial barriers (26). It should also be noted that even if a majority of spores or vegetative bacteria are cleared at the initial site of infection according to the Trojan horse hypothesis, the trafficking of a subset of spores to the lymph node could cause infection. In light of these observations, the Trojan horse hypothesis should be expanded to take into account all possible mechanisms of spore trafficking to draining lymph nodes. In summary, The Trojan horse hypothesis states that spores trafficking to the regional draining lymph node through an intermediate intracellular step leads to disseminated disease as demonstrated in Figure 1.1.

Challenges to the Trojan horse hypothesis

While study of the hypothetical Trojan horse mechanism of dissemination has led to a much greater understanding of how spores and the immune system interact in the lungs, there has been no direct evidence demonstrating whether spores in the draining mediastinal lymph nodes are the population of bacteria that give rise to disseminated anthrax. Establishing the location of the founding population of bacteria was particularly challenging until the recent development of BLI technologies. BLI-based studies have led to

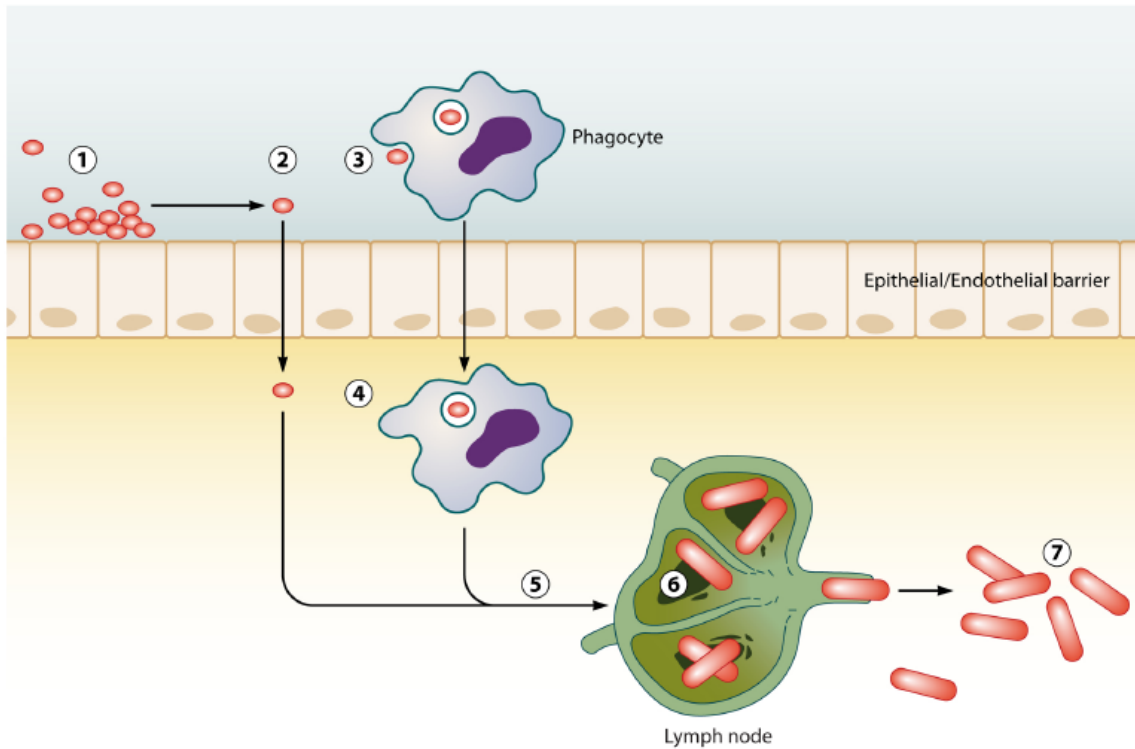


Figure 1.1: The Trojan horse hypothesis of infection.

Spores enter the lumen of the airways, gastrointestinal tract, or skin at exposure (1). Spores either invade epithelium directly (2), or are phagocytosed by host phagocytes (3). In the original model, this phagocyte was predicted to be an alveolar macrophage, but can likely also be a dendritic cell. Spores then cross the epithelium by transcytosis through the epithelial cell or within the phagocyte (4). Spores then traffic to the mediastinal lymph node (5). Once in the lymph node, spores germinate into vegetative bacteria, grow and produce exotoxins and capsule, eventually resulting in loss of structural integrity of lymph node (6). Bacteria escape lymph node and enter blood stream, leading to bacteremia and host death (7).

significant advances in the understanding of where infections initiate, and how dissemination of infection progresses temporally and spatially. BLI technologies rely on light-producing bacteria that can be tracked within an intact host using highly sensitive cameras. The major advantages of these methods are that subject animals do not need to be euthanized for every time point and data can be collected non-invasively in a dynamic fashion. Studies using a *B. anthracis* construct that expresses luminescence under a germination promoter demonstrated that spores could germinate in the lungs of mice (54, 126). These results were at odds with the original Trojan horse model that states that spores do not germinate in the lungs. However, germination in the lungs was only observed in animals that received a large bolus of spores' intranasally, and therefore may not represent the typical inhalational infection. Furthermore, multiple studies utilizing *B. anthracis* that produce light only during vegetative growth indicated that throughout early infection, when bacteria are growing in the upper airways, all bacteria in the mediastinal lymph nodes remained as dormant spores (56, 90).

The relationship between germination of spores and pathogenesis is complex (27). Germination alone does not necessarily mean establishment of infection, and can leave *B. anthracis* susceptible to destruction as demonstrated by Hu *et al* (69). Additionally, BLI studies raised concern about traditional experimental infection techniques. Glomski *et al* 2007 suggested that mucosal epithelial breaches caused by experimental techniques are more prone to infection (56). The propensity for traumatized epithelial barriers to be the initiation

site of infection is consistent with studies on cutaneous infection, in which breaks in the skin are more readily infected in mouse models of cutaneous infection (9). It is also important to note that Ross observed spores within a macrophage in transit to the regional lymph node after intratracheal intubation, which she noted to frequently cause breaks in the airway mucosa, and did not observe spore transport to the lymph after non-invasive aerosol challenge (119).

Experiments using BLI technologies found that in intranasal and aerosol spore challenges the first site that vegetative growth is detected in mice is the nasal-associated lymphoid tissue (NALT), and not in the mediastinal lymph nodes (54, 56, 90). A potential reason for why infection seems to initiate in the NALT and not the lymph node may be due to the particle size of the spore aerosol. Larger aerosols tend to accumulate in the upper respiratory tract in primates, as opposed to smaller ones which accumulate deeper in the lungs (65). Large aerosols likely reflect most natural infections and poorly executed bioweapon delivery because of the propensity of spores to clump. Infection studies following luminescent *B. anthracis* indicated that vegetative bacteria were multiplying and producing exotoxin in the NALT, and only ungerminated spores were found both in the lung and in mediastinal lymph nodes of mice (54, 56, 90). These data were later supported by research using a bioluminescent, fully virulent clinical isolate (39). These data suggest that in mouse infections spores in the lungs and mediastinal lymph nodes may be ancillary to the more robust infection in the NALT at early time points. These mouse studies supported Lincoln's monkey data, which demonstrated that after inoculation, infection next

spread into the lymphatic system then progressed into the blood stream, leading to death. A key difference between these two models was that in the mice bacterial growth initiated in the NALT then progressed to the cervical lymph node rather than the mediastinal lymph node as is suggested by the Trojan horse hypothesis. While a Trojan horse cell may be still be required for infection, BLI studies imply that bacteria are delivered into an unexpected anatomical location- the cervical lymph node rather than the mediastinal lymph node.

Reforming the Trojan horse hypothesis in light of new data

In both the gastrointestinal and subcutaneous forms of murine anthrax, vegetative bacilli grow at the initial sites of spore entry either in the intestines (Peyer's patches) or nasal-associated lymphoid tissues/oropharynx, bacteria then spread to lymphatic system before escaping into the blood (6). In cutaneous anthrax, spores germinate at the site of initial spore deposition, in the dermis (9, 56). The question becomes if *B. anthracis* does not require macrophages to act as a Trojan horse for dissemination in the case of gastrointestinal, cutaneous, or subcutaneous infections, why would a Trojan horse be required solely for the inhalational form?

New animal models of inhalational anthrax seem to contradict aspects of earlier observations of disease dissemination. However, it is possible to re-interpret previous findings in a new context. Since early inhalational anthrax exhibits some clinical manifestations similar to those of pneumonia, the disease has been referred to as "anthrax pneumonia" as early as 1882 (58). Despite the name there is typically little evidence of significant bacterial growth within the

alveolar space, as is characteristic of classical pneumonia. Today it remains difficult to diagnose inhalational anthrax. Many of the 2001 victims of the mailing of anthrax spores in the United States were initially diagnosed with bronchitis or pneumonia (99). Thus, it is not surprising that early research focused on the lungs and trachea. Once patients display symptoms of inhalational anthrax however, the infection has generally progressed to a point where even effective bactericidal antibiotic treatment can save only 45% of the infected individuals (15). This brings in the concept of a “point of no return”, where enough total exotoxin (or other bacterial products) is in circulation to kill the host even in the absence of viable bacteria (145). In the context of inhalational infections, this could reflect a point where infection has disseminated from the original site of infection and spread hematogenously into the lungs and mediastinum to cause the classical diagnostic mediastinal widening. This idea has some historical precedent, having first been proposed in 1925 by Fraenkel, who hypothesized that the initiating site of infection was in the tracheo-bronchial mucosa, and that pneumonia developed after infection had been established (47). BLI experiments using luminescent bacteria demonstrate that bacterial growth within NALT. These data suggest that past studies of inhalational anthrax have been mistakenly focused on the lungs, rather than an alternate sites as the origin of disseminated bacteria, possibly ones analogous to the NALT in mice.

The infection cycle of *B. anthracis* relies on killing grazing animals presumably through gastrointestinal anthrax. These infections result in an increase of spore concentrations in existing grazing areas and/or introduction of

spores into previously spore-free grazing areas (104). Therefore it is likely that *B. anthracis* has evolved to exploit the gut-associated lymphoid tissue (GALT), as observed in mouse models of infection (56), in order to kill grazing animals. When considering the similarities in structure between the NALT and GALT (56), it is conceivable that the deadly nature of inhalational anthrax is a byproduct of *B. anthracis* exploiting a similar niche as those that would be targeted in a gastrointestinal infection. Following this line of reasoning, the difference in mortality between mucosal and cutaneous infection could result from differences in the immune response between mucosal and non-mucosal infections. This possibility has been alluded to in the literature with mouse studies, where the role of polymorphonuclear cells (PMNs) and monocytes/macrophages in controlling subcutaneous versus inhalational infections has been assessed (28, 29, 88, 102). These studies report that PMNs are vital for clearance of subcutaneous infections (102). However, macrophages are the most important cell type mediating clearance of aerosol and intranasal infections (29, 102). Research examining cutaneous anthrax infections with nude mice, which lack most adaptive immunity but retain innate immune system function, showed that an influx of PMNs was associated with clearance of bacteria (148). Liu *et al.* found that selectively knocking out CMG2 in myeloid cells, eliminating their sensitivity to *B. anthracis* exotoxins, complete protection against subcutaneous *B. anthracis* infections was acquired (88). This would suggest that while macrophages and PMNs are protective against *B. anthracis* infection, exotoxins are capable of disarming the innate immune system to allow bacterial outgrowth and

dissemination. Differences in cellular subtypes that respond to mucosal compared to dermal infections could explain why inhalational *B. anthracis* has a higher mortality rate than cutaneous *B. anthracis*. Macrophages, which are protective in inhalational infection (28), rely heavily on oxidative killing which exotoxins have been shown to affect (64). PMNs, shown to be protective in cutaneous infection, do not rely solely on their oxidative burst to kill pathogens, but have granules that contain many different antimicrobial effectors (98). Indeed, human PMNs kill *B. anthracis* independently of oxidative burst with alpha defensins, which are a component of primary granules (98). The presence of PMNs non-oxidative killing ability perhaps suggests why PMN-controlled cutaneous infections have lower mortality rates than macrophage-controlled inhalational infections. It is important to point out that while cell-depletion experiments suggest that differential immune responses to a lung versus a subcutaneous infection occur, this phenomenon has not been conclusively demonstrated experimentally. Overall, small animal models suggest that rather than inhalational anthrax being unique among the forms of anthrax, requiring a host immune cell to escape the lumen of the lungs, it may progress like gastrointestinal anthrax, where infection is established in a mucosa-associated lymphoid tissue.

The Jailbreak hypothesis of dissemination

While Trojan horse-mediated movement of bacteria to the lymph nodes can occur (23), and spores are found in the mediastinal lymph nodes at early stages of infection (56), there is no experimental evidence that spores in draining

lymph nodes are the founders of disseminated disease. In light of recent findings using animal models, we propose that *B. anthracis* germinates at favorable sites in the host such as NALT, GALT, and damaged cutaneous soft tissues, where it begins producing its virulence factors (Fig. 1.2 steps 1 and 2). Exotoxins and proteases produced by *B. anthracis* act to dampen the immune response and permeabilize tissues, effectively allowing vegetative bacilli to drain into the regional lymph node (Fig. 1.2 steps 3-5). Once exotoxins and bacteria arriving from the initial site of infection have overwhelmed the draining lymph node, vegetative bacilli gain access to the blood stream causing bacteremia, leading to eventual host death (Fig. 1.2 steps 6 and 7). In summary, this model of dissemination proposes that differences in mortality between routes of infection are defined by the initial sites of spore contact with mucosa-associated lymphoid tissue or cutaneous lesions, and does not require intracellular transport of spores to the draining lymph node.

Summary

Often patients will die from *B. anthracis* infections even after treatment with antibiotics initiated after distinct manifestations of anthrax (such as mediastinal widening). Because of this a better understanding of where infection initiates and how *B. anthracis* disseminates is necessary in order to begin to design treatment options that interrupt crucial early events in infection. The proposed jailbreak hypothesis presents an alternative to the Trojan horse model of dissemination with the key difference that instead of spores requiring an intracellular step in order to establish infection in the lymph node the jailbreak

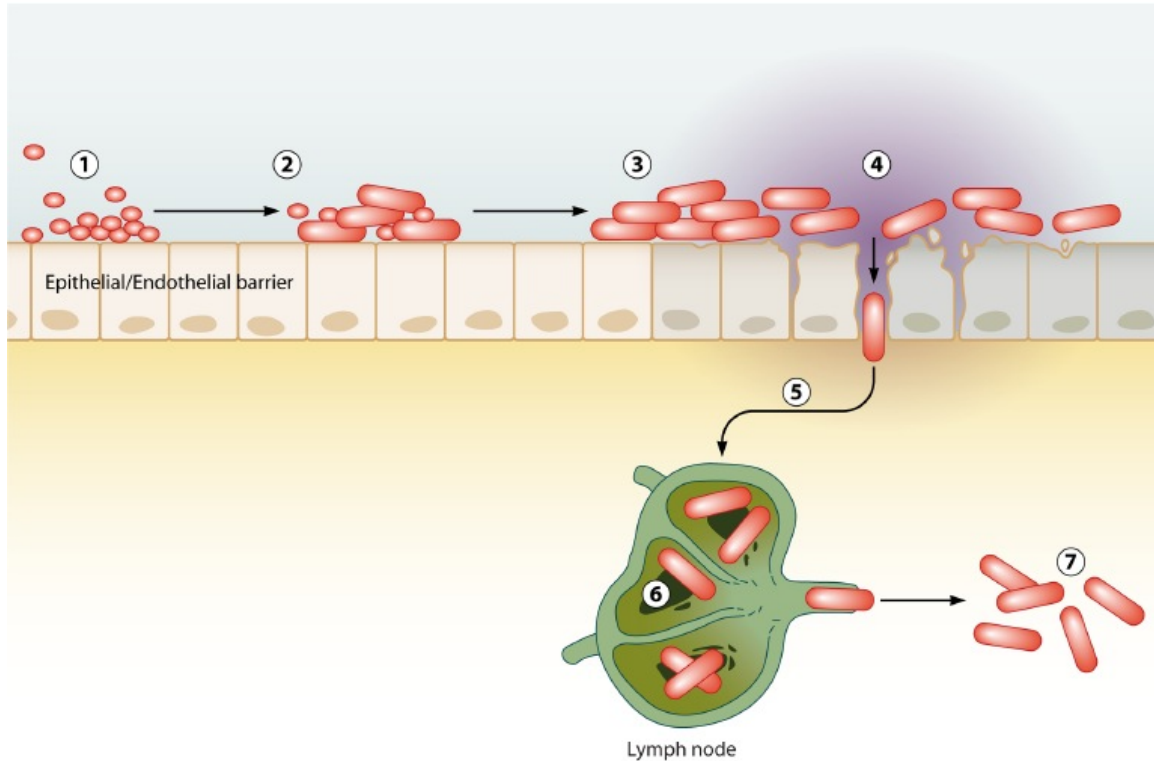


Figure 1.2: The Jailbreak hypothesis of infection.

Spores enter the lumen of the airways, gastrointestinal tract, or skin at exposure (1). Spores germinate and become exotoxin-producing encapsulated vegetative bacteria at the site of initial entry into the host tissues (2). Continued vegetative bacterial growth increases exotoxin and protease concentrations and leads to breakdown of endothelial/epithelial barrier function (3). Vegetative bacteria pass through the damaged barrier (4). Vegetative bacteria traffic to regional draining lymph nodes by bulk lymphatic flow without the necessity of phagocytic transport (5). Bacteria in lymph nodes continue to produce virulence factors and replicate, eventually causing loss of lymph node integrity (6). Bacteria escape the lymph node and enter blood stream, leading to bacteremia and host death (7).

model requires spore germination and exotoxin production at the initial site of spore exposure. Bacilli then gain access to the lymph and circulatory system after toxin-mediated damage to cellular barriers occurs. The proposed hypothesis of infection has several important ramifications for future research. Most importantly, the jailbreak suggests a shift away from the current focus on potential Trojan horses and the lumen of the lung. Instead, the jailbreak refocuses on the mucosal-associated lymphoid tissues in the upper respiratory tract in inhalational anthrax and the gastrointestinal tract for gastrointestinal anthrax. Additionally, the jailbreak model suggests that future research should have greater focus on differences in immune responses to mucosal compared to non-mucosal surfaces and mechanisms by which *B. anthracis* circumvents these responses. However, there are several caveats with the jailbreak model of infection. The most notable is that evidence for the jailbreak hypothesis has been primarily derived from mice, and results similar to those acquired with BLI have not been reproduced in other animal systems. Until more research is done, the universality of the jailbreak model of infection will need to be assessed using non-murine models of infection.

Research objectives

As this chapter demonstrates, the point where *B. anthracis* dissemination originates is currently ill defined. Accordingly, it is very difficult to study how *B. anthracis* is able to repress the immune response leading to dissemination and death, because if it is not known where a battle is fought, it is difficult to determine how the battle was won or lost. As such the first objective of this research was to

determine the primary site of *B. anthracis* outgrowth and dissemination in the subcutaneous model of infection, the initial site of spore deposit, or the regional draining lymph node. Once the site of infection initiation was determined the next objective was to determine what the *B. anthracis* exotoxins were doing to manipulate the PMN response to infection. The final goal of this research was to elucidate the mechanisms by which *B. anthracis* exotoxins accomplish the attenuation of the PMN response.

Chapter 2: Debridement Increases Survival in a Mouse Model of Subcutaneous Anthrax

Chapter 2 a large portion previously published as: Debridement increases survival in a mouse model of subcutaneous anthrax.

Weiner ZP, Boyer AE, Gallegos-Candela M, Cardani AN, Barr JR, Glomski IJ
Plos ONE 2012;7(2):e30201. doi: 10.1371/journal.pone.0030201. Epub 2012 Feb
29.

Introduction

Soft tissue debridement consists of surgically removing the infected and/or necrotic tissue to promote healing and physically eliminate the organisms infecting the tissue(124). Debridement is typically used, along with appropriate antibiotics, in the management of necrotizing fasciitis, gangrene, and soft-tissue infections caused by a wide range of organisms including *Staphylococcus aureus*, *Clostridium perfringens*, and other pathogens that are refractory to antibiotic treatment (46). In these situations, the infected tissues are sacrificed to prevent the rest of the body from becoming overwhelmed by the infection. Soft tissue infections by *B. anthracis* demonstrate similarities, including extensive tissue damage, necrotizing fasciitis, and have the potential to cause lethal systemic dissemination (115). Thus debridement serves as a means to reduce overall mortality (72, 100, 133). The question regarding use of surgical debridement for anthrax polarizes around whether it increases the risk of releasing bacteria into the circulatory system or removes the foci of infection to prevent future spread of bacteria. Recently debridement has been used as a treatment for patients that injected *B. anthracis*-contaminated heroin subcutaneously (“popping”) or intramuscularly (7, 115). We propose that any debate on whether or not to apply debridement during anthrax persists because the question has never been experimentally addressed, where one variable can be altered to assess cause and effect. The goal of this study was to develop and substantiate an animal model of debridement for anthrax to provide access the efficacy of its use for the treatment of *B. anthracis* infections.

As discussed in chapter one, the most widely cited hypothesis for *B. anthracis* dissemination is referred to as the Trojan horse model (52, 60). In this model, spores are phagocytosed by resident phagocytes and then transported to the draining lymph node where they germinate and grow. Once the lymph node can no longer contain the bacterial growth, the bacteria then gain access to the circulatory system via the efferent lymphatics. Most of the data that support this hypothesis were produced with the aim of deciphering the dynamics of inhalational anthrax. It is unclear how much of this hypothesis applies to other versions of anthrax. Multiple studies indicate that dissemination unfolds similarly after the draining lymph nodes have been infected irrespective of the initial site of infection (56, 92), implying that differences in the lethality observed between cutaneous, gastrointestinal, or inhalation anthrax are manifest upstream of the lymph nodes.

In the course of developing the debridement model in mice, it became apparent that the accumulating data had direct implications on the application of the Trojan horse hypothesis to subcutaneous infections. We hypothesized, based on the inhalation Trojan horse hypothesis, that *B. anthracis* spores injected subcutaneously will quickly enter the draining lymph node and that the spores that enter the lymph node early after inoculation are the founding population of bacteria of the disseminated infection. This hypothesis was tested by utilizing a luminescence-based mouse subcutaneous model of anthrax coupled with debridement to achieve delivery of a pulse of spores to the cervical lymph nodes (cLN) draining the injection site. By removing the initial site of inoculation, the

resultant infection is limited to those bacteria that have entered the cLN during the time interval from injection to excision of the injection site.

In this study, we report that debridement of the site of subcutaneous inoculation of *B. anthracis* spores in the mouse ear up to 48 hours post-infection significantly increased the likelihood of host survival. This observation questions the universality of the Trojan horse dissemination hypothesis, which posits that the early transit of *B. anthracis* into the lymph node is an essential step towards systemic infection. In subcutaneous infections, the early delivery of spores to the cLN was not sufficient to establish disseminated infection. Instead bacterial growth at the initial site of subcutaneous infection was necessary, an observation which does not support the Trojan horse hypothesis in subcutaneous anthrax. We propose that the initial site of cutaneous infection supplies bacteria and exotoxins to the lymph node at a later time to cause the disseminated infection. This mouse model of subcutaneous infection experimentally demonstrated that debridement improves the outcome of subcutaneous *B. anthracis* infections by limiting the influence of bacteria within the initial site of infection and thus should be further explored experimentally as an adjunct to antibiotic therapy.

Results

Debate about the appropriate application of debridement to soft tissue infections by *B. anthracis* has been hampered by lack of experimental evidence to indicate or contraindicate its use. We thus performed experimental debridement in mouse infections. To achieve this goal, spores from a *B. anthracis* Sterne strain that produces light during vegetative growth within a host

(BIG23) were injected subcutaneously in the ear of C5-deficient A/J mice.

Infection of A/J mice with non-capsulated toxigenic *B. anthracis* Sterne strain is a widely used animal model for anthrax that recapitulates many characteristics of infections caused by encapsulated toxigenic *B. anthracis* strains such as the Ames strain (57, 89). The major advantage of Sterne strain infections is that they pose less risk to researchers, thus making the BSL2 infections described here broadly accessible to researchers without BSL3 facilities. The ear was chosen as the anatomic site of infection for our studies because the ear architecture allows efficient debridement, its translucence permits greater sensitivity when detecting bacterial growth by light emission, and it has been frequently used for modeling infectious diseases (1, 8, 20, 39, 56). Bioluminescent *B. anthracis* strains were applied in order to qualitatively identify the initial site of infection, determine whether all infected tissues were removed during the debridement procedure, and allow the assessment of the dissemination of bacteria over time. Initial sites of infection were identified by bacterial luminescence at 12, 24, 48, and 72 hours and debrided by notching the ear to efficiently remove the initial site of infection (Fig. 2.1A), similar to general mouse husbandry ear tagging procedures. Control mice were infected but a section of ear was removed that did not contain the infection. As an additional control, no portion of the ear was removed.

Debridement at 12 hours significantly protected mice from subcutaneous infection with two different doses of spores (Fig. 2.1B and 2.1C). All mice that were inoculated with 1×10^5 spores and debrided survived, whereas 67% of the control groups succumbed to systemic infections (Fig. 2.1B). Similarly, in mice

inoculated with 1×10^6 spores (approximately 100 LD₅₀s), 50% of the debrided mice survived, while all mice from control groups succumbed to systemic infections (Fig. 2.1C). Debridement of the ear significantly decreased mortality when performed at 12, 24, and 48 hours post-infection, but no longer had an effect when done after 72 hours post-infection (Fig. 2.1D). We conclude that debridement significantly protected mice from subcutaneous infection if performed within 48 hours of subcutaneous inoculation.

There are multiple mechanisms by which debridement could promote survival, one of which would be by preventing bacterial dissemination from the site of inoculation into the draining lymph node. We thus investigated the timing of entry of *B. anthracis* into the draining lymph node post-inoculation and determined if bacteria had indeed entered the draining lymph nodes during the interval between inoculation and debridement as is predicted by the Trojan horse hypothesis of infection. Accordingly, at 1, 12 and 24 hours post-infection the cervical draining lymph nodes were removed and bacterial colony-forming units (CFU) were measured. The total number of bacteria (spores + vegetative cells) were established by plating without heat treatment, and the number of spores was determined by heating the samples to 65° C for 20 minutes, and then plating for CFU (29). Independent of the initial dose, approximately 3-4% of injected spores arrived in the draining lymph nodes as early as one hour after injection (Fig. 2.2). The number of spores in the lymph node remained constant, and no outgrowth occurred as late as 24 hours after infection (Fig. 2.2A). To test the effect of debridement on subsequent bacterial loads, lymph nodes were

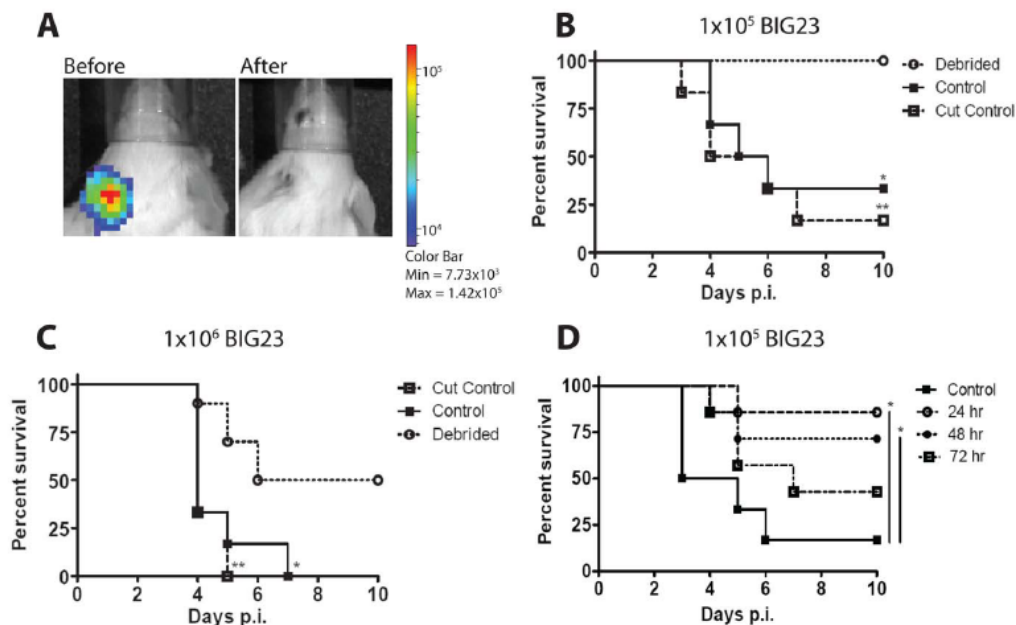


Figure 2.1: Debridement significantly increases mouse survival from subcutaneous *B. anthracis* infection. (A) Black and white photos of a single A/J mouse infected with 1×10^5 BIG23 spores in the left ear overlaid with false-color representation of photon emission intensity as indicated by the scale on the right in p/s/cm-2/sr. At 12 hours post injection luminescent infected tissue (left photo- before) was removed (debrided) to eliminate all bacterial luminescence (right photo- after). (B to D) BIG23 spores were injected subcutaneously into the left ear of 4-12 week old A/J mice. Control mice either had their left ear unperturbed (control) or non-infected tissue on the same ear was removed (cut control). Mice were then monitored for infection and dissemination using in vivo bioluminescent imaging. Mice were monitored for a total of ten days post-infection (p.i.), until luminescence was detected in a major organ, or mouse

appeared moribund (indicating imminent death). (B) Mice were inoculated with 1×10^5 spores of BIG23. Luminescent tissue was debrided at 12 hours p.i. Survival data from a total of seven mice from three independent experiments were analyzed with the log rank test to determine significant differences in survival between debrided and control mice (*, $p = 0.0108$), and debrided and cut control mice (**, $p = 0.0021$). There was no statistical difference between control and cut control mice. (C) Mice were inoculated with 1×10^6 spores of BIG23. Luminescent tissue was debrided at 12 hours p.i. Survival data were analyzed with the log rank test on a total of ten debrided mice and seven mice each for the control groups from three independent experiments to determine significant differences in survival between debrided and control mice (*, $p = 0.0109$) and debrided and cut control mice (**, $p = 0.0026$). There was no statistical difference between control and cut control mice. (D) Mice were infected with BIG23 as described above, but debridement of luminescent tissue was performed at 24, 48, or 78 hour p.i. Survival data were analyzed with the log rank test on a total of seven mice from each experimental group, with the exception of the control mice that totaled six, from three independent experiments to determine significant differences from control mice. The survival of mice debrided at 24 hours (*, $p = 0.0110$) and 48 hours (*, $p = 0.0477$) p.i. was significantly increased. The survival of mice debrided at 72 hours p.i. was not significantly different than control mice ($p = 0.1734$).

removed at 24 and 72 hours from mice that underwent debridement at 12 hours or from non-debrided control mice. At 72 hours post-injection the CFU had dropped more than 90%, and as at earlier time points, all CFU were comprised of spores (Fig. 2.2B). After debridement there were significantly fewer spores in the cLN at 24 hours post-infection ($p = 0.0144$), but no difference at 72 hours post-infection compared to 24 hours ($p = 0.0066$) (Fig. 2.2B). These findings were unaffected by the dose of spores, but as expected the number of CFU was proportionally lower with the lower inoculum (Fig. 2.2A and 2.2C). At no time were CFU isolated from the contralateral lymph nodes draining the uninoculated right ear (data not shown). Similar cLN CFU were observed in infections using spores from a *B. anthracis* strain that had PA, LF, and EF production eliminated (TKO) (Fig. 2.2D), suggesting that the above findings are spore-mediated and not LT- or ET-dependent. In total, these data suggest that at the time of debridement at 12 hours post-inoculation spores can be found in the draining lymph nodes and these spores are typically not sufficient to cause systemic infections since debridement effectively increased the likelihood of mouse survival.

The ineffectiveness of treatment, even after the bacteria have been eliminated with antibiotics, has been attributed to residual exotoxin activity within the host. Likewise, *B. anthracis* exotoxins have been reported to modulate chemotaxis and activation of host innate immune cells (30, 55, 116, 120). We thus questioned whether exotoxins were present at the time of debridement,

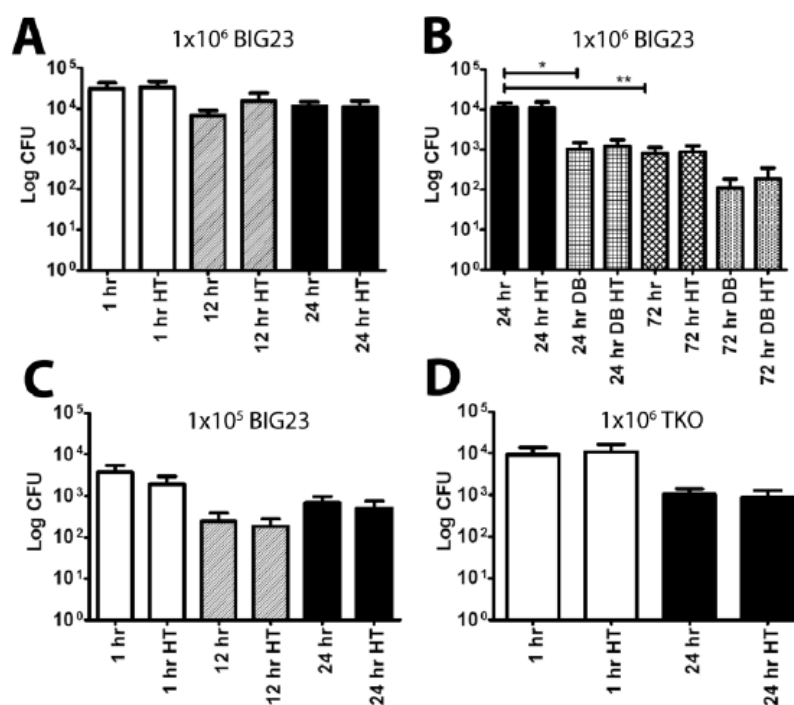


Figure 2.2: *B. anthracis* spores are found in the draining cervical lymph node early in infection. (A-C) BIG23 spores were inoculated subcutaneously into the left ear of 4-12 week old A/J mice. At the indicated times cervical draining lymph nodes were removed and CFU derived from vegetative cells versus spores were differentiated by quantifying samples with and without heat treatment (HT). Bars denote the mean and error bars represent the standard error of the mean. Significance was determined using Student's T-test. (A) Quantification of bacteria within the draining lymph node at 1, 12, and 24 hours post-infection (p.i.) from mice inoculated with 1×10^6 spores. There were no significant differences with or without heat treatment or between different time points using a total of six mice in three independent experiments. (B) Quantification of bacteria within the draining lymph node at 24 and 72 hours p.i.

with and without debridement (DB) performed at 12 hours after inoculation with 1×10^6 spores. Significant differences were observed in a total of six mice in three independent experiments between 24 hr and 24 hr DB (*, $p = 0.0144$) and 24 hr and 72 hr (**, $p = 0.0066$). There were no significant differences between heated and unheated samples at either time with or without debridement. (C) Bacteria within the lymph node were quantified similarly to A at 1, 12, and 24 hours p.i., but with an inoculation of 1×10^5 spores in a total of six mice in three independent experiments. There were no significant differences with or without heat treatment. (D) Bacteria within the lymph nodes were quantified similarly to A at 1 and 24 hours p.i., but instead, 1×10^6 spores of the mutant strain that produced no exotoxins (TKO) were inoculated in six mice in three independent experiments. There were no significant differences with or without heat treatment.

since they could be locally influencing the chemotaxis of potential Trojan horse cells, altering the activation state of innate immune defenses, or contributing to overall mortality even after the bacteria were surgically removed. At 12 hours, the earliest time of debridement, 458 ± 216 pg LF was isolated from the ear, 28 ± 10 pg in the draining lymph node, and 476 ± 82 pg/ml in the serum of mice that received 1×10^6 BIG23 spores subcutaneously (Table 2.1). When TKO spores were co-inoculated with purified LT (100ng LF + 650ng PA), levels of LF distributed into the ear, lymph nodes, and serum was similar to the LF actively produced by the exotoxin-producing BIG23. Both conditions had relatively equal proportions of the total LF distributed to the ear and serum and approximately one-twentieth of the quantity found in the cLN as in the ear and serum (Table 2.1). These LF amounts were assessed using a highly sensitive mass spectrometry-based assay for LF enzymatic activity that was originally designed to assess LF concentrations in serum (12), but was adapted here to study solid tissues. To date this is the most sensitive assay for detecting any of the components of the *B. anthracis* exotoxins and reflects total exotoxin production since the individual exotoxin components are coordinately regulated (128). Notably, the majority of debrided mice did not succumb to infection, even with measurable circulating exotoxins, implying that these concentrations of LF alone are not sufficient to mediate death. Likewise, when TKO spores were used to initiate infection, a similar number of spores was found in the cLN as wild-type Sterne strain bacteria during the same time period (Fig. 2.2D). This suggests that LT or ET does not affect spore entry into the cLN,

Table 2.1: Lethal Factor is measurable in the ear, draining cervical lymph nodes and serum at the time of debridement 12 hours after spore inoculation:

Strain	Ear^C	cLN^{CD}	Serum/ml^E
BIG23 ^A	458 ± 216	28 ± 10	476 ± 82
TKO + LT ^B	1592 ± 681	49 ± 13	2354 ± 223

^A Injection of 1×10^6 luminescent 7702 (BIG23) spores subcutaneously into left ear of 3 A/J mice

^B Injection of 1×10^6 triple exotoxin knockout (TKO) spores with 100ng LF plus 650ng PA into left ear of 3 A/J mice

^C LF detected by anatomic locations (pg/tissue ± SE) 12 hours post inoculation. Average of three separate experiments with three mice

^D Cervical lymph node

^E LF detected in the serum (pg/ml ± SE) 12 hours post inoculation. Average of three separate experiments with three mice

counter to what may have been predicted based on published cell culture analyses that demonstrated exotoxin-based alterations in phagocyte activation and chemotaxis towards lymph nodes (3, 55, 78, 138, 139).

Since exotoxins were present at the earliest time of debridement, we next asked whether they had any measurable effect on innate immune cell activation within the draining lymph nodes. Accordingly, spores from *B. anthracis* Sterne or the TKO mutant were injected subcutaneously into the left ear of mice at a dose of 1×10^6 spores and at 24 hours cLN were removed, homogenized, and stained for flow cytometric analysis. Expression of the activation markers CD69, CD80 and CD86 was chosen as measures of activation since previous publications have demonstrated that these cell markers are down regulated by *B. anthracis* exotoxins (19, 67, 157). Specifically, CD80 and CD86 are down regulated in dendritic cells (95, 157), and CD69 is down regulated in response to LT in T cells at 24 hours (67). Flow cytometry revealed that expression of CD69 and CD86, but not CD80, were significantly up-regulated in mice that had been infected with Sterne or TKO spores as compared to internal control lymph nodes (Fig. 2.3A to C). The degree of up-regulation was the same regardless of the ability of bacteria to produce exotoxin. cLN analyzed at 12 hours post-infection demonstrated no increase in CD69, CD80, or CD86 under any conditions (data not shown). These findings suggest that exotoxins are not present in the lymph node in sufficient quantities to alter cellular response to inflammatory stimuli in the first 24 hours of *B. anthracis* infection.

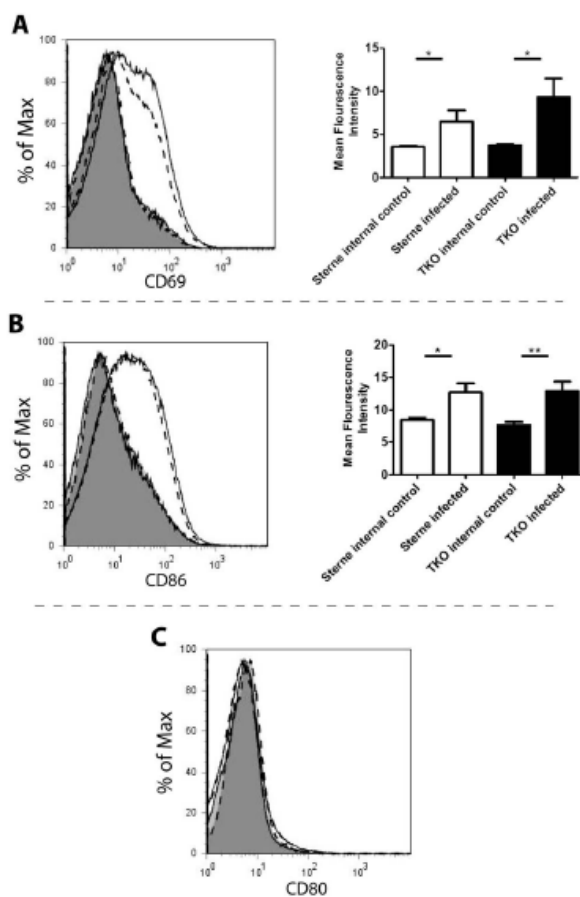


Figure 2.3: Presence of lethal factor in cervical draining lymph node does not alter cellular activation. Mice were infected with 1×10^6 Sterne strain or TKO spores subcutaneously in the left ear. At 24 hours cLN were taken from mice including: Sterne infected mice (solid line non-shaded) along with control non-infected contralateral lymph nodes from Sterne infected mice (solid line shaded), and TKO infected (dashed line non-shaded) and control non-infected contralateral lymph nodes from TKO infected mice (dashed line shaded). cLN were homogenized and cells were stained for flow cytometry. Flow plots were gated for single event live CD45 positive cells. (A) Left- a representative histogram comparing expression of CD69 in draining cLN. Right- The mean

fluorescence intensity of lymph nodes draining either Sterne (*, $p = 0.0464$) or TKO (*, $p = 0.0256$) infections from seven mice was significantly higher than contralateral control lymph nodes as determined using Student's T test. (B) Left- a representative histogram comparing expression of CD86 in draining cLN. Right- The mean fluorescence intensity of lymph nodes draining either Sterne (*, $p = 0.0119$) or TKO (**, $p = 0.0063$) infections from seven mice was significantly higher than contralateral control lymph nodes as determined using Student's T test. (C) A representative comparison of CD80 expression in draining cLN. The mean fluorescence intensity of lymph nodes draining either Sterne or TKO infections from seven mice was not significantly higher than lymph nodes that were not.

Discussion

Early events in *B. anthracis* infections are crucial in determining the ultimate outcome of infection. Antibiotic treatment can eliminate most vegetative bacteria growing in a host, yet frequently the sequelae of infection exacerbated by lingering exotoxins still lead to death (153). It is therefore vital that the early events in *B. anthracis* infections are better understood so that properly conceived therapeutic interventions can be administered to promote survival. The studies described above explored early events in subcutaneous *B. anthracis* infections and support the following major conclusions: 1) debridement can effectively reduce the mortality of subcutaneous infections in a mouse model of infection, and 2) early delivery of spores into the draining lymph nodes during subcutaneous infections is not sufficient to cause disseminated disease.

In addition to appropriate antimicrobial therapy, debridement has been an effective method in the management of certain soft tissue infections for over a century (124). The data derived from the mouse model of subcutaneous infection support the use of debridement as therapy for some cases of subcutaneous anthrax. This is because survival was significantly improved in mice debrided within 48 hours of infection, though it should be noted that debridement at 72 hours post-infection trended towards greater protection as well. These findings may have particular relevance to infections initiated by subcutaneous introduction of illicit drugs, such as those documented in Scotland in 2010 and Norway in 2000 (115, 118). To our knowledge, this is the first controlled experimental evidence to support debridement in anthrax-associated with soft tissues.

Although there are important caveats to using this approach, the major advantages offered by murine models of infection include the availability of genetically manipulated mice, and the extensive array of immunological reagents. Subsequent corroboration of that which was learned in mice to studies in non-human primates or retrospective studies where debridement was applied to human anthrax would ultimately be necessary to demonstrate practical utility in human anthrax. Likewise, it should not be overlooked that the model system applied in these studies utilizes a BSL2 *B. anthracis* Sterne strain that does not produce capsule. The lack of capsule production has been demonstrated to alter aspects of pathogenesis in mouse models of infection (53, 56). Some strains of capsulated exotoxin-producing *B. anthracis*, such as the Ames strain, do not require exotoxins to maintain full virulence in subcutaneous infection (152), yet others such as UT500 do require exotoxin production for full virulence (18). Thus, it is unknown how bacterial capsule production may affect the observations reported here, but should be addressed by future research.

As proposed by the Trojan horse model of infection, spores that enter the lymph nodes at the earliest stages of infection eventually cause the disseminated infection (60). This model would predict that removal of the site of infection by debridement after spores had entered the draining lymph nodes should have minimal effect on the outcome of infection, since these spores should establish a lethal infection. This was not observed, instead, mice were more likely to survive with debridement. A similar sequence of events would then unfold in the lymph node, such that when bacteria and/or exotoxins overcome its resistance

thresholds, the bacteria and exotoxins then spill into the lymphatics and blood to cause bacteremia and/or toxemia leading to eventual death. Indeed, *B. anthracis* exotoxins were detected at the site of infection, in the circulatory system and in the draining lymph nodes at 12 hours post-infection as described above. Thus, debridement may improve outcomes by simultaneously removing bacteria and eliminating the source of exotoxins that disperse to tissues not containing bacteria. That which defines the thresholds controlling the infection locally has not been clearly established, but likely includes effector cells of the innate immune response. This would imply that the immune status of the host is vital in defining the outcome of infection.

Considering the Trojan horse model, the improved survival with debridement was unexpected, especially considering that the primary inoculation dose would have been lethal otherwise. However, the totality of results presented above for the cLN provides evidence that supports a different mechanism of dissemination in subcutaneous infections. Approximately 4% of the spores that were inoculated subcutaneously could be isolated from the draining cervical lymph node within 1 hour of infection. The number of spores in the lymph node remained unchanged for the first 24 hours and then decreased by more than a log by 72 hours. At no point were vegetative bacteria detected in the cLN during this time course. Spores are resistant to immune cell killing until they germinate (68), thus the constant number of spores detected over the first 24 hours in undebrided mice may represent either a static population of spores or a dynamic balance achieved by the influx of new spores countered by germination and rapid

killing of nascent vegetative bacteria. A significant decrease in spores was detected in the cLN at 24 hours after debridement at 12 hours, which supports the second scenario, where total spore counts represent a balance between influx and destruction.

Another unexpected finding was that early exotoxin production had no effect on the ability of spores to enter or persist in the lymph nodes or activate immune cells. The Sterne strain and the TKO mutant showed no significant differences in bacterial CFU in the lymph nodes at any point. TKO and Sterne strains also activated cells within the lymph nodes equivalently, despite evidence for production of exotoxins in the tissues by the Sterne strain after infection. This was unexpected because ET has been proposed to promote the chemotaxis of phagocytes towards lymph nodes (44, 78, 95) and LT has been extensively characterized for its ability to modulate the immune system (3, 55, 138). For these reasons, we predicted that a greater number of spores from an exotoxin-producing strain would be found in the lymph nodes. We also hypothesized that there would be a less robust immune response characterized by the expression of fewer activation markers by cells within the lymph nodes. In the context of a subcutaneous infection, our data do not support these roles for the exotoxins, especially since measurable exotoxin was present at the time of debridement at 12 hours post-infection. The cause of this discrepancy is unclear but may reflect the fact that the quantities and timing of the addition of exotoxins in previously published systems may not accurately represent those during an active infection *in vivo*. Indeed, the concentrations of LF detected in the model described above

are orders of magnitude lower than those measured in the serum of Rhesus macaques two to four days post-inhalation of spores (12). The serum of these monkeys contained LF in the hundreds of nanogram per milliliter range, which is closer to the concentration of LF typically used in cell culture assays assessing the effects of LT on cellular functions. It thus may follow that the reported effects of *B. anthracis* exotoxins on cells of the immune system better represent phenomena in later stages of infection rather than the early stages of infection that were explored in this study. In total these data suggest that during the first day post-inoculation the host response in the lymph nodes, 1) is not affected by the presence or absence of the anthrax exotoxins as indicated by the measures described above, and 2) is effective at eliminating *B. anthracis*.

The observation that the lymph nodes are the site of considerable host defense is not surprising in view of the fact that they consist of a diverse collection of immune effector cells. It does raise some doubt that Trojan horse phagocytes carry sufficient spores to the lymph node at the early stages of infection to suppress the lymph node defenses. All indications from this study are that the lymph node is an effective bulwark against systemic infection unless the initial site of infection continues to feed bacteria and/or spores and exotoxins into the lymph node. Thus the early movement of spores into the lymph nodes in subcutaneous infection, either by phagocyte transport or as extracellular bacteria, is unlikely to have a significant effect on the ultimate outcome of the infection.

In summary, this study describes the first animal model system to experimentally assess debridement as a method of treating subcutaneous anthrax. In addition, the debridement model was readily applied to exploring basic aspects of subcutaneous *B. anthracis* infection. In particular it was effective at assessing the most common model explaining early stages of *B. anthracis* infection, whereby spores are seeded into the draining lymph node where they grow and eventually cause disseminated disease. The data acquired from this analysis suggest that spores initially entering the draining lymph nodes have less of an influence on the ultimate disseminated disease than those spores that germinate and multiply at the initial site of inoculation.

Materials and Methods

Ethics Statement: All mouse husbandry and manipulation were performed following protocols approved by the University of Virginia Animal Care and Use Committee (protocol #3671) conforming to AAALAC International accreditation guidelines. When at all possible we have strived to replace the use of animals in our studies with *in vitro* or non-invasive assays, reduce the number of animals utilized, and refine our use of animals to minimize their suffering and maximize the data extracted from each experiment.

Bacterial Strains and growth conditions: *B. anthracis* Sterne strain 7702 was obtained from BEI Resources (Manassas, VA). The *B. anthracis* Sterne 7702 strain with deletion of the *pagA*, *lef*, and *cya* genes (referred to in the text as the triple exotoxin knockout or TKO) was graciously provided by Dr. Scott Stibitz from the Center for Biologics Evaluation and Research, Food and Drug

Administration (73). BIG23 was constructed by integrating plasmid pIG6-19, a kind gift from Michele Mock at the Pasteur Institute, into *B. anthracis* strain 7702 using previously described conjugative methods (56). The resultant BIG23 expressed the *luxABCDE* genes from *Photobacterium luminescens* under the control of the protective antigen promoter, therefore the vegetative cells of this strain as luminescent when growing with the host. Spores of each *B. anthracis* strains were generated on NBY 5 µg/ml erythromycin agar plates with subsequent purification on an Omnipaque (GE Healthcare, Inc., NJ) gradient as previously published (56).

Mouse infection: 4-12 week old female A/J mice were obtained from Jackson labs, or bred in specific pathogen-free conditions within vivaria at UVA. Mice were anesthetized with 3% isoflurane (Piramal Healthcare, Andhra Pradesh, India) mixed with oxygen using an Isotec 5 vaporizer (Absolute Anesthesia, Piney River, VA). Purified *B. anthracis* spores at a dose of 1×10^6 or 1×10^5 spores in 10 µl PBS (Invitrogen, Carlsbad, CA) were injected subcutaneously in the left ear using a 0.5 cc insulin syringe as previously published (56).

Lymph node isolation: At designated time points infected mice were euthanized and lymph nodes were surgically removed and placed in sterile PBS on ice. The left cervical lymph node from the infected side of the mouse was harvested as the experimental sample and the right lymph node was harvested as an internal control. The location of the lymph node draining the subcutaneous compartment of the left ear was established by injecting India ink in the same manner as the spore inoculum and then identifying which lymph node turned black (142). Only

one cervical lymph node turned black and subsequent analysis found CFU solely within this lymph node. No other cervical lymph nodes turned black or contained CFU at early stages of infection, suggesting that only the lymph node that directly drains the subcutaneous compartment was infected by *B. anthracis* and not other lymph nodes or surrounding tissues.

Tissue CFU determination: Lymph nodes were isolated as previously described, immediately stored on ice, and dissociated by grinding between two glass slides. Cells were lysed in distilled water for 15 minutes on ice. Serial dilutions were performed in 1x sterile PBS on ice. Samples were plated onto BHI agar plates, and incubated at 37 °C overnight. Determination of dormant spores' verses vegetative bacilli was established by placing samples in a 65°C water bath for twenty minutes to kill vegetative bacteria but leave dormant spores unaffected.

Flow cytometry staining: Single cell suspensions of individual lymph nodes were resuspended in 100 µl flow cytometry staining buffer (1xPBS 3% FBS 0.05% Sodium Azide). Fc receptor-blocking antibody (CD16/32, eBioscience San Diego, CA) was added and incubated on ice for thirty minutes. Samples were centrifuged and resuspended in 100 µl flow staining buffer. Antibodies against specific cell surface markers were added, incubated for one hour on ice, and then washed. Samples were then fixed overnight with 4% paraformaldehyde at 4°C. Antibodies used were: anti-Ly6C FITC (RB6-8C5, BD Biosciences), anti-CD86 PE (PO3.1, eBioscience San Diego, CA), anti-CD11b APC (M1/70, eBioscience), anti-MHC II PacBlue (M5/114.15.2, eBiosciences), anti-CD80 PE

Cy5 (16-10A1, eBioscience), anti-CD69 PE Cy7 (H1.2F3, eBioscience), and anti-CD45 Alexa780 (30-F11, eBioscience). Live/Dead staining was performed with fixable Aqua Dead Cell Stain kit (Invitrogen).

Infection monitoring and luminescent imaging: In order to monitor the progression of infections using luminescent BIG23, mice were anesthetized using 3% isoflourane mixed with oxygen from the XGI-8 gas anesthesia system supplied with a Xenogen IVIS Spectrum. Images were acquired as previously reported and analyzed using Living Image software (version 2.50.1, Xenogen) (56). Once any detectible luminescent signal was detected in a vital organ, or a mouse appeared moribund, mice were euthanized per animal use protocol and scored as dead in the survival assays.

Measurement of Lethal Factor concentration in tissue samples: Mice were infected with 1×10^6 spores of BIG23 spores or TKO spores with 100ng LF (*B. anthracis* recombinant exotoxin, BEI Resources) + 650ng PA (*B. anthracis* recombinant exotoxin, BEI resources) subcutaneously in the left ear. At 12 hours ears, draining cervical lymph nodes, and blood were removed from infected mice and samples were placed on ice. Then 100 μ l of cell lysis cocktail consisting of 0.2% Triton X-100 (Promega), 0.56mg/ml Pefablock (AppliChem. Darmstadt, Germany), 3.125mg/ml 6-aminohexanoic acid (Spectrum chemical. Brunswick, NJ), 0.3125mg/ml Antipain (VWR. West Chester, PA), and 22 μ g/ml of E64-D (Cayman Chemical. Ann Arbor, MI) in PBS were added to samples. Samples were then homogenized using kontes pellet pestles (Fisher Scientific. Waltham, MA). Samples then sat on ice for 1 hour. Samples were then spun down and

supernatants were removed and stored at -80 C. Blood samples were allowed to clot for 20 minutes then spun down to collect serum, which was then stored at -80° C. Quantification of LF was performed using matrix assisted laser desorption/ionization (MALDI) time of flight (TOF) mass spectrometry (MS) to detect peptide cleavage products generated by LF as previously described (12).

Statistical Analysis

All statistical analysis and was performed using GraphPad Prism software (version 5, GraphPad Software, San Diego, CA) with log rank test for survival studies, and unpaired t-test for differential CFU in draining lymph node.

**Chapter 3: Circulating lethal toxin decreases
the ability of neutrophils to kill vegetative
Bacillus anthracis by preventing the
oxidative burst**

Introduction

PMNs are among the first cells to arrive at sites of bacterial and fungal infections (10, 151). PMNs are terminally differentiated cells which do not divide or synthesize large amounts of RNA or proteins (132). PMNs have short half lives in circulation, although reports vary suggesting anywhere between 1.5 to 12.5 hours in mice and 8 hours to five days in humans (82). However, when exposed to inflammatory stimuli PMNs will become activated increasing their half life substantially (25).

PMNs are capable of killing both intracellularly and extracellularly by NADPH oxidase-dependent and -independent mechanisms (82). The NADPH oxidase complex used by PMNs to produce superoxide consists of three cytosolic proteins, p47 phox, p67 phox, and rac, as well as two membrane proteins, gp91 phox and p22 phox (43). Upon induction by phagocytosis or engagement of cellular receptors with pathogen-associated molecular patterns (PAMPs) the complex will assemble and start the process of reducing O_2 into $\cdot OH$ radicals (43). PMNs are capable of producing a much stronger oxidative burst than other phagocytes, attributed to the ability to recruit a greater number of NADPH oxidase complexes to the phagosome (105). In addition to NADPH oxidase, PMNs also produce Myeloperoxiase, which generates hypochlorous acid from chloride and hydrogen peroxide (11). In addition to oxidative burst, PMNs possess granules which contain an array of antimicrobial effectors including cathepsins, lysozyme, and defensins (11). PMNs contain three different types of granules: azurophilic (primary), specific (secondary), and gelatinase

(tertiary), each of which are defined by their contents and degree of activation necessary to initiate exocytosis (10). These granules can either fuse to a phagolysosome to aid internal killing or be exocytosed to kill bacteria extracellularly (82).

In the context of *B. anthracis* infections, it is becoming increasingly clear that PMNs play an important role in bacterial clearance and delaying time to death (28, 29, 102). In addition to studies utilizing monoclonal antibody and chemical depletion of PMNs in mice, PMNs have been shown to surround tissues infected by *B. anthracis* during cutaneous infections in humans, dogs, and pigs (13, 101). However it is clear by high mortality rates reported for all forms of anthrax that *B. anthracis* effectively counteracts the PMNs response during the course of many infections (15). While there is robust literature examining the effects of *B. anthracis* LT on various tissue systems and cellular subtypes such as alveolar macrophages, endothelial cells, T cells, and NK cells, comparatively little has been explored regarding toxins' affects on PMNs, and what has been reported is contradictory across publications (91, 108). In human PMNs, LT was found to prevent fMLP receptor-mediated, but not PMA-induced, oxidative burst. Another study published contrary results, finding that C57Bl/6 mouse PMNs isolated from LT-intoxicated mice displayed increased oxidative burst in response to PMA (30, 156). Neither of these studies linked alterations in oxidative burst to a defect in PMN's ability to kill *B. anthracis*. Human PMNs may not require oxidative burst to kill *B. anthracis*, since they are capable of killing through use of α -defensin, which mouse PMNs do not possess (41, 98). Previous studies have

also noted that treatment of human PMNs with LT *in vitro* leads to a defect in actin polymerization in the context of PMN migration towards fMLP (40). While this study focused on the role of actin polymerization during PMN migration, the defects in actin polymerization described could also result in a defect in phagocytosis.

We reported in chapter two that LF can be found circulating in the blood stream of infected mice 12 hours post subcutaneous *B. anthracis* spore inoculation. At this time the bacteria have not spread from the initial site of inoculation into the draining lymph node (149). Since LT, and not ET, is necessary for *B. anthracis* Sterne infection to progress from the initial inoculation site into deeper tissues (90), circulating LT may thus function to dampen the host innate immune response at the systemic level. In this study we use unique and comprehensive methods to establish the levels of circulating LF throughout *B. anthracis* infection. We found that sub-lethal quantities of circulating LT diminish PMN's ability to kill vegetative bacilli *in vitro*. We then determined that mouse PMNs require oxidative burst and phagocytosis in order to kill vegetative TKO, and that circulating LT attenuates oxidative burst. The experiments presented here are the first to address how circulating *B. anthracis* LT influences immune cell function remotely from an infection site, avoiding some pit falls of *in vitro* intoxication studies.

Results

LF levels increase in major organs over time during *B. anthracis* infection

While we previously reported that LF can be found in measurable amounts in the serum of mice as early as 12 hours post infection, the concentration of LF in circulation and in organs throughout infection has not been defined (149). Our studies rely on the mouse model of infection, which has many advantages over other animal models, such as the availability of a wide variety of genetic tools, and a BSL2 infection system using the Sterne strain of *B. anthracis* that lacks pX02 (57). The range of biologically relevant LF levels was determined in both serum and organs throughout infection in 6-8 week old female AJ mice. Mice were infected subcutaneously in the left ear with 1×10^6 spores of BIG23, a *B. anthracis* Sterne strain that emits light when producing toxins within a host as vegetative bacilli. Infection and dissemination were then monitored via bioluminescence. *B. anthracis* infection is asynchronous and time to death can vary by multiple days despite identical spore doses administered within a small time-frame (56, 90). Because of this, the stage of infection cannot be established solely by the passage of time, and must instead be defined by the stage of infection as indicated by the location of bacterial bioluminescence within the mouse. Early infection is defined as when luminescence representing vegetative bacilli can only be detected at the initial site of inoculation (Fig. 3.1). The mid stage of infection occurs when luminescence has spread to the regional draining lymph node. The late stage of infection is when luminescence can be detected in the kidneys, a time when we have determined mice are bacteremic. At each stage of infection, serum and major organs were removed for quantification of LF with a mass spectrometry-based assay, as previously reported (12). At the early

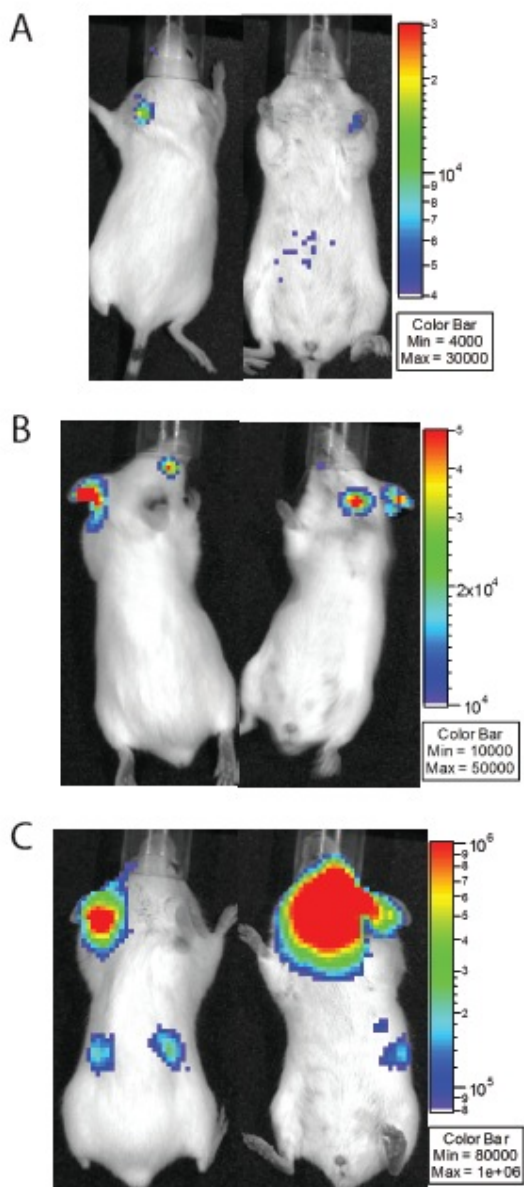


Figure 3.1: Three defined stages of *B.*

***anthracis* infection.** (A-C) Black and white photos of a single A/J mouse injected subcutaneously in the left ear with 1×10^5 luminescent *B. anthracis* Sterne strain (BIG23) spores, overlaid with a false color representation of photon emission intensity as indicated by the scale on the right in p/s/cm²/sr at different stages of infection.

(A) Early stage of infection defined by vegetative bacilli, represented by luminescence, being confined to the initial site of spore inoculation. (B) Mid stage of infection defined by vegetative bacilli spread to the regional draining lymph node. (C) Late stage infection defined by bacterial spread to the kidneys.

stage of infection, LF was found primarily in the infected ear extracts (4.57 ± 4.13 ng/ml) containing vegetative bacilli, circulating in serum at 0.89 ± 0.55 ng/ml, and at very low levels in extracts from most of the major organs where luminescence was absent ($\leq 0.07 \pm 0.02$ ng/ml) (Table 3.1). At the mid-stage of infection when luminescence is found in the draining lymph node, there was a corresponding increase in LF levels in the infected lymph node extracts (33.36 ± 10.61 ng/ml). LF concentrations were similarly elevated in serum and infected ear extracts, and had low levels in all other organs sampled (Table 3.1). In the late stage of infection, high concentrations of LF were detected in all sampled organs, with highest levels (1973.92 ± 1725.4 ng/ml) observed in the serum (Table 3.1). LF was not quantified in kidneys due to interferences from high levels of proteases in this tissue.

Circulating LT attenuates PMN's ability to kill vegetative *B. anthracis*

Human PMNs kill vegetative bacilli through deployment of α -defensins (98). Mice, however, lack α -defensins (41). Despite this, PMNs isolated from mice after being elicited using injections of sterile starch *in vivo*, were capable of phagocytosing and killing Sterne strain *B. anthracis in vitro* (151). Mouse PMNs are vital for the clearance and control of *B. anthracis* infections since pharmacological or antibody depletion of PMNs raises the severity of outcome to infection (29, 88). The ability of mouse PMNs that have not been elicited by starch to kill vegetative bacilli *in vitro* was determined. PMNs from six-week-old C57BL/6 female mice were isolated from femur bone marrow and mixed with

Table 3.1: LF levels increase in all major organs over time during *B. anthracis* infection

Sample	Early infection^A	Mid infection^A	Late infection^A
Serum	0.89±0.55	27.33±18.18	1973.92±1725.4
Infected ear	4.57±4.13	37.16±25.03	586.53±126.83
Control ear	0.03±0.01	0.13±0.06	5.11±2.43
Infected lymph	0.02±0.01	33.36±10.61	667.64±378.4
Control lymph	<LOD ^B	0.11±0.05	93.89±77.78
Heart	0.07±0.02	4.08±3.72	85.89±71.58
Lungs	0.05±0.02	1.78±1.55	207.48±163.02
Spleen	0.04±0.01	0.46±0.34	107.75±80.50
Liver	0.05±0.02	8.36±7.98	760.65±335.64
Right bone marrow	<LOD ^B	0.15±0.10	27.68±24.42
Left bone marrow	<LOD ^B	0.13±0.09	22.27±17.10
Brain	<LOD ^B	0.10±0.05	46.51±31.32

^A Injection of 1×10^5 spores of luminescent 7702 (BIG23) spores subcutaneously into the left ear of three A/J mice. Samples were collected and processed when mice reached the indicated stage of infection, LF values reported in ng/ml \pm SE

^B Samples below the limit of detection for LF (0.005 ng/ml) were labeled <LOD.

opsonized TKO to eliminate the confounding influence of secreted toxins while establishing the assay. PMN bactericidal activity was assessed by determining bacterial colony-forming units over a time course of one and a half hours in PMN-exposed and bacteria-only controls (Fig. 3.2A). One and a half hours was the maximum time for determining differences since significant TKO growth occurred after this time, making interpreting results difficult. At one and a half hours the CFU of the TKO bacilli dropped by 65% in the presence of PMNs, compared to samples without PMNs where CFU increased 46% above initial inoculum (Fig. 3.2A).

The reported inability of toxin-producing *B. anthracis* strains to alter *in vitro* PMN bactericidal function (98) may be due to an insufficient concentration of LT. This would occur during the time course of the cell culture assay if *B. anthracis* could not produce enough toxin. Likewise, the time required for cells to manifest the biological effects of intoxication may also be an issue. Previous reports have concluded that PMNs must be exposed to LT for at least 2 hours *in vitro* for any measurable defects to manifest (40). The short lifespan of circulating PMNs (approximately 6.5 hours in humans) (97), and the similar half-life of PMNs outside the host (114), the length of time needed for mouse PMNs incubation with LT *in vitro*, may make it difficult to assess the effect of LT on PMN function. We previously found that in the subcutaneous mouse model of *B. anthracis* infection, LF can be found in measurable amounts in serum after 12 hours (149), prior to measurable bacteremia. This finding leads to the possibility that circulating toxins emanating from the site of infection may be capable of

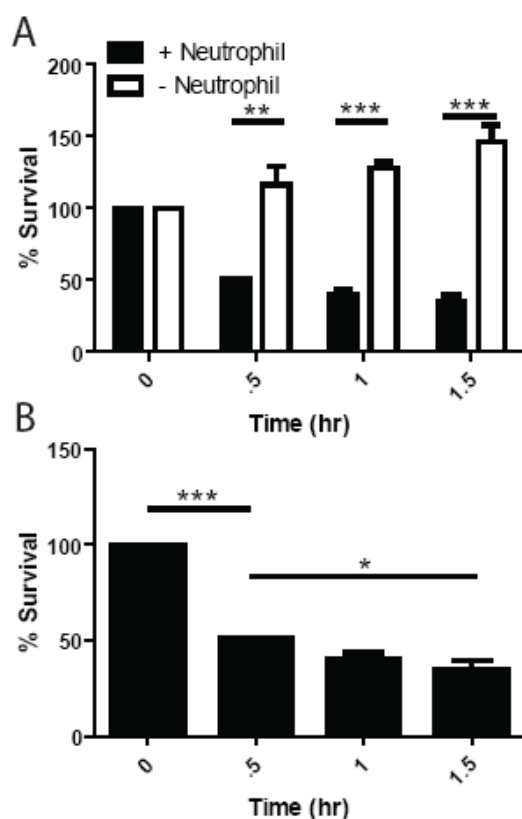


Figure 3.2: Mouse PMNs kill vegetative *B. anthracis*. (A and B) PMNs isolated from C57B/6 mice were inoculated with vegetative *B. anthracis* at an MOI of 1:1 and incubated at 37°C. At indicated time points samples were put on ice and mixed with 0.1% Saponin for 10 min. Samples were then serially diluted and plated for enumeration on LB agar. (A) Comparison between samples where TKO alone and TKO mixed with PMNs with significant differences at 0.5 hr (**, $p=0.0072$), 1 hour (***, $p=0.0001$), and 1.5 hour (***, $p=0.0001$). (B) PMN reduction of TKO CFU over time with significant differences between 0 and 0.5 hours (***, $p<0.0001$) and 1.5 hours (*, $p=0.0252$). $n=3$ mice per condition.

manipulating the innate immune system in sites distal from areas with bacterial growth.

Due to the variability of circulating LF levels of mice infected with *B. anthracis*, LT was injected intraperitoneally (i.p.) to ensure PMNs received consistent exposure to LT. Serum and bone marrow LF concentrations were determined in C57Bl/6 mice 24 hours post injection of 1.56 μ g LT (1.56 μ g LF + 3.12 μ g PA), 6.25 μ g LT (6.25 μ g LF + 12.5 μ g PA), and 6.25 μ g LF (Table 3.2). The measured LF concentrations from LT-injected mice were much less variable between animals compared to LF levels measured during bacterial infections. For example, LF was measured as 1.25 ± 0.32 ng/ml in serum of mice injected 24 hours previously with 6.25 μ g LT had a lower standard error compared to 1.78 ± 1.55 ng/ml in the lungs of mid-stage infected mice (Table 3.1). The results also showed that a 1.56 μ g injection of LT yielded circulating LF levels similar to those found during early infection, and an injected dose of 6.25 μ g LT was 10-fold higher than observed for 1.56 μ g LT injections but lower than LF levels found in the mid stage infection. The addition of PA decreases the concentration of LF in serum, presumably due to PA binding LF causing cellular internalization. Mice injected with LF only had 10-fold higher levels of LF in serum compared to LT injected mice, while levels measured in the bone marrow were equivalent (Table 3.2). To confirm that LT injected into a mouse is active in bone marrow PMNs were isolated and a western blot to detect MEK3 cleavage was performed, which observed MEK3 cleavage 24 hours post-injection (Fig. 3.3).

Table 3.2: LF concentration after injection of purified toxin components are consistent with levels found during active infection

Sample	1.56μg LT^{AB}	6.25 μg LT^{AC}	6.25 μg LF^{AD}
Serum	0.10 \pm 0.08	1.25 \pm 0.32	19.43 \pm 1.13
Right bone marrow	<LOD ^E	0.04 \pm 0.01	0.04 \pm 0.01
Left bone marrow	<LOD ^E	0.03 \pm 0.01	0.04 \pm 0.01

^A LF concentrations reported in ng/ml \pm SE

^B Three C57Bl/6 mice were injected with 1.56 μ g LT (1.56 μ g LF + 3.12 μ g PA) in 100 μ l PBS i.p. and indicated samples measured for LF concentration 24 hours post intoxication.

^C Three C57Bl/6 mice were injected with 6.25 μ g LT (6.25 μ g LF + 12.5 μ g PA) in 100 μ l PBS i.p. and indicated samples measured for LF concentration 24 hours post intoxication.

^D Three C57Bl/6 mice were injected with 6.25 μ g LT in 100 μ l PBS i.p. and indicated samples measured for LF concentration 24 hours post intoxication.

^E Samples below the limit of detection for LF (0.005 ng/ml) were labeled <LOD.

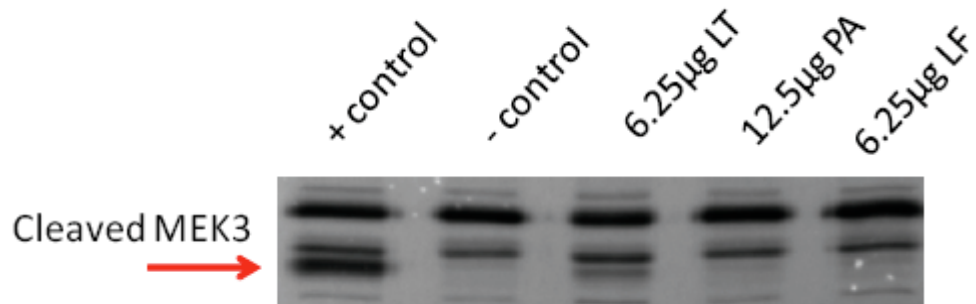


Figure 3.3: Injected LT is enzymatically active in PMNs isolated from mouse bone marrow. Western blot analysis determined LT was acting on PMNs to cleave MEK3 *in vivo* before cell isolation, when mice were injected with indicated amounts of LT, LF, or PA. 1×10^6 PMNs were isolated 24 hours post injection. Positive control PMNs were treated *in vitro* with LT for 2 hours.

In order to determine if *in vivo* LT-intoxicated PMNs displayed a defect in the ability to kill vegetative TKO, LT was injected i.p. in mice and PMNs were isolated 24 hours post-intoxication as before, and the ability to kill vegetative bacilli were compared to that of non-intoxicated PMNs *ex vivo*. Significant differences in TKO CFU between unintoxicated PMNs and LT-treated PMNs were measured. A dose of 6.25 μ g of LT permitted 84% of the bacteria to survive after 1.5 hours, and 54% of the bacteria survived when a dose of 1.56 μ g LT was administered as compared to 35% survival with unintoxicated PMNs (Fig. 3.4A). At a dose of 0.1 μ g LT no statistically significant differences were seen from unintoxicated control PMNs. Treatments with LF or PA alone also resulted in no significant differences when compared to untreated PMNs (Fig. 3.4B). Purified PMNs were analyzed for differences in viability by flow cytometry after 24hr after injection of 6.25 μ g of LT. No differences were found when compared to non treated control mice indicating the PMN's viability was not affected by LT (Fig. 3.5). Next we wanted to assess how long the effects of circulating LT on PMNs persist. Mice were injected i.p. with 6.25 μ g LT and PMNs were harvested at 24, 48, and 72 hours post-administration to assess their ability to kill vegetative TKO. At 48 hours-post treatment with 6.25 μ g LT PMNs demonstrated no attenuation in their ability to kill vegetative TKO, after 72 hours no differences were seen compared to untreated PMNs (Fig. 3.4C).

Mouse PMNs require oxidative burst to kill vegetative *B. anthracis*

Human PMNs utilize α -defensin to kill vegetative *B. anthracis* (98), mice however, lack α -defensin (41). Despite this, mouse PMNs effectively kill

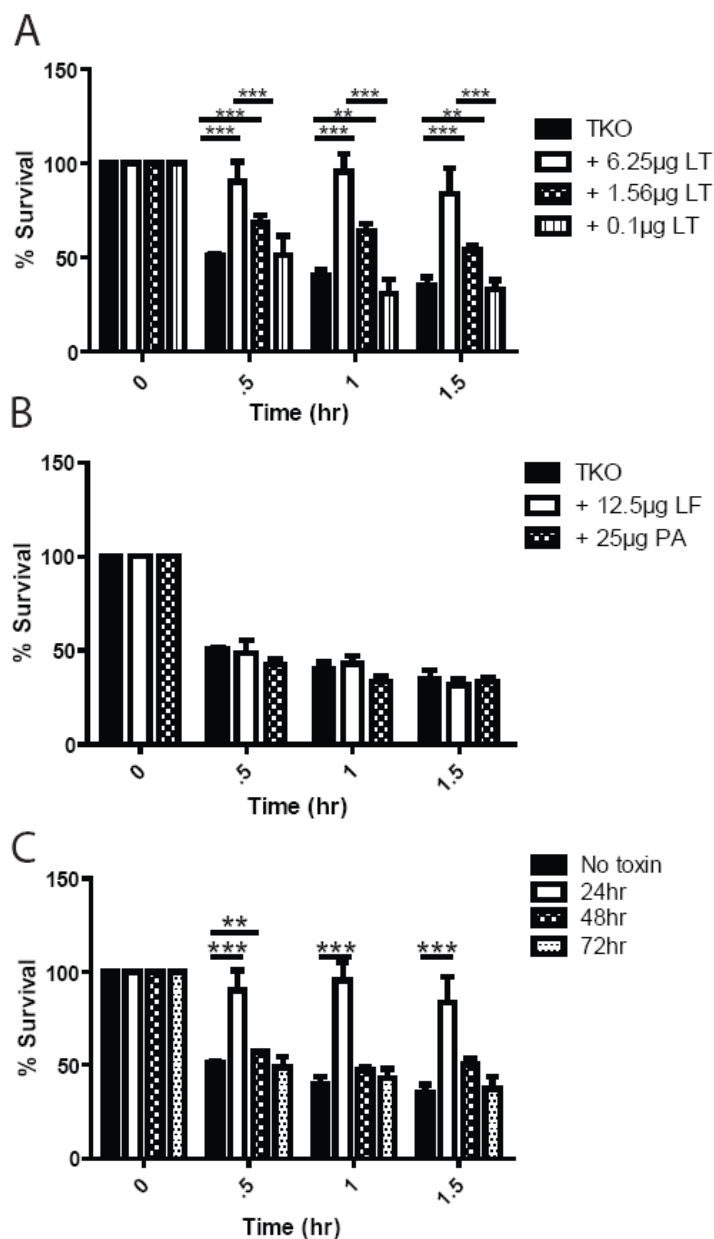


Figure 3.4: Circulating LT attenuates PMNs killing of vegetative *B. anthracis*.

(A-C) C57Bl/6 mice were injected with toxin components (LF, PA) and PMNs were isolated at the indicated times. PMNs were then inoculated with TKO at an MOI of 1:1 and incubated at 37°C. At indicated time points samples were put on ice and mixed with 0.1% Saponin for 10 min and vigorously mixed by pipetting. Samples were then serially diluted and plated for enumeration on LB

agar. (A) Mice were injected i.p. with the indicated doses of LT, PMNs were isolated at 24 hours post injection and CFU were determined at indicated time points. Significant differences in % CFU over time were found between TKO alone and + 6.25 μ g LT (0.5 hour *** $p < 0.0001$, 1 hour *** $p < 0.0001$, 1.5 hour *** $p < 0.0001$), TKO alone and + 1.56 μ g LT (0.5 hour *** $p = 0.0003$, 1 hour ** $p = 0.0025$, and 1.5 hour ** $p = 0.0026$), and 6.25 μ g LT and 1.56 μ g LT (0.5 hour *** $p = 0.0005$, 1 hour *** $p = 0.0003$, and 1.5 hour *** $p < 0.0001$). (B) Mice were injected i.p. with LF or PA, PMNs were isolated 24 hours post injection and CFU were determined at indicated time points. (C) Mice were injected with 6.25 μ g LT and PMNs were isolated at 24, 48, and 72 hours. Significant differences were found between TKO and PMNs treated for 24 hours (for P-value ranges see 3A), and at 0.5 hour between no toxin and 48 hour LT treatment (**, $p = 0.0021$). $n = 3$ mice per condition.

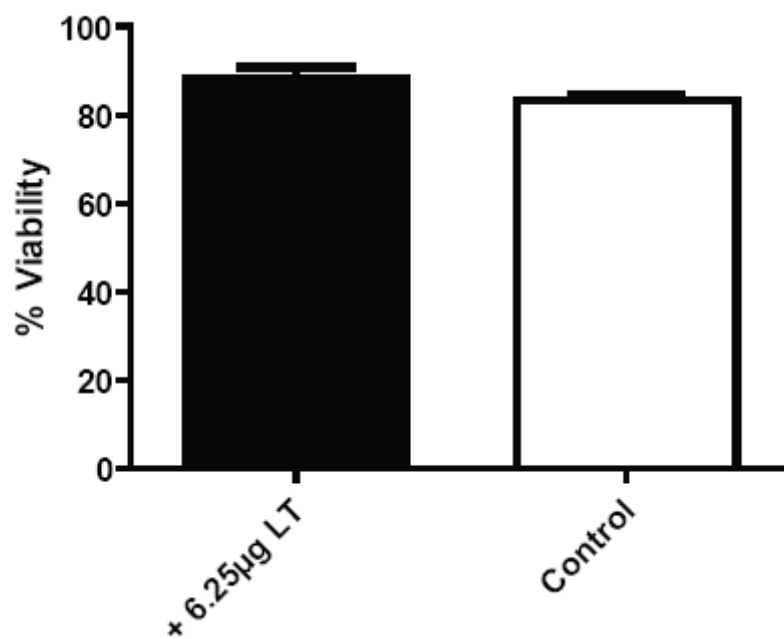


Figure 3.5: Circulating LT does not decrease viability of bone marrow

PMNs. C57Bl/6 mice were injected with 6.25µg of LT and PMNs were isolated from the bone marrow of intoxicated and non-intoxicated mice 24 hours later. Cells were then stained for flow cytometry with Aqua Dead Cell Stain kit. PMNs were gated for by Ly-6G and side scatter, the bar graph represents % viability of cells in that subset. No significant differences were detected ($p>0.05$). $n=3$ mice per condition.

vegetative TKO in *in vitro* killing assays. In order to determine if human and mouse PMNs are similarly bactericidal, or if lack of α -defensin by mouse PMNs leads to a lesser degree of killing, mouse PMNs were isolated from the bone marrow of C57Bl/6 mice or human venous blood. PMNs were then mixed with freshly opsonized TKO. PMN bactericidal activity was indicated by reduction in TKO CFU over the course of one and a half hours. No statistical difference between mouse and human PMN killing of vegetative TKO *in vitro* was found (Fig. 3.6). PMNs are capable of killing bacteria by production of reactive oxygen species (ROS) as well as antimicrobial peptides (10). *B. anthracis* demonstrates some resistance to ROS because it encodes for four separate superoxide dismutases (SODs) which are capable of detoxifying oxidative free radicals produced by NADPH oxidase (109, 140). There is some debate as to the role of these SODs in *B. anthracis* infection. One study demonstrated that the deletion of a single SOD gene results in no difference in virulence (31), but in a different study Passalacqua and Bergman demonstrated that deletion of *soda1* resulted in a decrease of virulence (109). However, deletion of all four SODs is associated with a major loss of virulence in an inhalational Sterne strain model of infection (31). In order to determine if oxidative burst is the mechanism by which mouse PMNs kill *B. anthracis*, two different approaches were taken. The first was isolating and analyzing the bactericidal activity of PMNs isolated from gp91^{phox} ^{-/-} knockout mice (112), which are unable to form the NADPH oxidase complex, in comparison to wild type C57Bl/6 PMNs (Fig. 7A). Secondly, WT C57Bl/6 PMNs were treated with a chemical inhibitor of NADPH oxidase, diphenylene iodonium

(DPI) (Fig. 3.7B). When the PMN's oxidative burst was inhibited genetically or DPI-treated there is a resultant statistically significant decrease in the ability of PMNs to kill vegetative TKO, where DPI treated PMNs have 76% survival, and $gp91^{\text{phox}^{-/-}}$ PMNs had 91% survival at one and a half hours compared to 35% survival in control PMNs (***, $p < 0.001$) (Fig. 3.7A). PMNs treated with DMSO as a vehicle control for DPI demonstrated no significant difference in killing ability versus WT PMNs (Fig. 7B). In order to determine if human PMNs require oxidative burst to kill vegetative bacilli human PMNs were treated with 10 μ M DPI and incubated with TKO. As reported previously (98), inhibition of NADPH oxidase in human PMNs with DPI resulted in no defect in their ability to kill *B. anthracis* (Fig. 3.7C).

Circulating LT prevents TKO-induced oxidative burst

Since mouse PMNs use oxidative burst to kill vegetative bacilli and circulating LT is capable of preventing bacilli from being killed *in vitro* the effects of LT on oxidative burst were assessed. Previous studies have examined the effects of LT on PMN oxidative burst with mixed conclusions. Crawford et al. found that human PMNs treated with LT *in vitro* exhibited a defect in producing oxidative burst in response to stimulation by fMLP, but had no defect when stimulated with PMA (30). This defect was reportedly due to inhibition of p38 and MEK1, which were cleaved by LT (38). However Xu et al. found that C57Bl/6 PMNs isolated from mice intoxicated i.p. with LT had increased oxidative burst after stimulation with PMA *in vitro* (156). Data presented in figure 3.4 used much lower doses of LT injected i.p. than those reported by Xu et al., whose work

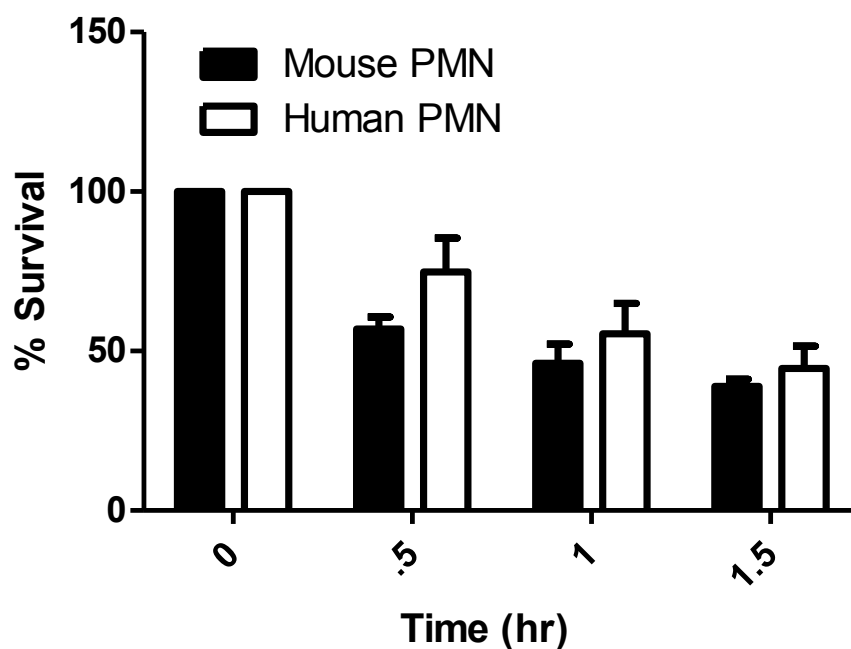


Figure 3.6: Human and mouse PMNs kill vegetative TKO to a similar degree.

PMNs were isolated from C57Bl/6 mice and human venous blood were inoculated with vegetative *B. anthracis* at an MOI of 1:1 and incubated at 37°C. At indicated time points samples were put on ice and mixed with 0.1% Saponin for 10 min. Samples were then serially diluted and plated for enumeration on LB agar. No significant differences were seen between any time points ($p > 0.05$). (n=3)

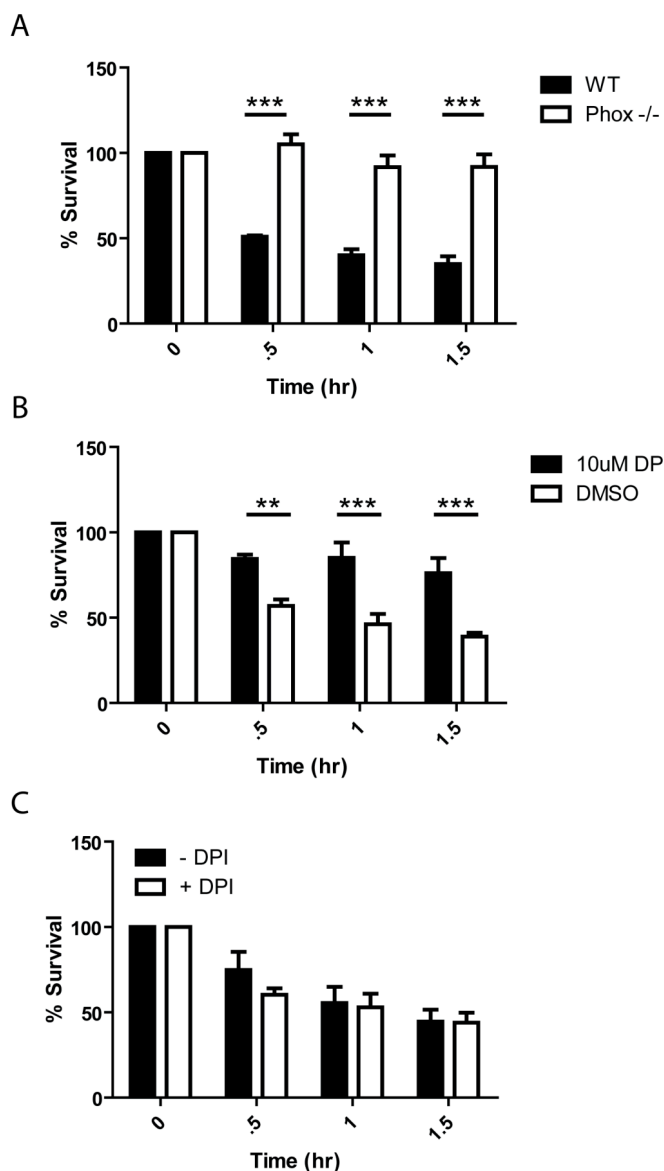


Figure 3.7: Oxidative burst is required for mouse PMNs to kill vegetative TKO. (A-B)

PMNs were isolated from C57B/6 mice, gp91^{phox-/-} mice, and human venous blood were inoculated with vegetative TKO *B. anthracis* at an MOI of 1:1 and incubated at 37°C. At indicated time points samples were put on ice and mixed with 0.1% Saponin for 10 min. Samples were then serially diluted and plated for enumeration on LB agar. (A)

Comparison of PMN's killing ability between WT C57BI/6 mice and C57BI/6 gp91^{phox-/-} mice. Significant differences in % survival of TKO were seen at 0.5, 1, and 1.5 hours ($p < 0.001$). (B) WT C57BI/6 PMNs were treated with 10 μ M of DPI in DMSO or DMSO vehicle control for 15 minutes on ice prior to mixing with vegetative TKO. Significant differences were seen at 0.5 hour ($p < 0.01$) one 1 hour and 1.5 hours ($p < 0.001$). $n = 3$ for all experiments. (C) Comparison of human PMN's ability to kill TKO with and without pre-treatment using DPI.

demonstrated an increase in ROS production by PMNs, in order to determine if low doses of circulating LT prevent oxidative burst in vitro, C57Bl/6 mice were injected with either 1.56 μ g (1.56 μ g LF + 3.12 μ g PA) or 6.25 μ g (6.2 μ g LF + 12.5 μ g PA) of LT i.p. and PMNs were isolated from the femur 24 hours post toxin injection. PMNs were then stimulated with either freshly opsonized TKO at an MOI of 1:1 or PMA in a luminol assay, where luminol produces chemiluminescence upon exposure to oxidizing agents. PMNs isolated from mice intoxicated with 6.25 μ g of LT had a significant reduction in oxidative burst compared to unintoxicated controls when stimulated by opsonized TKO at 20 min (*, $p < 0.05$), 40 min (***, $p < 0.001$) and 60 min (***, $p < 0.001$) (Fig. 3.8A). PMNs isolated from mice intoxicated with 1.56 μ g LT also exhibited significant reductions in oxidative burst at 40 min (***, $p < 0.001$) and 60 min (**, $p < 0.01$) (Fig. 3.8A). The 6.25 μ g dose of LT provided more inhibition of oxidative burst compared to the 1.56 μ g dose at 40 min (**, $p < 0.01$) and 60 min (***, $p < 0.001$), suggesting that the effects of circulating LT are dose-dependent (figure 8A). Mice injected with the individual toxin components, PA or LF, demonstrated no statistical defect in production of oxidative burst (Fig. 8B). In contrast PMA stimulated PMNs isolated from intoxicated mice demonstrated no defect in production of oxidative burst (Fig. 8C), which mirrors Crawford et al. human PMN studies. Taken together these results suggest that LT may function to inhibit receptor-based activation of NADPH oxidase (30), although this possibility requires further study.

Phagocytosis of vegetative *B. anthracis* is required for killing

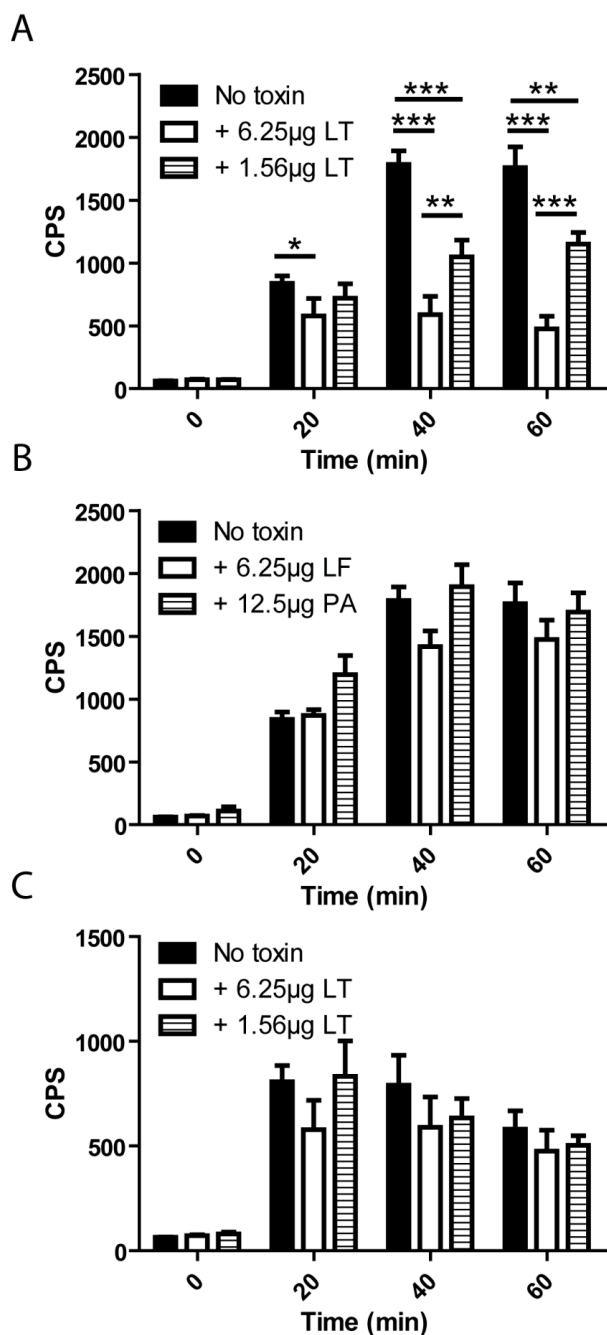


Figure 3.8: Circulating LT causes a decrease in oxidative burst in response to TKO but not PMA. (A-C) PMNs from C57Bl/6 mice were isolated and activated by TKO or PMA in the presence of luminol and degree of oxidative burst was established by measurement of chemiluminescence. (A) Mice were injected with LT i.p. 24 hours prior to isolation of PMNs, which were exposed to TKO at a 1:1 MOI, and luminescence was measured over the course of an hour. Significant differences were seen between non intoxicated PMNs and PMNs intoxicated with 6.25µg LT at 20 minutes ($p < 0.05$), 40 minutes, and

60 minutes ($p < 0.001$). Significant differences were seen between non intoxicated PMNs and PMNs intoxicated with 1.56µg LT at 40 minutes ($p < 0.001$) and 60 minutes ($p < 0.01$). Significant differences were seen between PMNs intoxicated with 6.25µg LT and 1.56µg LT at 40 minutes ($p < 0.01$) and 60 minutes ($p < 0.001$).

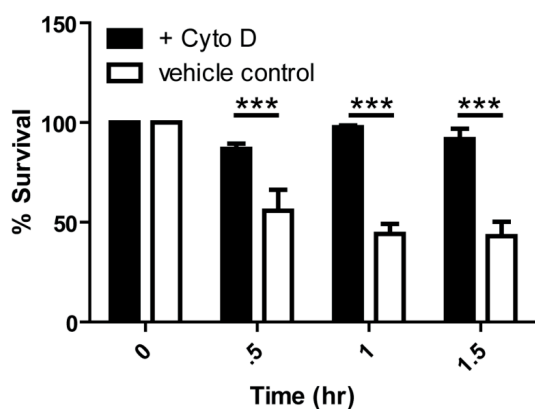
(B) Mice were injected with LF or PA i.p. 24 hours prior to isolation of PMNs, which were exposed to TKO at a 1:1 MOI, and luminescence was measured over the course of an hour. No significant differences were seen. (C) Mice were injected with LT i.p. 24 hours prior to isolation of PMNs, which were exposed to 10ng PMA, and luminescence was measured over the course of an hour. No significant differences were seen ($p>0.05$). $n=3$ mice for all conditions shown.

Despite the ability of PMNs to secrete antimicrobial granule components extracellularly, human PMNs require phagocytosis in order to eliminate vegetative *B. anthracis in vitro* (98). PMNs are also capable of producing extracellular reactive oxygen species in response to stimulation by PMA and fMLP (147). In order to determine if mouse PMNs require phagocytosis for killing of vegetative *B. anthracis*, C57Bl/6 PMNs were isolated and incubated with 10µg/ml of the actin polymerization inhibitor Cytochalasin D. When compared to DMSO vehicle controls there were significant defects in Cytochalasin D-treated cells' ability to kill vegetative TKO at a half hour, hour, and hour and a half (***, $p < 0.001$) (Fig. 3.9A). However, because Cytochalasin D has multiple cell biological effects, including PMN altering granule exocytosis (76), we additionally prevented phagocytosis by performing the PMN killing of TKO assay at 4°C. Similar to the results obtained with Cytochalasin D treatment, killing of TKO was significantly reduced at all time points past time zero (***, $p < 0.001$) (Fig. 3.9B). Taken together it can be concluded that phagocytosis of vegetative TKO is essential for mouse PMNs to kill vegetative *B. anthracis*.

Discussion

These studies provide valuable insights into how *B. anthracis* utilizes LT to subvert the host PMNs response to infection. While in the mouse model of anthrax intoxication of PMNs by LT is necessary for *B. anthracis* to disseminate and cause animal death, there have been few studies examining the functional ramifications of LT intoxication of PMNs (88, 90). Here we have demonstrated

A



B

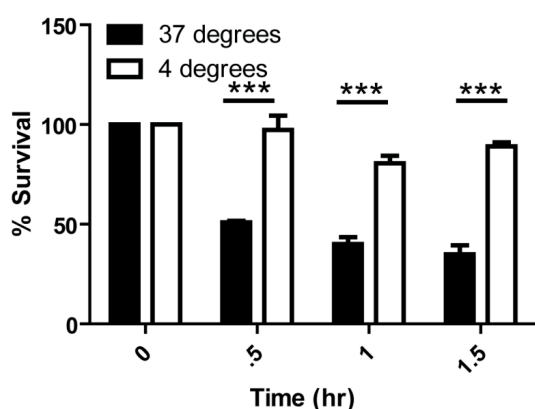


Figure 3.9: Phagocytosis is

necessary for PMNs killing of

vegetative TKO. (A and B) PMNs

were isolated from C57Bl/6 mice and

inoculated with vegetative *B. anthracis*

at an MOI of 1:1. At indicated time

points samples were put on ice and

mixed with 0.1% Saponin for 10 min.

Samples were then serially diluted

and plated for enumeration on LB

agar. (A) PMNs were treated with

10 μ g/ml of Cytochalasin D in DMSO

or a DMSO vehicle control throughout

the duration of the experiment. Significant differences in % survival of TKO were

seen at 0.5, 1, and 1.5 hours ($p < 0.001$). (B) PMN's killing of TKO was assessed

at both 37°C and 4°C. Significant differences in % survival of TKO were seen at

0.5, 1, and 1.5 hours ($p < 0.001$). $n = 3$ mice for all conditions shown.

that circulating LT is capable of significantly impairing PMN functions crucial to resolving infections. These observations help to answer the question of whether LT prevents PMNs from killing vegetative *B. anthracis*. Our studies also form a connection between injected quantities of LT and biologically relevant concentrations found in an active infection. However, these results require several caveats. First, there are many variables unaccounted for, such as the number of vegetative bacilli contributing to LF levels over time, and the rate of cellular uptake and clearance of LF during infection. This study also did not differentiate between LT and LF, or intra- versus extracellular toxin and because of this no conclusions can be made about whether LF is enzymatically active within the cytosol of cells within tissues where it was detected.

Understanding the mechanisms by which LT secretion by *B. anthracis* promotes bacterial growth and dissemination in a host is vital to developing means to reduce anthrax mortality. We have focused our research on the effects of LT on PMN function because of the critical role PMNs play in curing and controlling *B. anthracis* infections, and since LT and not ET is necessary for dissemination in the Sterne strain mouse model of infection (28, 29, 88, 90). Our work demonstrates that LT circulating in the blood stream independently of vegetative bacteria is capable of having dramatic effects at sites distal to the infection. However, gaps in knowledge remain regarding the role that circulating LT might play in the context of active infection. It will be important for future studies to implement new methods that differentiate between total-LF and LT and intra- versus extra- cellular toxin in various organs during the course of *B.*

anthracis infection. This information would result in a much greater understanding of how *B. anthracis* is so effective at causing lethal infection. *B. anthracis* capsule may also play a supporting role in modulation of the immune system. Capsule components shed during infection can be found in circulation and may function to activate the complement cascade at sites remote from infection disrupting the chemoattractant gradient (94). Circulating capsule may also increase the efficiency of cellular intoxication by stabilizing intracellular PA pore formation (79).

The majority of studies focusing on the effects of bacterial products on components of the immune system concentrate on immune cells that have been exposed to toxins *in vitro*, or immune cells that have been isolated directly from the infected sites. Our studies utilized low concentrations of LT *in vivo*, which resulted in circulating LF levels that were consistent with concentrations found in infected mice in the early stages of Sterne infection. However, these LT injections intoxicate PMNs resulting in quantifiable defects in their ability to respond to infection despite demonstrating no defects in viability (Fig 5). While exotoxins produced by other pathogens such as *Clostridium* species and *Staphylococcus aureus* are reported to cause effects remote from infection sites, these phenotypes are generally seen at late stages of disease progression or at concentrations which result in outward symptoms (107, 130). In C57Bl/6 mice, we demonstrate that doses of LT that are not detectable in the bone marrow even with very sensitive detection methods are capable of attenuating neutrophil function (Table 2, Fig 4). This suggests that minute concentrations of circulating

exotoxin have the potential to greatly affect the host immune response to infection. The degree of early intoxication of host immune cells may play a greater role in determining a lethal versus non-lethal infection than previously thought. By further study of *B. anthracis* toxin kinetics during the course of anthrax, it will be possible to determine the thresholds of LT intoxication needed for infection to progress beyond the initial site of infection. These studies and techniques can be applied broadly to other exotoxin-secreting pathogens to better understand how initial slight differences in toxin concentrations can precipitate differences in patient outcomes.

These results do not take into account the differences between injected purified toxin and the toxin produced throughout an infection. In an infection PMNs are exposed to toxin throughout the entire course of infection and the concentration of LF and/or LT would gradually increase the closer the PMNs got to the site of infection. In contrast, injected LT is a single bolus of toxin that is no longer active after 48 hours and does not establish a toxin gradient centered at the site of bacteria growth. Therefore, the injected toxin model may not accurately reflect the true toxin dynamics during an active infection.

These studies demonstrate that as in the case of humans, mouse PMNs require phagocytosis in order to kill vegetative *B. anthracis* (98), however unlike human PMNs, they also require oxidative burst. Here we show that low levels of circulating LT present in mice are capable of reducing the amount of oxidative burst the PMNs are capable of producing in a dose-dependent manner. It is important to note that this reduction in oxidative burst is only seen when TKO

stimulates PMNs but not when stimulated by PMA, which is similar to the results reported by Crawford et al. who used human PMNs treated with LT *in vitro* (30). However, these results are contradictory to those reported by Xu et al. who used C57Bl/6 mice injected with LT *in vivo* much like our model (156). There are several possible explanations as to why the results reported here do not match what was previously seen in mice. The oxidative burst assays performed by Xu utilized much larger doses of LT than were used in our assays, and did not use a bacterial activator in addition to PMA (156). PMNs were also incubated for up to 72 hours *in vitro* while primed with LPS and Pam₃ and exposed to LT before stimulation with PMA directly before measuring oxidative burst. Our assays use PMNs isolated from mice 24 hours after they had been injected with LT, and were not primed prior to activation with TKO or PMA. This was done to attempt to replicate the same conditions by which we monitor for PMN killing of vegetative TKO.

A remaining question is why LT only affects the oxidative burst in response to TKO and not PMA. Crawford et al. demonstrated that LT does not directly affect the components of NADPH oxidase system in a cell free system, but is preventing activation of NADPH oxidase through disrupting the MEK1-signaling cascade (30). Activation of NADPH oxidase from the fMLP receptor relies on activating MEK1 and 2 which phosphorylates ERK1 which directly phosphorylates p47 (35). In this case, LT is likely cleaving MEK1 and 2 preventing the downstream activation of p47, although this mechanism of LT action should be explored in future experiments. PMA stimulation activates p47

by a different mechanism. PMA activates PKC which in turn can activate c-Src which will phosphorylate p47 on a different serine residue than ERK (33). These separate pathways of NADPH activation most likely account for differences seen in LT effects on oxidative burst.

While oxidative burst is important for mouse PMN killing of vegetative TKO, and LT is capable of dampening this response, human PMNs do not require oxidative burst in order to kill *B. anthracis*, because α -defensin is sufficient. It is possible circulating LT also acts to prevent phagocytosis of vegetative bacilli, since many of the same signaling cascades regulate phagocytosis. Future experiments will concentrate on the possibility that circulating LT is capable of preventing phagocytosis and if it does whether the inhibition is caused by prevention of cellular signaling or phagocytosis machinery.

Materials and methods

Ethics Statement: All mouse husbandry and manipulation were performed following protocols approved by the University of Virginia Animal Care and Use Committee (protocol #3671) conforming to AAALAC International accreditation guidelines. When at all possible we have strived to replace the use of animals in our studies with *in vitro* or non-invasive assays, reduced the number of animals utilized, and refined our use of animals to minimize their suffering and maximize the data extracted from each experiment.

Mice: All Mouse strains used were bred in specific pathogen-free conditions within vivaria at University of Virginia All experiments used female mice between 6-8 weeks of age. Strains used were C57Bl/6 mice (Jackson labs, Bar Harbor

Maine), AJ mice (Jackson labs), FVB.129S6(B6)-Gt(ROSA)26Sor^{tm1(luc)kael}/J mice (Jackson labs), 129-Elane^{tm1(cre)Roes}/H mice (Medical Research Council, London, United Kingdom), and NEC cre luc mice bred at University of Virginia.

Bacterial Strains and growth conditions: *B. anthracis* Sterne strain 7702 was obtained from BEI Resources (Manassas, VA). The *B. anthracis* Sterne 7702 strain with deletion of the *pagA*, *lef*, and *cya* genes (referred to in the text as the triple exotoxin knockout or TKO) was graciously provided by Dr. Scott Stibitz from the Center for Biologics Evaluation and Research, Food and Drug Administration (73). BIG23 was constructed by integrating plasmid pIG6-19, a kind gift from Michele Mock at the Pasteur Institute, into *B. anthracis* strain 7702 using previously described conjugative methods (56). The resultant BIG23 expressed the *luxABCDE* genes from *Photobacterium luminescens* under the control of the protective antigen promoter. Therefore the vegetative cells of this strain are luminescent when growing with the host. Cultures of TKO *B. anthracis* were grown in Luria-Bertani (LB) broth overnight and then separated into 500µl aliquots with 15% glycerol and stored at -80°C. For recovery of experimental aliquots from -80°C, samples were thawed on ice and then 200µl was added to 800µl of LB broth and allowed to shake for one hour at 37°C.

Bacterial toxin components: The following reagents were obtained through BEI Resources, NIAID, NIH: Anthrax Protective Antigen (PA), Recombinant from *Bacillus anthracis*, NR-140, and Anthrax Lethal Factor (LF-HMA), Recombinant from *Bacillus anthracis*, NR-723. Toxin components were resuspended in PBS

+1 mg/ml of bovine serum albumin to a concentration of 1 mg/ml and stored at -80°C.

Mouse infection: AJ mice were anesthetized with 3% isoflurane (Piramal Healthcare, Andhra Pradesh, India) mixed with oxygen using an Isotec 5 vaporizer (Absolute Anesthesia, Piney River, VA). Purified BIG23 *B. anthracis* spores at a dose of 1×10^5 spores in 10 μ l PBS (Invitrogen, Carlsbad, CA) were injected subcutaneously in the left ear using a 0.5 cc insulin syringe as previously published (56).

Infection monitoring and luminescent imaging: In order to monitor the progression of infections using luminescent BIG23, mice were anesthetized using 3% isoflurane mixed with oxygen from the XGI-8 gas anesthesia system supplied with a Xenogen IVIS Spectrum. Images were acquired as previously reported and analyzed using Living Image software (version 2.50.1, Xenogen) (56). Once any detectable luminescent signal was detected in a vital organ, or a mouse appeared moribund, mice were euthanized per animal use protocol.

Measurement of Lethal Factor concentration in tissue samples: Organs from infected AJ or LT intoxicated C57Bl/6 mice were removed and placed into 100 to 1000 μ L of a cell lysis cocktail, depending on the organ, consisting of 0.2% Triton X-100 (Promega), 0.56mg/ml Pefablock (AppliChem. Darmstadt, Germany), 3.125mg/ml 6-aminohexanoic acid (Spectrum chemical. Brunswick, NJ), 0.3125mg/ml Antipain (VWR. West Chester, PA), and 22 μ g/ml of E64-D (Cayman Chemical. Ann Arbor, MI) in PBS. Samples were then homogenized using kontes pellet pestles (Fisher Scientific. Waltham, MA). Samples then sat on

ice for 1 hour then were then centrifuged and supernatants were removed and stored at -80 C until later use. Blood samples were allowed to clot for 20 minutes then spun down to collect serum, which was then stored at -80° C until later use. Quantification of LF was performed using matrix assisted laser desorption/ionization (MALDI) time of flight (TOF) mass spectrometry (MS) to detect synthetic peptide cleavage products generated by LF as previously described (12). LF levels in serum were reported in ng/ml.

Opsonization of *B. anthracis*: Blood was collected from mice by cardiac puncture and allowed to clot at room temperature for 10 minutes. Clotted blood was centrifuged at 1,800 x g for 15 minutes at room temperature and serum was collected. 95µl of *B. anthracis* from aliquots stored at -80°C which was diluted 1:5 in fresh LB broth and shaken for 1 hour at 37°C, was then added to 500µl of serum and allowed to incubate 37°C shaking for 30 minutes.

Isolation of PMNs: Mice were euthanized by cervical dislocation while under anesthesia and femurs were removed. Bone marrow was removed from femur using a 1 ml syringe and a 26 gauge half inch needle with 500µl of 1x Hanks balanced salt solution (HBSS). Once collected 1ml of bone marrow suspension was carefully layered over 1.5ml of Lympholyte Mammal (Cedar lane laboratories, Ontario, Canada) and centrifuged for 20 minutes at 800xg at room temperature. After centrifugation the pellet consisting of red blood cells (RBCs) and PMNs was resuspended in 4.5ml of dH₂O on ice, and after 30 seconds 0.5ml of 10x HBSS was added. PMNs were centrifuged at 4°C for 5 minutes at 500xg, supernatant was discarded and PMNs were resuspended in 1ml of 1x HBSS and

counted by hemocytometer. Purity and viability of PMNs was established using flow cytometry.

Assessment of PMN killing of vegetative bacteria: Heat-treated mouse serum was made by collecting blood from C57Bl/6 mice by cardiac puncture and allowing blood to clot at room temperature for 10 minutes. After clotting blood was centrifuged at 1,800 x g for 15 min and serum was collected. Serum was then heated at 55°C for 20 minutes before being frozen at -20°C for later use. Purified PMNs and opsonized bacteria were mixed at an MOI of 1:1 in a master mix of 1x HBSS and 10% heat-inactivated mouse serum. 200µl of the master mix were pipetted in triplicate for each time point into U- bottomed 96 well tissue culture plates (Corning, Corning, New York). Plates were centrifuged at 450 x g for 10 minutes at 4°C, and then placed at 37°C + 10% CO₂ for the times indicated in the figures. At designated time points PMNs were lysed by addition of 0.5% Saponin and vigorous pipetting with subsequent incubation on ice for 10 minutes. After lysis samples were diluted appropriately onto LB agar plates and incubated at 37°C overnight to enumerate CFU.

Western blotting for MEK3 cleavage: PMNs were harvested from mice with and without pretreatment with LT. As a positive control 1x10⁶ PMNs were treated with 100 ng of LT (100 ng LF, 200 ng PA) for one hour at 37°C with 10% CO₂. For each condition 1x10⁶ PMNs were lysed using SDS running buffer with β-mercaptoethanol and heated to 95°C for 4 minutes. Samples were loaded onto a SDS 10% polyacrylamide gel along with 10µl of a pre-stained protein ladder (Bio-Rad, Hercules, CA). The gel was run at 161 volts and transferred to a PVDF

transfer membrane (Biotechnology systems, Boston MA) at 100 volts for one hour. Membrane was first treated with rabbit anti mouse MEK3 (C-19, Santa Cruz Biotechnology, Santa Cruz CA) at a 1:500 dilution in 1% milk (0.4 µg/ml), following with goat anti-rabbit alkaline phosphatase conjugate (Millipore, Billerica MA) at 1:1000 (1 µg/ml). Blot was visualized using SigmaFast BCIP/NBT tablets (Sigma-Aldrich, St. Louis MO).

Flow cytometry staining: Single cell suspensions of bone marrow isolated PMNs were resuspended in 100 µl flow cytometry staining buffer (1xPBS 3% FBS 0.05% sodium azide). Fc receptor-blocking antibody (CD16/32, eBioscience San Diego, CA) was added and incubated on ice for thirty minutes. Samples were centrifuged and resuspended in 100 µl flow staining buffer. Antibodies against specific cell surface markers were added, incubated for one hour on ice, and then washed. Samples were then fixed overnight with 4% paraformaldehyde at 4°C. Antibodies used were: anti-Ly6C FITC (RB6-8C5, BD Biosciences), anti-CD86 PE (PO3.1, eBioscience San Diego, CA), anti-CD11b APC (M1/70, eBioscience), anti-MHC II PacBlue (M5/114.15.2, eBiosciences), anti-CD80 PE Cy5 (16-10A1, eBioscience), anti-CD69 PE Cy7 (H1.2F3, eBioscience), and anti-CD45 Alexa780 (30-F11, eBioscience). Live/Dead staining was performed with fixable Aqua Dead Cell Stain kit (Invitrogen).

Isolation of human PMNs: Human venous blood was collected from healthy human subjects. PMNs were then isolated from heparinized blood first by sedimentation in a 3% dextran 0.9% NaCl solution for 20 minutes, followed by purification on a Histopaque-1083 gradient (Sigma, St. Louis MO). Afterwards the

pellet containing PMNs underwent red blood cell lysis. PMNs were then centrifuged at 4°C and resuspended in 1ml of 1x HBSS and counted by hemocytometer.

Inhibition of oxidative burst by DPI: Human and mouse PMNs were treated on ice with 10µM of diphenylene iodonium (DPI) in 400µl of HBSS for 15min. PMNs were then centrifuged at 500xg for 10 minutes and resuspended in 1ml of HBSS.

Inhibition of phagocytosis by Cytochalasin D: Mouse PMNs were treated with 10µg/ml of in HBSS Cytochalasin D (Sigma) throughout the course of PMN killing of vegetative TKO assay.

Measurement of the oxidative burst: PMN reactive oxygen species (ROS) production was measured by luminol-dependent chemiluminescence assay and measured using a Victor 3 multiple plate reader. PMNs were isolated from intoxicated and non intoxicated mice, and 1×10^5 PMNs in 50µl of HBSS + 0.25% heat inactivated C57Bl/6 mouse serum were added to 96 well white opaque tissue culture plates (Beckton Dickinson, Franklin lakes NJ). PMNs were then stimulated with opsonized TKO at an MOI of 1:1 or 10ng of phorbol-12-myristate-13-acetate (PMA).

Statistical Analysis: All statistical analysis and was performed using GraphPad Prism software (version 5, GraphPad Software, San Diego, CA). Unless otherwise noted all statistical values reported were determined using a two tailed t-test and graphed to display mean with the standard error of the mean.

**Chapter 4: Circulating LT prevents PMNs
accumulation at sites of PMA induced
inflammation**

Introduction

Besides affecting the ability of PMNs to kill vegetative bacilli, there is a possibility that LT can attenuate the PMN response by preventing the accumulation of PMNs at the site of infection. PMNs arrive at sites of infection through the process of chemotaxis, which is the ability of a leukocyte to migrate along chemical gradient (22). PMNs initiate chemotaxis *in vivo* when resident macrophages and dendritic cells are exposed to bacterial PAMPs and start producing inflammatory cytokines which stimulate epithelial and endothelial cells to up-regulate expression of adhesion molecules such as P and E-selectin (85, 111). Inflammatory cytokines CXCL1 and CXCL2, which both signal through CXCR2, then reach the bone marrow, triggering PMN release from the bone marrow into circulation (32). These activating signals also induce PMNs to mobilize secretory vesicles to the plasma membrane, exposing Mac-1, which is necessary for cellular adhesion to ICAM-1 (63). After PMNs enter circulation, endothelial cells expressing selectins capture them, allowing them to start to roll along the endothelium driven by blood flow. As PMNs roll towards the site of inflammation, priming occurs by exposure of PMNs to PAMPs and increased concentrations of chemoattractants (132). Priming of PMNs promotes tight adhesion to the endothelium through binding of PMN expressed CAMs to endothelial expressed ICAMs, as well as increases the life span of PMNs (132). PMNs then pass through the endothelial barrier into the site of inflammation through a process called transmigration, characterized by PMNs cytoskeletal

rearrangements and secretion of proteases to degrade the extracellular matrix (82).

Studies investigating LT effects on PMN chemotaxis have consisted of *in vitro* treatment of human PMNs with toxin components, and have generated conflicting reports, some claiming an increase in chemotaxis (144, 154), while others reported inhibition (40, 134). However, these previous studies have several drawbacks. Different effects on chemotaxis can be seen with PMNs depending on how long PMNs were treated with LT *in vitro* (40). Additionally *in vitro* PMN migration assays cannot mimic the complex *in vivo* environment. For example, most *in vitro* PMN migration assays utilize a single chemoattractant such as MIP-2 or fMLP, where *in vivo* there are several distinct chemoattractant gradients that can be divided into two categories, intermediate and end target (82). This is made possible because PMNs possess hierarchical intracellular signaling cascades where intermediate chemoattractants signal through the PI3K signaling pathway and end target chemoattractants signal through the p38 pathway (82). This allows for the potential for LT to affect the ability of PMNs to migrate via one pathway while the other is not affected/remains intact.

In order to address the limitations and drawbacks of *in vitro* PMN migration assays here we demonstrate the development of an *in vivo* PMN accumulation assay. This system uses transgenic mice in which PMNs selectively express firefly luciferase, which can be detected by an IVIS camera to access the abundance of PMNs in a tissue non-invasively. The effects of *B. anthracis* LT on PMN accumulation can then be determined by comparing

luminescence at the site of PMA induced inflammation between LT intoxicated and non-intoxicated mice. Here we demonstrate that low concentrations of circulating LT are capable of attenuating the quantity of PMNs at the site of PMA induced inflammation.

Results

Circulating LT attenuates PMNs accumulation at sites of inflammation

While many studies have been able to examine PMN migration and accumulation in response to a chemotactic gradient *in vitro*, the real-time analysis of PMN accumulation dynamics *in vivo* is ideal. This is because the complex interplay among many cell types defines PMN accumulation dynamics. In order to analyze PMN populations *in vivo*, transgenic mice were created by crossing mice expressing Cre recombinase under a neutrophil elastase promoter (129-Elane^{tm1(cre)Roes}/H mice) (137) with floxed stop luciferase mice (FVB.129S6(B6)-Gt(ROSA)26Sor^{tm1(luc)kael}/J mice) (125). The resulting progeny (NECre luc mice) expressed luciferase in PMNs only. Luminescence could then be detected within the mouse by use of an IVIS camera. The resulting light signal intensity in mice is proportional to the density of PMNs in the tissue. In order to track PMNs in real time, a chemical inducer of inflammation phorbol 12-myristate 13-acetate (PMA) dissolved in DMSO was spotted onto the left ear of mice, and luciferin was then introduced i.p. Mice were imaged using an IVIS Spectrum imaging apparatus over a time course of 48 hours (Fig. 4.1A). To quantify the accumulation of PMNs in the inflamed area luminescent signal was measured in both ears and at each time point the percent increase in luminescent signal over

background was calculated using the non-inflamed right ear as the background measurement. These results demonstrated that there was a statistically significant increase in the PMN-generated light signal over time in the inflamed ear, increasing from $31 \pm 6.12\%$ to $213 \pm 27.47\%$ over background from 0 to 48 hours (Fig. 4.1B). It was noted that the light signal from PMNs in the background ear fluctuated at each time point, making it necessary to determine if both ears fluctuate in a synchronous manner in the absence of inflammation. Mice were injected with luciferin without induction of inflammation and imaged at multiple time points. Light signals in both ears were quantified over the 48 hour time period. Independent of any inflammatory stimuli the PMN content in the ears fluctuated uniformly in both ears over time (Fig. 4.2), validating the right ear as a proper background light-emission control.

Although we demonstrated that LT decreases overall mouse PMN chemotaxis through a porous membrane towards MIP-2 *in vitro*, it was not clear what effect would be exhibited *in vivo* since many more chemotactic stimuli and inflammatory processes exist within a complete tissue system. To assess the effect that circulating LT might have on PMN migration to inflammation *in vivo*, NECre luc mice were treated with increasing doses of LT and PMA was spotted onto the left ear to induce inflammation. Light production was monitored over a time period of 48 hours (Fig. 4.3A). It was found that mice treated with $6.25\mu\text{g}$ of LT showed a significant decrease in light signal at both 24 and 48 hours post LT injection, while a dose of $1.56\mu\text{g}$ induced no significant differences at any time point (Fig. 4.3B). Treatment of mice with equivalent quantities of PA alone or LF

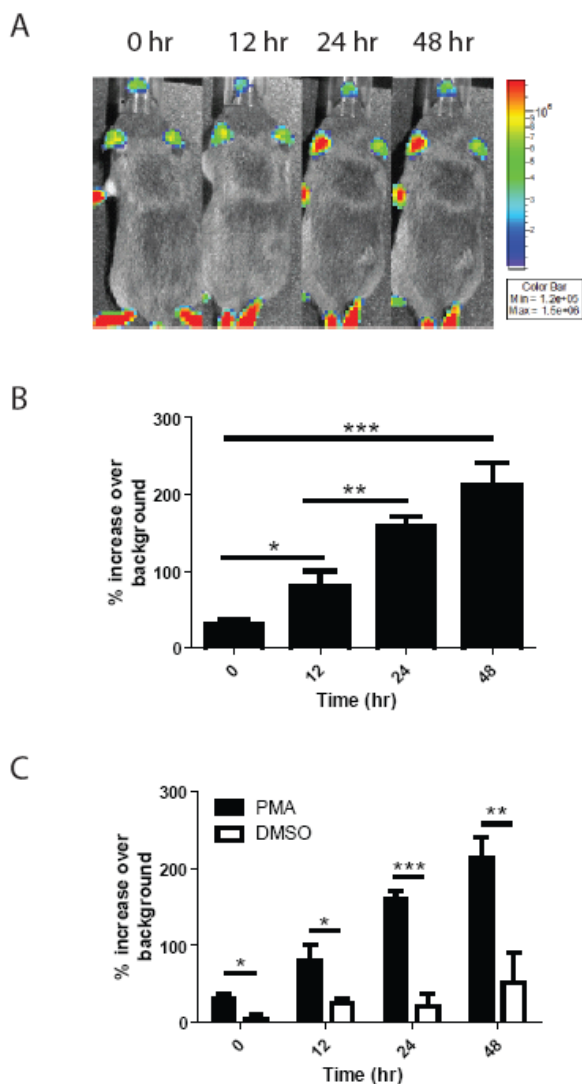


Figure 4.1: PMN accumulation at sites of inflammation can be measured in real-time. (A) Black and white photos of a single representative NEC Luc mouse

with 2.5 μ g PMA in 5 μ l DMSO pipetted onto the ear, overlaid with a false color representation of photon emission intensity as indicated by the scale on the right in p/s/cm-2/sr over a 48 hour time course. (B) Luminescence was quantified for both the PMA-treated and non-treated ear. Percentage increase in luminescence over background was then calculated,

where non-PMA ear was set as background for each time point. Significant increases were seen from 0 to 12 hours (*, $p=0.0349$) from 0 to 48 hours (***, $p<0.0001$), and 12 to 24 hours (**, $p=0.0056$). (C) Comparison between PMN recruitment to PMA ($n=6$) and DMSO vehicle control ($n=5$) ears where significant differences were seen at time 0 (*, $p=0.0106$) 12 hours (*, $p=0.0318$), 24 hours (***, $p<0.0001$), and 48 hours (**, $p=0.0070$). $n=6$ mice per condition.

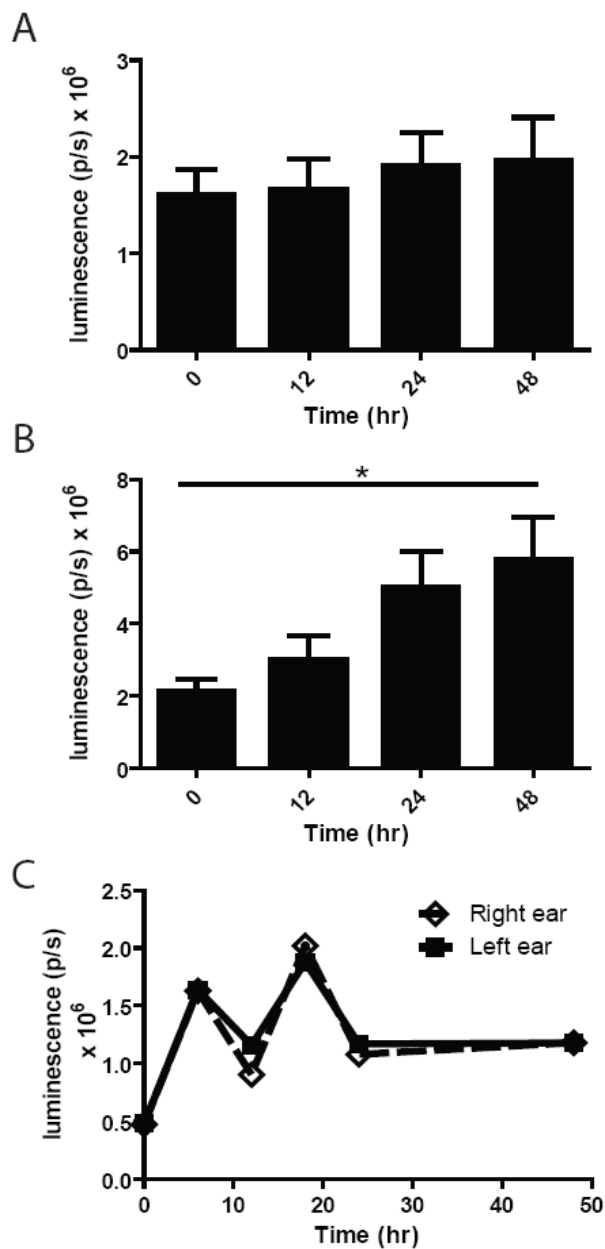


Figure 4.2: PMN

accumulation at sites of inflammation can be measured in real-time. (A

and B) NEC Luc mouse with

2.5 μ g PMA in 5 μ l DMSO pipetted onto the ear had net luminescence measured over

the course of 48 hours in both the non-inflamed right ear (A), and the inflamed left ear (B)

where a significant increase

was found from time zero to 48 hours (*, $p=0.0213$) where $n=6$ mice per condition. (C)

luminescence was measured in both ears of a NEC Luc

mouse over the course of 48 hours. Results are representative of 3 separate mice.

mouse over the course of 48 hours. Results are representative of 3 separate mice.

alone yielded no significant difference in PMN accumulation compared to control mice (Fig. 4.3C). Injection of LT did not decrease the number of PMNs in circulation as determined by luminescence levels in the non-PMA inflamed background ear over the experimental time course (Fig. 4.4).

Circulating LT causes a decrease in PMN *in vitro* migration

Previous assays to determine LT effects on PMN migration have been performed using human cell culture assays with contradictory results (40, 120, 134, 144), and involved directly intoxicating PMNs with LT *in vitro*. Our previous assays to assess the effects of circulating LT on PMNs were performed in C57Bl/6 mice. In order to determine if circulating LT is capable of altering C57Bl/6 PMNs, mice were treated with LT i.p. and PMNs were isolated at 24 hours post inoculation. The PMN's ability to chemotax to MIP-2 (CXCL2) was determined by enumerating PMNs that migrated through a porous membrane (Fig. 4.5). PMNs exposed to as little as 1.56 μ g of LT showed a significant defect in transmigration across the membrane (60.77%, $p=0.0454$) when compared to single toxin component controls that do not intoxicate cells alone (Fig. 4.6).

NECre luc mice demonstrate less susceptibility to circulating LT than C57Bl/6 mice

Because previous experiments utilized two distinct mouse strains (C57Bl/6 and NECre luc) it was necessary to corroborate the differences and similarities of NECre luc and C57Bl/6 mouse PMNs in the presence of circulating LT. First, the ability of NECre luc PMNs to kill vegetative TKO was assessed and compared to

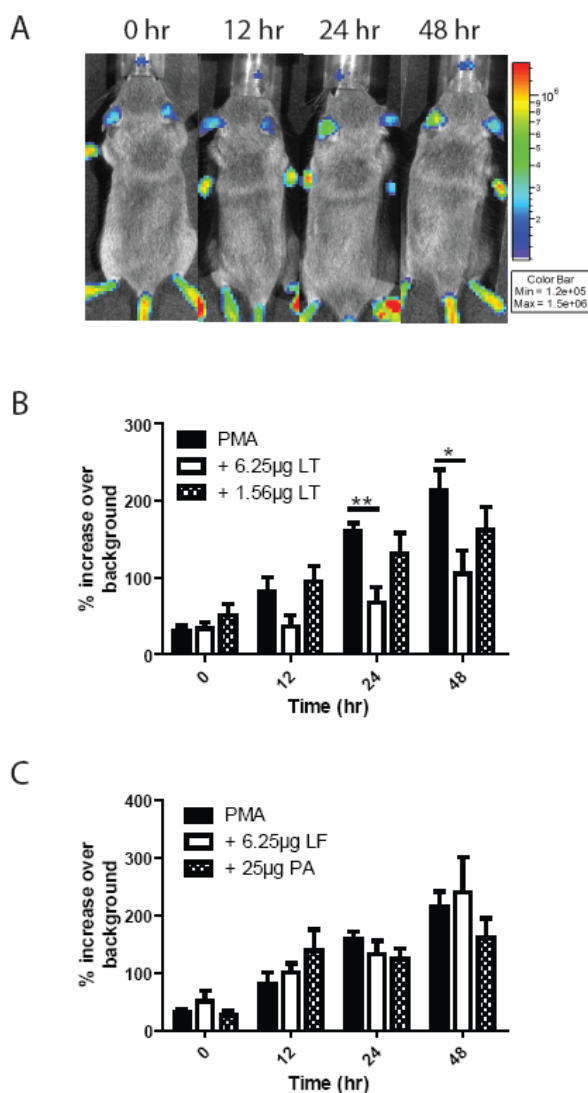


Figure 4.3: Circulating LT

attenuates PMN accumulation at sites of PMA induced inflammation.

(A) Black and white photos of a single representative

NEC Luc mouse with 2.5µg PMA

in 5µl DMSO pipetted onto the ear and injected i.p. with 6.25µg LT,

overlaid with a false color

representation of photon emission intensity as indicated by the scale

on the right in p/s/cm²/sr over a 48 hour time course. (B)

Comparison of left-ear

luminescence over background

between mice treated with the indicated amounts of i.p. LT and non-intoxicated mice. Significant differences were found between PMA and PMA +6.25µg LT mice at 24 (**, p=0.0026) and 48 hours (*, p=0.0234). (C) Comparison between mice treated with PA or LF to non-intoxicated mice. No significant differences were found. n=6 mice per condition.

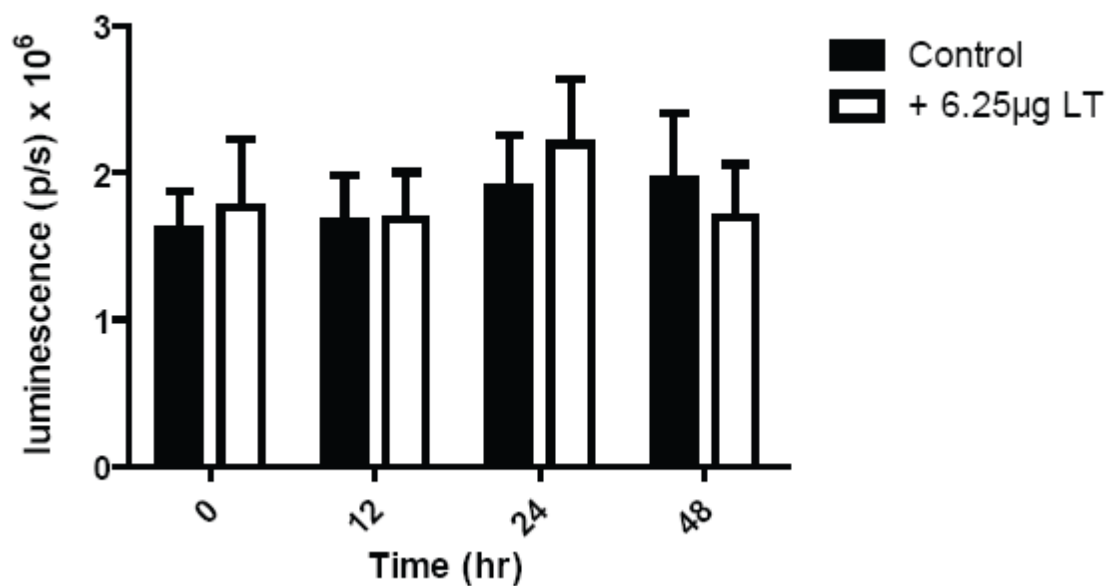


Figure 4.4: Circulating LT does not affect circulating PMN levels. NEC Luc mice had 2.5µg PMA in 5µl DMSO pipetted onto the left ear and injected i.p. with 6.25µg LT. Luminescence was measured in the non-PMA right ear at each indicated time point and compared to luminescence in the control ear of non-intoxicated mice. n=6 mice per condition (p>0.05).

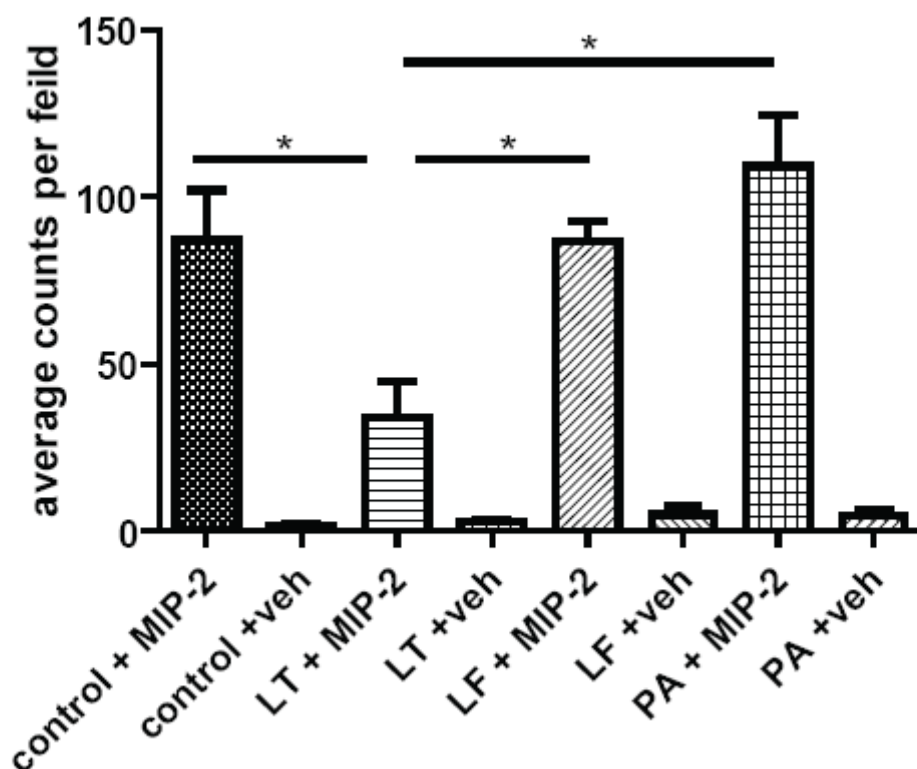


Figure 4.5: Circulating LT causes a decrease in PMN migration. C57Bl/6

Mice were injected with 1.56 μ g LT, 1.56 μ g LF, or 3.12 μ g PA i.p. and PMNs were isolated 24 hours later. PMN migration through a membrane with 3 μ m pores was induced with MIP-2 or a BSA vehicle control. Average count per 40x field recorded for each condition where statistically significant differences were found between non-intoxicated PMNs and LT treated PMNs (*, $p=0.0454$), LF and LT treated (*, $p=0.0120$), and PA and LT treated PMNs (*, $p=0.0153$) to MIP-2. $n=3$ mice for each condition.

that of C57Bl/6 PMNs (Fig. 4.6A). It was found that NECre luc PMNs kill vegetative TKO to a similar degree as C57Bl/6 PMNs. There was a statistical difference at 30 minutes but no statistical differences between PMNs from the two mouse strains at other time points. NECre luc PMN killing of TKO was then reassessed with the presence of circulating 6.25 μ g LT, as previously described (Fig. 4.6B). While there were significant differences in the ability of NECre luc PMNs to kill vegetative TKO caused by treatment with circulating LT, there was less impairment of bactericidal activity compared to C57Bl/6 PMNs with the same dose of LT (Fig. 4.6C). When PMNs from NECre luc mice were compared for their ability to migrate through a porous membrane towards MIP-2 there were no significant differences between PMNs with and without pretreatment with circulating 1.56 μ g LT (Fig. 4.6D). The *in vitro* NECre luc results are similar to what was found in the *in vivo* PMN migration/accumulation assay, where a dose of 1.56 μ g LT was insufficient to cause a significant change in PMN accumulation in inflamed tissues. These results suggest that while both NECre luc and C57Bl/6 mouse PMNs are influenced by circulating LT, C57Bl/6 PMNs are affected by lower doses than NECre luc mice.

Discussion

These studies present several methodological advantages over those previously published. First is that PMNs from intoxicated mice were used instead of intoxicating PMNs *in vitro*. Because PMNs have a short half-life and variable intoxication times can lead to different biological results, differences in *in vitro*

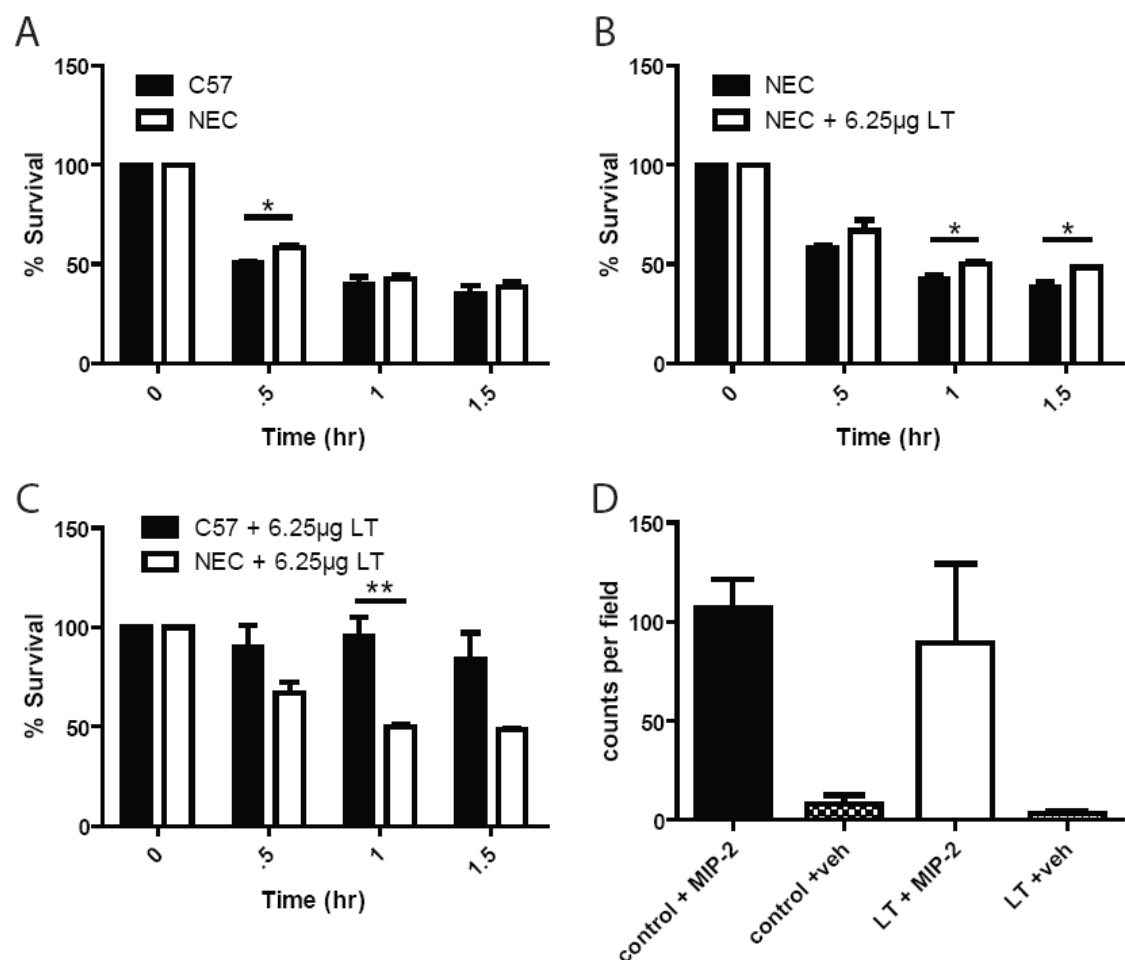


Figure 4.6: NECre luc mice demonstrate less susceptibility to circulating LT than C57BI/6 mice. (A-C) C57BI/6 and NEC luc mice were injected with toxin components (LF, PA) and PMNs were isolated after 24 hours. PMNs were then inoculated with TKO at an MOI of 1:1 and incubated at 37°C. At indicated time points samples put on ice and mixed with 0.1% Saponin for 10 min. Samples were then serially diluted and plated for enumeration on LB agar. (A) Comparison between C57BI/6 and NEC luc PMN ability to kill vegetative TKO, a significant difference was seen at one half hour ($p= 0.0101$). (B) Comparison between non-

intoxicated and intoxicated NEC luc PMN ability to kill vegetative TKO. Significant differences were seen at one hour (*, $p= 0.0330$) and one and a half hours (*, $p= 0.0193$). (C) Comparison between intoxicated C57Bl/6 and NEC luc PMN ability to kill vegetative TKO. A significant difference was seen at one hour (**, $p= 0.0097$). (D) NEC luc mice were injected with $1.56\mu\text{g}$ LT and PMNs were isolated from bone marrow after 24 hours. Intoxicated and non-intoxicated PMNs then migrated through a membrane with $3\mu\text{m}$ pore to MIP-2 or a BSA vehicle control. Average count per 40x field recorded for each condition. Results are representative of 3 separate experiments.

intoxication protocols could have led to the inconsistencies in the literature (134). As mentioned previously, intoxication *in vivo* allows PMNs to interact with LT in a similar physiologic context as would happen during active infection. The second advantage is the development of an *in vivo* PMN accumulation assay. The *in vivo* assay represents a major advance in technologies to aid understanding factors that influence how PMNs act *in vitro*. Current *in vitro* PMN migration assays do not reflect many of the factors influencing PMN function within the highly integrated immune response to infection. These factors include failing to account for multiple chemoattractant gradients occurring simultaneously and that the use of diffusion-based assays leads to temporary and unstable gradients (meaning the slope of chemoattractant gradient will change as cells migrate across the gradient) (84, 86). In addition previous chemotaxis assays rely on treatment of PMNs *in vitro*, where it has been shown that short incubation times (< 2 hrs) with LT can lead to different results in the assay (120, 134). Importantly, data acquired with our novel *in vivo* PMN accumulation assay are consistent with our *in vitro* migration assays which together support the conclusion that LT inhibits PMN migration into inflammatory sites (84).

Materials and Methods

Mice: All Mouse strains used were bred in specific pathogen-free conditions within vivaria at University of Virginia All experiments used female mice between 6-8 weeks of age. Strains used were C57Bl/6 mice (Jackson labs, Bar Harbor Maine), FVB.129S6(B6)-Gt(ROSA)26Sor^{tm1(luc)kael}/J mice (Jackson labs), 129-

Elane^{tm1(cre)Roes}/H mice (Medical Research Council, London, United Kingdom), and NEC cre luc mice bred at University of Virginia.

Bacterial Strains and growth conditions: *B. anthracis* Sterne strain 7702 was obtained from BEI Resources (Manassas, VA). The *B. anthracis* Sterne 7702 strain with deletion of the *pagA*, *lef*, and *cya* genes (referred to in the text as the triple exotoxin knockout or TKO) was graciously provided by Dr. Scott Stibitz from the Center for Biologics Evaluation and Research, Food and Drug Administration (73). Cultures of TKO *B. anthracis* were grown in Luria-Bertani (LB) broth overnight and then separated into 500µl aliquots with 15% glycerol and stored at -80°C. For recovery of experimental aliquots from -80°C, samples were thawed on ice and then 200µl was added to 800µl of LB broth and allowed to shake for one hour at 37°C.

Bacterial toxin components: The following reagents were obtained through BEI Resources, NIAID, NIH: Anthrax Protective Antigen (PA), Recombinant from *Bacillus anthracis*, NR-140, and Anthrax Lethal Factor (LF-HMA), Recombinant from *Bacillus anthracis*, NR-723. Toxin components were resuspended in PBS +1 mg/ml of bovine serum albumin to a concentration of 1 mg/ml and stored at -80°C.

Opsonization of *B. anthracis*: Blood was collected from mice by cardiac puncture and allowed to clot at room temperature for 10 minutes. Clotted blood was centrifuged at 1,800 x g for 15 minutes at room temperature and serum was collected. 95µl of *B. anthracis* from aliquots stored at -80°C which was diluted 1:5

in fresh LB broth and shaken for 1 hour at 37°C, was then added to 500µl of serum and allowed to incubate 37°C shaking for 30 minutes.

Isolation of PMNs: Mice were euthanized by cervical dislocation while under anesthesia and femurs were removed. Bone marrow was removed from femur using a 1 ml syringe and a 26 gauge half inch needle with 500µl of 1x Hanks balanced salt solution (HBSS). Once collected 1ml of bone marrow suspension was carefully layered over 1.5ml of Lympholyte Mammal (Cedar lane laboratories, Ontario, Canada) and centrifuged for 20 minutes at 800xg at room temperature. After centrifugation the pellet consisting of red blood cells (RBCs) and PMNs was resuspended in 4.5ml of dH₂O on ice, and after 30 seconds 0.5ml of 10x HBSS was added. PMNs were centrifuged at 4°C for 5 minutes at 500xg, supernatant was discarded and PMNs were resuspended in 1ml of 1x HBSS and counted by hemocytometer. Purity and viability of PMNs were established using flow cytometry.

Assessment of PMN killing of vegetative bacteria: Heat-treated mouse serum was made by collecting blood from C57Bl/6 mice by cardiac puncture and allowing blood to clot at room temperature for 10 minutes. After clotting blood was centrifuged at 1,800 x g for 15 min and serum was collected. Serum was then heated at 55°C for 20 minutes before being frozen at -20°C for later use. Purified PMNs and opsonized bacteria were mixed at an MOI of 1:1 in a master mix of 1x HBSS and 10% heat-inactivated mouse serum. 200µl of the master mix were pipetted in triplicate for each time point into U- bottomed 96 well tissue culture plates (Corning, Corning, New York). Plates were centrifuged at 450 x g

for 10 minutes at 4°C, and then placed at 37°C + 10% CO₂ for the times indicated in the figures. At designated time points PMNs were lysed by addition of 0.5% Saponin and vigorous pipetting with subsequent incubation on ice for 10 minutes. After lysis samples were diluted appropriately onto LB agar plates and incubated at 37°C overnight to enumerate CFU.

PMN accumulation monitoring and luminescent imaging: Mice were anesthetized using 3% isoflourane mixed with oxygen from the XGI-8 gas anesthesia system supplied with a Xenogen IVIS Spectrum. To induce inflammation 5µl of a 0.5 µg/µl phorbol 12-myristate 13-acetate (PMA) suspended in dimethyl sulfoxide (DMSO) was pipetted onto the left ear of mice. At indicated time points 150µl of luciferin at a concentration of 30 mg/ml suspended in DPBS (Perkin Elmer, Waltham MA) was injected i.p. into mice and 8-10 minutes were allowed to elapse for diffusion throughout the mouse. Images were acquired as previously reported and analyzed using Living Image software (version 2.50.1, Xenogen)(56).

PMN *in vitro* chemotaxis assay: PMNs isolated from LT intoxicated mice and non-intoxicated control mice were tested for chemotactic ability as previously described (131). Briefly, to the bottom wells of a blind well chemotaxis chamber (Neuroprobe Inc, Cabin John MD) 160µl of HBSS containing 0.03ng/µl of MIP-2 (Peprtech, Rocky Hill NJ) or vehicle control were added in triplicate for each experimental condition. A 3µm pore size polycarbonate filter (Neuroprobe Inc) was placed over the bottom wells and 100µl containing 2.6×10^5 PMNs were added to the top wells. Chemotaxis assembly was incubated at 37°C with 5%

CO₂ for 45 minutes. Afterward filters were removed and, fixed and stained using the Diff-Quick staining system (Dade Behring, Newark DE). PMNs that had migrated through the filter were counted in 5 high powered fields (40X) using a Zeiss Primostar microscope (Carl Zeiss, Oberkochen Germany). Chemotactic activity was established by averaging the number of PMNs per field from three separate experiments compared to vehicle only controls.

Statistical Analysis: All statistical analysis and was performed using GraphPad Prism software (version 5, GraphPad Software, San Diego, CA). Unless otherwise noted all statistical values reported were determined using a two tailed t-test and graphed to display mean with the standard error of the mean.

**Chapter 5: Examining circulating *B.*
anthracis edema toxin effects on PMN
function**

Introduction

While the effects of LT on PMN's ability to both kill vegetative bacilli and accumulate at sites of PMA-induced inflammation have been the concentration of this dissertation, most of our effort was spent investigating any similar roles of ET. ET is a calmodulin-dependent adenylate cyclase, which is capable of increasing cAMP levels over 1000x what would be produced endogenously (5). As its name implies ET is responsible for causing edema in the host, and injection of purified ET results in extensive lesions in many tissues (45). The role of ET during an infection is not understood as well as that of LT, and was not shown to be lethal on its own until recently (45). It is clear that ET plays a vital role during pathogenesis, when it is knocked out virulence is reduced, and dissemination patterns are altered (39, 110).

Most reports on *B. anthracis* toxin effects on PMNs demonstrate that ET plays a complementary role to LT, in that independently ET is capable of preventing *in vitro* chemotaxis and oxidative burst of human PMNs (30, 134). ET has also reduces the β 2 integrin CD11b/CD18 in PMNs, which would hypothetically prevent PMN's ability to transmigrate through capillaries to sites of inflammation (134). However these data are in contrast to studies demonstrating increases in PMNs at sites of ET injection (136). ET has been shown to directly prevent phagocytosis in human PMNs when directly intoxicated, most likely because of ET effects on actin dynamics (106).

Unlike circulating LT, here we demonstrate that ET in circulation does not affect PMN's ability to kill vegetative bacilli *ex vivo* at large or small doses at a

broad variety of time points and injection routes. ET may play a role in *in vivo* PMN accumulation. Studies showing that large doses of ET injected i.p. are capable of preventing accumulation. However, the same effects were seen with EF alone suggesting that the defects in PMN accumulation were not dependent on whole toxin. Taken together this suggests that circulating ET may not play a significant role in remotely intoxicating PMNs. These studies do not rule out that ET may play a vital role at the initial site of infection or at the end stages of infection. These results suggest that EF could function extracellularly through a previously un-described mechanism to prevent PMN accumulation at sites of inflammation.

Results

Circulating ET does not affect PMN's ability to kill vegetative *B. anthracis*.

Like LT the potential role of ET to prevent killing of vegetative *B. anthracis* by PMNs has not been established. Unlike LT however, the concentration of ET in circulation has not yet been established in the mouse model of infection. In order to determine if injected ET could alter the ability of C57Bl/6 PMNs to kill vegetative bacilli, PMNs isolated from mouse bone marrow were combined with TKO or an LF knockout strain of *B. anthracis* at an MOI of 1:1. Percent survival of bacteria was determined throughout a time course of one and a half hours. The ability of *B. anthracis* to produce ET does not lead to a significant difference in PMN's ability to kill *B. anthracis* (Fig. 5.1). However as in the case of LT, the ability of *B. anthracis* to generate ET does not take into account the concentration of ET

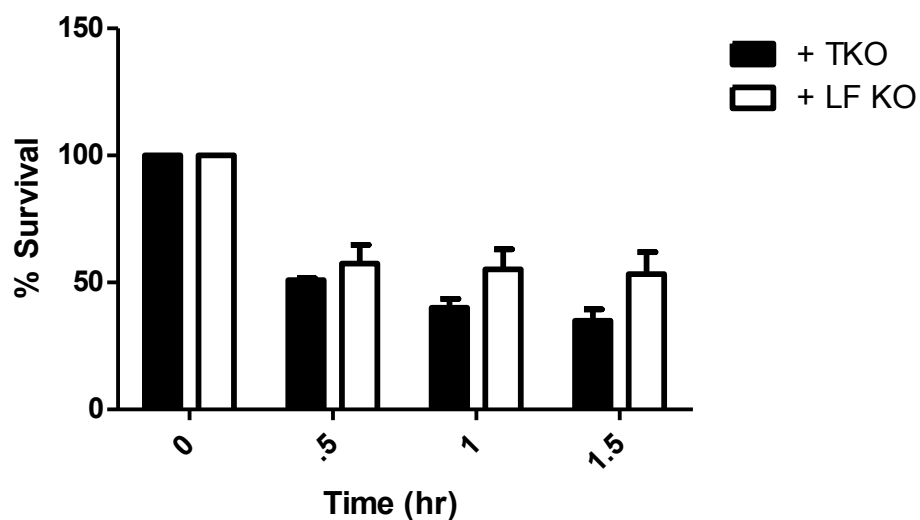


Figure 5.1: Ability of *B. anthracis* to produce ET does not alter PMN's ability to kill vegetative bacilli. PMNs were isolated from C57Bl/6 mice. PMNs were then inoculated with TKO or LF KO at an MOI of 1:1 and incubated at 37°C. At indicated time points samples were put on ice and mixed with 0.1% Saponin for 10 min and vigorously mixed by pipetting. Samples were then serially diluted and plated for enumeration on LB agar and CFU were determined ($p > 0.05$).

which would be present, and the time course of the experiment may be insufficient ET to act on PMNs. Because of this concentrations (25 μ g to 1.56 μ g) of ET were injected i.p. into C57Bl/6 mice and PMNs were isolated from the bone marrow 24 hours post injection. ET-exposed PMNs were then combined with opsonized TKO at a 1:1 MOI and % survival was determined over a time course of one and a half hours (Fig. 5.2). No significant effect on ability of ET to prevent PMN killing of TKO was seen at any concentration tested.

One reason that no effect of circulating ET on PMNs was seen could be due to ET having a shorter functional half-life than was demonstrated for LT. In order to test if ET effects on PMNs could be seen at earlier times post injection of ET, C57Bl/6 mice were injected i.p. with 6.25 μ g of ET and bone marrow PMNs were isolated at both 1 and 12 hours post injection. In both cases there was no difference in ability of PMNs to kill TKO as compared to EF only controls (Fig. 5.3), suggesting that circulating ET does not affect PMN's ability to kill vegetative TKO within 24 hours post i.p. injection.

After injection of ET i.p. local edema was noticed around the site of injection. This led to suspicion that ET was not able to diffuse into circulation as easily as LT may, leading to little or no ET making it into circulation or the bone marrow to act on PMNs. To account for this possibility ET was injected retro-orbitally (r.o.), and PMNs were isolated from the bone marrow at 1 and 24 hours post injection and assayed for ability to kill opsonized vegetative TKO. At both 1 and 24 hours post i.v. injection there was no difference in ability of PMNs to kill vegetative TKO compared to EF controls (Fig. 5.4). This demonstrates that

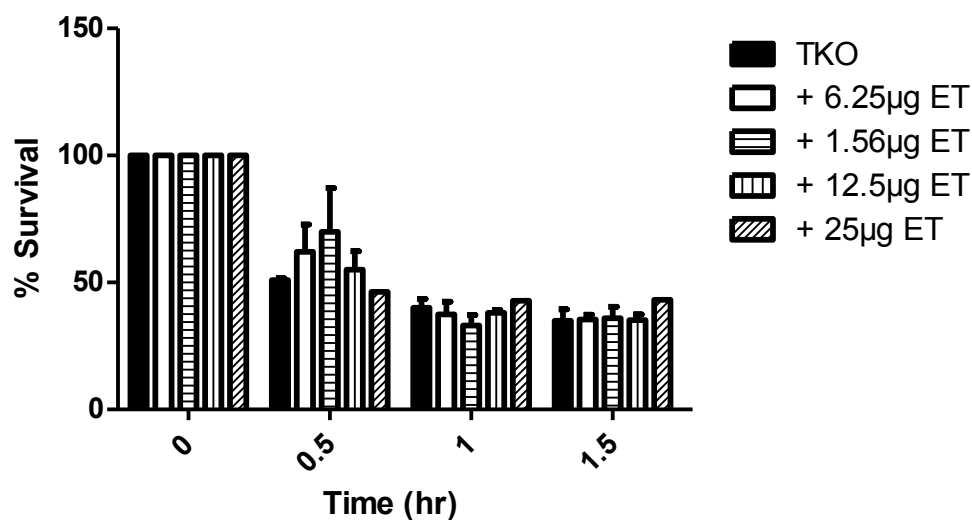


Figure 5.2: i.p. injected ET does not attenuate the ability of PMNs to kill vegetative *B. anthracis*. C57Bl/6 mice were injected with toxin components (EF, PA) and PMNs were isolated at the indicated times. PMNs were then inoculated with TKO at an MOI of 1:1 and incubated at 37°C. At indicated time points samples were put on ice and mixed with 0.1% Saponin for 10 min and vigorously mixed by pipetting. Samples were then serially diluted and plated for enumeration on LB agar. Mice were injected i.p. with the indicated doses of ET, PMNs were isolated at 24 hours post injection and CFU were determined at indicated time points. n=2 for all conditions.

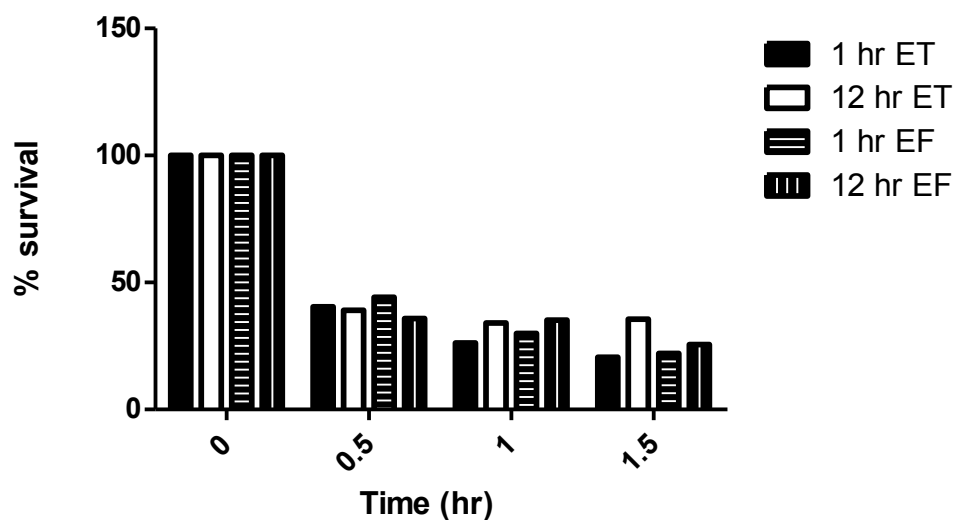


Figure 5.3: ET does not affect PMN's ability to kill vegetative TKO at earlier time points. C57Bl/6 mice were injected with toxin components (EF, PA) and PMNs were isolated at the indicated times. PMNs were then inoculated with TKO at an MOI of 1:1 and incubated at 37°C. At indicated time points samples were put on ice and mixed with 0.1% Saponin for 10 min and vigorously mixed by pipetting. Samples were then serially diluted and plated for enumeration on LB agar. Mice were injected i.p. with 6.25µg of ET, PMNs were isolated at the indicated time post injection and CFU were determined at indicated time points. n=1 for all conditions.

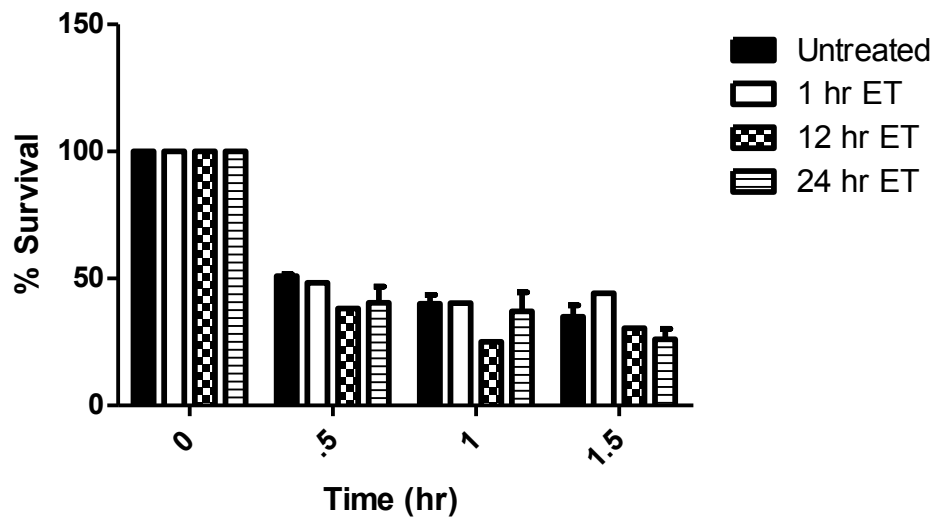


Figure 5.4: Retro-orbital injection of ET does not lead to alteration in PMN's ability to kill vegetative TKO. C57Bl/6 mice were injected with toxin components (EF, PA) and PMNs were isolated at the indicated times. PMNs were then inoculated with TKO at an MOI of 1:1 and incubated at 37°C. At indicated time points samples were put on ice and mixed with 0.1% Saponin for 10 min and vigorously mixed by pipetting. Samples were then serially diluted and plated for enumeration on LB agar. Mice were injected r.o. with 6.25µg of ET, PMNs were isolated at the indicated time post injection and CFU were determined at indicated time points. n=1 or 2 (indicated by presence of error bars) for all conditions.

injected ET is not capable of diminishing the ability of PMNs under the conditions we have outlined.

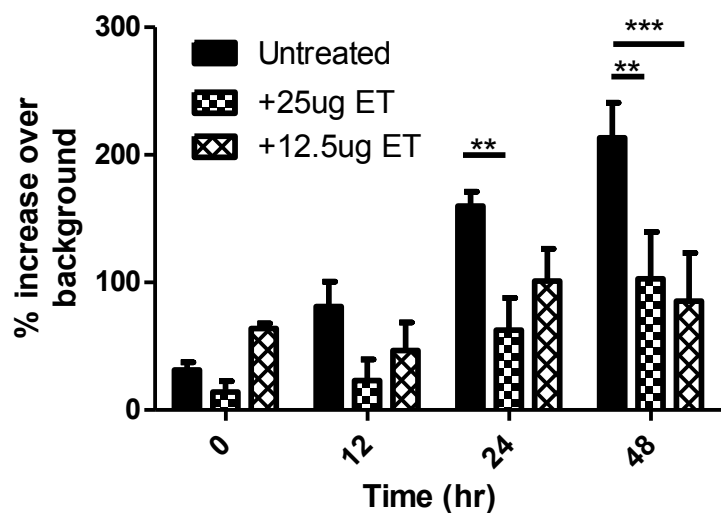
Circulating ET prevents PMN accumulation at sites of inflammation

Like LT, ET prevents PMN chemotaxis *in vitro* by interfering with actin filament polymerization (134). In order to determine if circulating ET is capable of preventing PMN accumulation *in vivo*, NECre luc mice were injected i.p. with either 25 μ g or 12.5 μ g ET and 2.5 μ g of PMA was spotted onto the left ear. PMN accumulation at the site of PMA induced inflammation was monitored for 48 hours using the IVIS spectrum. Both the 12.5 μ g and 25 μ g dose demonstrated a significant decrease in PMN accumulation in at sites of PMA induced inflammation (Fig. 5.5). However, the 12.5 μ g dose only had a significant difference at 48 hours (***, $p < 0.001$) while the 25 μ g dose had significant decreases in luminescence at both 24 and 48 hours (**, $p < 0.01$) (Fig. 5.5A). When a dose of 25 μ g of EF alone was injected i.p. and PMN's ability to accumulate at sites of PMA induced inflammation was assessed, a significant decrease was found at 24 hours (*, $p < 0.05$), suggesting that EF alone may be capable of preventing PMN accumulation at sites of inflammation (Fig. 5.5B).

Discussion

These studies suggest that while circulating LT plays an important role in preventing PMNs from killing vegetative bacilli, circulating ET does not. However, both ET and EF are capable of preventing PMNs from accumulating at sites of PMA induced inflammation *in vivo*. The amount of injected ET required to prevent

A



B

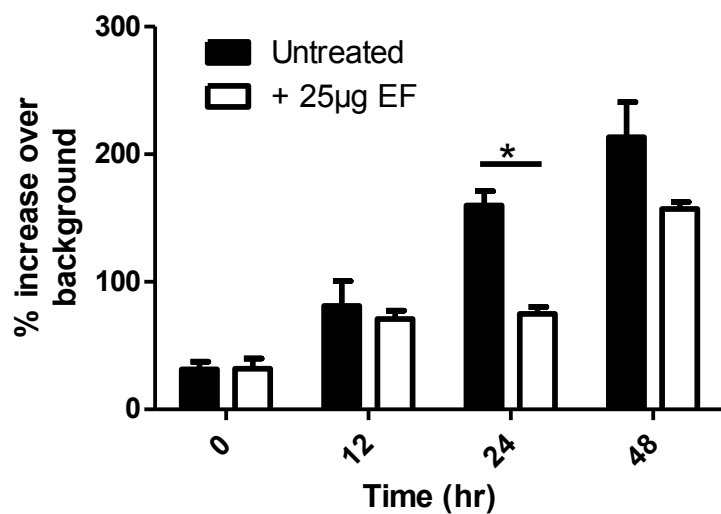


Figure 5.5: ET and EF attenuate PMN accumulation at sites of PMA induced inflammation. (A and B) NECre luc mice were injected with either ET or EF and 2.5μg of PMA in 5μl of DMSO was pipetted onto the left ear. Luminescence, which represents an increase in PMNs was monitored over 48 hours. (A) Luminescence in the left ear of NECre luc mice which have been i.p. injected

with indicated amounts of ET were compared to un-injected mice. Significant differences were found between untreated and mice injected with 12.5 μ g ET at 48 hours (***, $p < 0.001$) and untreated and mice injected with 25 μ g ET at 24 hours (**, $p < 0.01$) and 48 hours (**, $p < 0.01$). (B) Comparison between mice which were untreated or injected with 25 μ g EF. A significant difference was seen at 24 hours (*, $p < 0.05$). $n=6$ for untreated mice and 3 for ET injected mice. $n=3$ for all conditions.

PMN accumulation is double the amount of injected LT required. Because during infection EF is produced at a lower amount than LF it is unlikely that circulating ET would play a large role in preventing the PMNs response. However, there are several caveats to the data as currently presented. Primarily, we did not check to see if ET was acting on bone marrow-purified PMNs. There are several possibilities that could prevent ET from acting on bone marrow PMNs. It is possible that endothelial cells or blood vessels rapidly absorb ET where as LT is not, or EF may have a very short half-life compared to LF in the serum. Also, in several cases the numbers of experiments done were not enough to determine statistical significance between treated and untreated controls, however the amount performed as pilots did not suggest there would be a change if more experiments were performed. Any future experiments investigating the potential role of circulating ET should take into account these possibilities before moving forward.

According to Dr. Anne Boyer, in the non-human primate model of infection there is almost no EF found in circulation during the early or mid stages of infection while in the late stages there is a sudden increase (personal communication). However, these data have not been replicated in mice and a comprehensive ET survey has not been completed as was done for LT. In the future, it will be important to continue to work with our CDC collaborators in order to accomplish this. Taking into account the current data it appears that circulating ET does not have an important role in influencing PMN dynamics. ET could play several important alternative roles in subverting the immune response at the

initial infection site and aiding in bacterial escape from the initial site of infection. Alternatively, ET function might be more important in the late stage of infection. Future experiments should be directed to address these possibilities. Another potential role of ET would be to increase the action of circulating LT. In this case future experiments should focus on using LT and ET together and test the ability of PMNs to kill and accumulate at sites of inflammation.

Materials and methods

Ethics Statement: All mouse husbandry and manipulation were performed following protocols approved by the University of Virginia Animal Care and Use Committee (protocol #3671) conforming to AAALAC International accreditation guidelines. When at all possible we have strived to replace the use of animals in our studies with *in vitro* or non-invasive assays, reduced the number of animals utilized, and refined our use of animals to minimize their suffering and maximize the data extracted from each experiment.

Mice: All Mouse strains used were bred in specific pathogen-free conditions within vivaria at University of Virginia All experiments used female mice between 6-8 weeks of age. Strains used were C57Bl/6 mice (Jackson labs, Bar Harbor Maine), AJ mice (Jackson labs), FVB.129S6(B6)-Gt(ROSA)26Sor^{tm1(luc)kael}/J mice (Jackson labs), 129-Elane^{tm1(cre)Roes}/H mice (Medical Research Council, London, United Kingdom), and NEC cre luc mice bred at University of Virginia.

Bacterial Strains and growth conditions: *B. anthracis* Sterne strain 7702 was obtained from BEI Resources (Manassas, VA). The *B. anthracis* Sterne 7702 strain with deletion of the *pagA*, *lef*, and *cya* genes (referred to in the text as the

triple exotoxin knockout or TKO) was graciously provided by Dr. Scott Stibitz from the Center for Biologics Evaluation and Research, Food and Drug Administration (73). BIG23 was constructed by integrating plasmid pIG6-19, a kind gift from Michele Mock at the Pasteur Institute, into *B. anthracis* strain 7702 using previously described conjugative methods (56). The resultant BIG23 expressed the *luxABCDE* genes from *Photobacterium luminescens* under the control of the protective antigen promoter. Therefore the vegetative cells of this strain are luminescent when growing with the host. Cultures of TKO *B. anthracis* were grown in Luria-Bertani (LB) broth overnight and then separated into 500µl aliquots with 15% glycerol and stored at -80°C. For recovery of experimental aliquots from -80°C, samples were thawed on ice and then 200µl was added to 800µl of LB broth and allowed to shake for one hour at 37°C.

Bacterial toxin components: The following reagents were obtained through BEI Resources, NIAID, NIH: Anthrax Protective Antigen (PA), Recombinant from *Bacillus anthracis*, NR-140, and Anthrax Edema Factor (EF-HMA), Recombinant from *Bacillus anthracis*, (NR-2585). Toxin components were resuspended in PBS +1 mg/ml of bovine serum albumin to a concentration of 1 mg/ml and stored at -80°C.

Mouse infection: AJ mice were anesthetized with 3% isoflurane (Piramal Healthcare, Andhra Pradesh, India) mixed with oxygen using an Isotec 5 vaporizer (Absolute Anesthesia, Piney River, VA). Purified BIG23 *B. anthracis* spores at a dose of 1×10^5 spores in 10 µl PBS (Invitrogen, Carlsbad, CA) were

injected subcutaneously in the left ear using a 0.5 cc insulin syringe as previously published (56).

Infection monitoring and luminescent imaging: In order to monitor the progression of infections using luminescent BIG23, mice were anesthetized using 3% isoflourane mixed with oxygen from the XGI-8 gas anesthesia system supplied with a Xenogen IVIS Spectrum. Images were acquired as previously reported and analyzed using Living Image software (version 2.50.1, Xenogen) (56). Once any detectible luminescent signal was detected in a vital organ, or a mouse appeared moribund, mice were euthanized per animal use protocol.

Opsionization of *B. anthracis*: Blood was collected from mice by cardiac puncture and allowed to clot at room temperature for 10 minutes. Clotted blood was centrifuged at 1,800 x g for 15 minutes at room temperature and serum was collected. 95µl of *B. anthracis* from aliquots stored at -80°C which was diluted 1:5 in fresh LB broth and shaken for 1 hour at 37°C, was then added to 500µl of serum and allowed to incubate 37°C shaking for 30 minutes.

Isolation of PMNs: Mice were euthanized by cervical dislocation while under anesthesia and femurs were removed. Bone marrow was removed from femur using a 1 ml syringe and a 26 gauge half inch needle with 500µl of 1x Hanks balanced salt solution (HBSS). Once collected 1ml of bone marrow suspension was carefully layered over 1.5ml of Lympholyte Mammal (Cedar lane laboratories, Ontario, Canada) and centrifuged for 20 minutes at 800xg at room temperature. After centrifugation the pellet consisting of red blood cells (RBCs) and PMNs was resuspended in 4.5ml of dH₂O on ice, and after 30 seconds 0.5ml

of 10x HBSS was added. PMNs were centrifuged at 4°C for 5 minutes at 500xg, supernatant was discarded and PMNs were resuspended in 1ml of 1x HBSS and counted by hemocytometer. Purity and viability of PMNs were established using flow cytometry.

Assessment of PMN killing of vegetative bacteria: Heat-treated mouse serum was made by collecting blood from C57Bl/6 mice by cardiac puncture and allowing blood to clot at room temperature for 10 minutes. After clotting blood was centrifuged at 1,800 x g for 15 min and serum was collected. Serum was then heated at 55°C for 20 minutes before being frozen at -20°C for later use. Purified PMNs and opsonized bacteria were mixed at an MOI of 1:1 in a master mix of 1x HBSS and 10% heat-inactivated mouse serum. 200µl of the master mix were pipetted in triplicate for each time point into U- bottomed 96 well tissue culture plates (Corning, Corning, New York). Plates were centrifuged at 450 x g for 10 minutes at 4°C, and then placed at 37°C + 10% CO₂ for the times indicated in the figures. At designated time points PMNs were lysed by addition of 0.5% Saponin and vigorous pipetting with subsequent incubation on ice for 10 minutes. After lysis samples were diluted appropriately onto LB agar plates and incubated at 37°C overnight to enumerate CFU.

PMN accumulation monitoring and luminescent imaging: Mice were anesthetized using 3% isoflourane mixed with oxygen from the XGI-8 gas anesthesia system supplied with a Xenogen IVIS Spectrum. To induce inflammation 5µl of a 0.5 µg/µl phorbol 12-myristate 13-acetate (PMA) suspended in dimethyl sulfoxide (DMSO) was pipetted onto the left ear of mice.

At indicated time points 150 μ l of luciferin at a concentration of 30 mg/ml suspended in DPBS (Perkin Elmer, Waltham MA) was injected i.p. into mice and 8-10 minutes were allowed to elapse for diffusion throughout the mouse. Images were acquired as previously reported and analyzed using Living Image software (version 2.50.1, Xenogen)(56).

Statistical Analysis: All statistical analysis and was performed using GraphPad Prism software (version 5, GraphPad Software, San Diego, CA). Unless otherwise noted all statistical values reported were determined using a two tailed t-test and graphed to display mean with the standard error of the mean.

Chapter 6: Summary, discussion, and future directions

Summary

The aim of this chapter is to contextualize the research presented in this document by describing where the field was when this research started and how each chapter answered a specific question. This chapter will also discuss areas that should be expanded upon in the future, but were not addressed directly by these studies. An additional simplified representation of the questions answered by this research can be seen in figure 6.1.

When I entered the *B. anthracis* field, research focusing on the interactions with *B. anthracis* and the host immune system was primarily operating under the “Trojan horse” hypothesis of dissemination. Accordingly, the vast majority of literature was focused on how *B. anthracis* virulence factors manipulate cells thought to be Trojan horses, primarily macrophages and dendritic cells. However the “Trojan horse” hypothesis was coming under increasing scrutiny, summed up in chapter one and its correlating literature review (150). A collection of articles were published which started to suggest that something other than the “Trojan horse” was occurring. First was data which observed that spore germination and outgrowth seems to start at the initial site of spore deposit and then spread into the draining lymph node (56). Multiple papers then demonstrated that PMNs were responsible for protection against many forms of anthrax, whereas protection from other cell types was not (29, 88). Liu et al. demonstrated that if innate immune cells, particularly PMNs, were not capable of being intoxicated, then dissemination would not occur in the mouse model of infection (29, 88). Finally a paper which demonstrated that in the mouse Sterne

strain model of infection, LT is required for dissemination, while ET is not (90). Taken together, these collected studies suggested that *B. anthracis* outgrowth occurs where spores are first deposited, and does not require an intracellular step for dissemination. During this process LT produced by the bacteria controls the PMN response in order to lead to disseminated infection. My research set out to further explore an alternative hypothesis of *B. anthracis* dissemination and control of the innate immune system.

The first question that I attempted to address was based on the observation by Glomski et al. that germination and outgrowth of *B. anthracis* spores occurred first at the site of initial spore deposit and not the regional draining lymph node (56). This suggested that the trafficking and germination of spores in the regional draining lymph node was not the vital part of dissemination. However those data did not demonstrate whether that was the case, and it remained quite possible that germination occurring in the ear or lung was not as important in the outcomes of infection as any germination that was occurring in the lymph node. Finding the principle site which would lead to dissemination would be vital for future research in the field of *B. anthracis*. In order to study how *B. anthracis* overcomes the PMN response through production of LT, the location where these interactions are taking place must be identified. The experiments described in chapter two made this distinction by demonstrating that germination and outgrowth at initial site of spore inoculation is where dissemination originates, and not spores within the draining lymph node. Not only does this research have implications for studying host pathogen

interactions, but also has medical ramifications with the emergence of a subcutaneous form of anthrax from heroin injection in Europe. These results allowed for us to make the claim that the appropriate place to study toxin output and *B. anthracis* outgrowth was not the lymph node, but the site of subcutaneous injection. This study also resulted in clinically significant findings. With the rise of subcutaneous anthrax cases resulting from injection of contaminated heroin in Scotland and elsewhere in Europe, there is a debate in clinical journals on whether or not to use debridement as a means of treatment. Since the Trojan horse hypothesis poses that bacteria found in the draining lymph nodes are the bacteria that ultimately establish the disseminated disease and not the bacteria within the initially-infected tissues, physicians debated if performing highly invasive surgical debridement would increase the survival of infected patients. Our study demonstrated that surgical debridement increases survival and thus that early and effective removal of infected tissues is advised.

The next question I attempted to answer stemmed from papers stating the necessity of LT to overcome the PMN response in order for dissemination to occur. While previous studies collectively suggested that this was the case, very little work was done to determine what aspect of PMN function LT was inhibiting. The first major hurdle for studying how LT manipulates PMNs came from the fact that the relevant levels of LT during infection had not been determined. Most of the previous *B. anthracis* research on toxins in mice relied on injecting purified toxin components into the mice, while having little idea if the toxin doses administered were physiologically relevant. The question of what toxin levels are

physiologically relevant throughout infections was addressed in chapter three, where our collaboration with Drs. Anne Boyer and John Barr resulted in a mapping of LT concentrations throughout infection. By addressing the question of relevant toxin concentrations, it became possible to investigate mechanisms utilized by LT to manipulate PMNs at each stage of infection. This is an important distinction to make, because different concentrations of LT may result in different effects on PMNs. With LT levels clearly defined for each stage of infection, research into the possibility that different toxin concentrations control PMNs differently can be explored.

Once physiologically relevant toxin levels were determined, experimental focus shifted back to potential avenues LT would utilize to attenuate PMN's ability to clear *B. anthracis* infections. This question is very broad, so it was broken into two primary areas where LT could prevent PMNs from properly responding to infection. The two most likely ways to prevent PMN clearance of infection would be to attenuate PMN killing ability and/or ability to accumulate at sites of infection. Previous research into these areas was quite limited or controversial. Mayer-Scholl et al. found that human PMNs were capable of killing vegetative bacilli, but did not investigate if LT was capable of attenuating killing (98). Research into PMN accumulation at sites of inflammation was limited to *in vitro* chemotaxis experiments, which drew opposing conclusions (40, 144). Chapter three demonstrates that concentrations of LT that are similar to those found in early and mid stages of infection are capable of preventing PMNs from killing vegetative bacilli, while chapter four demonstrates that those same LT

concentrations prevent PMNs from accumulating at sites of inflammation.

Answering these very basic questions about LT control of PMNs led to the novel observation that low levels of LT are present in circulation during the early stages of infection and that these concentrations can effectively disarm PMNs at sites far from the actual infection. Likewise the development of the *in vivo* PMN accumulation assay provides a powerful tool which can test for defects at all stages of PMN migration to sites of infection, not just the ability to chemotax across a single gradient.

The next obvious question raised from this work was the mechanism of LT effects on PMNs. Chapter four represents the beginnings of investigations into this question by determining what is required for mouse PMNs to kill TKO, demonstrating that NADPH oxidase and phagocytosis are required. Determining that circulating LT diminishes the ability of PMNs to produce oxidative burst when stimulated by TKO but not when stimulated with PMA, confirming human PMN work done by Crawford et al., but inconsistent with mouse work done by Xu et al. (30, 156). Future plans include investigating if circulating LT prevents PMN phagocytosis in addition to oxidative burst, and determining if LT prevents all receptor-based, oxidative-burst activation.

Collectively these data add to the *B. anthracis* field by providing a better understanding of the events of early and mid-stage infection. Chapter one proposes the jail break hypothesis, here figure 6.2 presents a subcutaneous specific model supplemented by recent data demonstrating how LT alters PMNs during infection. In brief, *B. anthracis* spores are deposited in a skin abrasion,

NALT, or lung and then germinate into vegetative bacilli. The cellular endothelial layer along with resident macrophages and dendritic cells activate to produce a chemotactant gradient and inflammatory signals which signal for PMN chemotaxis to the site of inflammation. Meanwhile vegetative *B. anthracis* start to produce LT which intoxicates cells within the immediate environment preventing PMNs at the site of infection from killing it. LT also starts to diffuse into the lymphatic and circulatory system preventing additional PMN accumulation at the site of infection. The PMNs that do make it to the site of PMA stimulation are likewise prevented from killing the bacteria.

Discussion

The data presented here have larger implications in the study of *B. anthracis* infections and host pathogen interactions than could be discussed in individual chapters. This section will cover many different topics. I will discuss concepts that were briefly discussed in earlier chapters but were not resolved, and observations that were not shown in the manuscript but merit discussion. Future directions based on these ideas, which are peripherally related to the data presented in this dissertation, will also be proposed.

Much of the research presented in this document has focused on the role of the lymph node during *B. anthracis* infection. The Trojan horse hypothesis suggests that the lymph node plays a very important role in infection. However, chapter two demonstrated that spores deposited in the lymph node were not able to cause disseminated disease, while vegetative growth at the site of initial spore

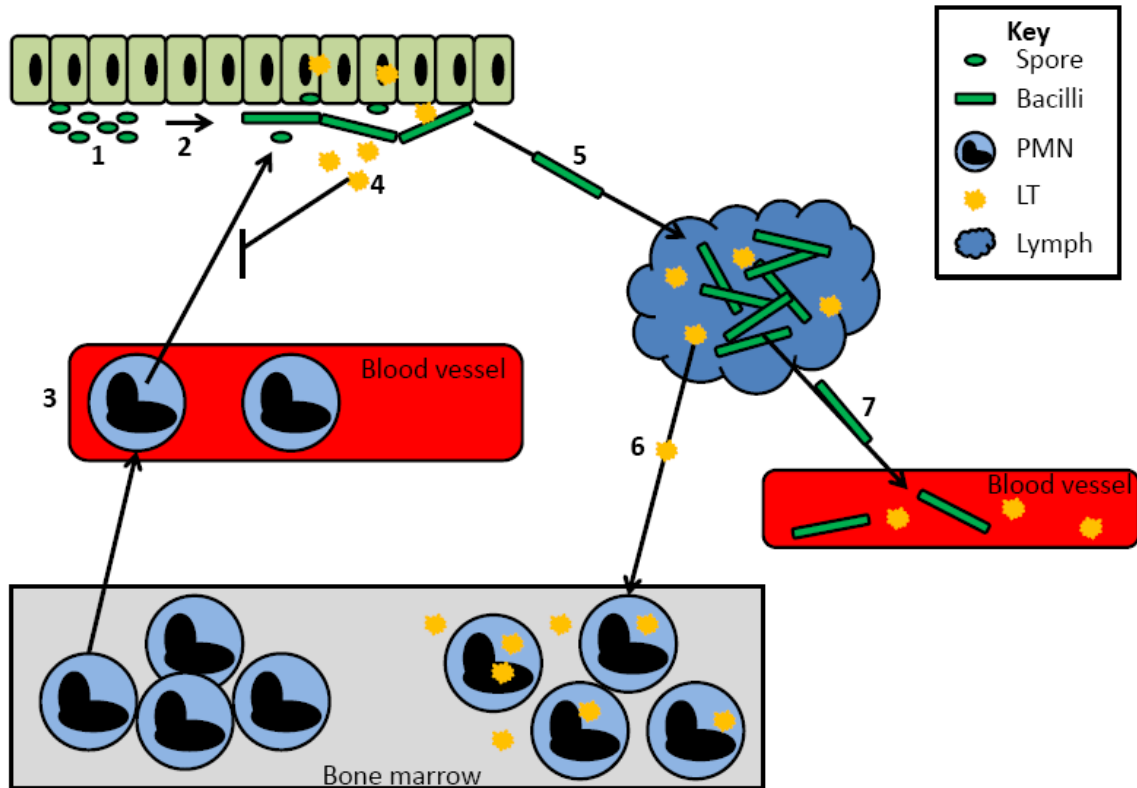


Figure 6.2: Model of early events during subcutaneous *B. anthracis* infection. 1, spores are deposited in the subcutaneous tissue. 2, germination of spores occurs causing inflammation. 3, PMNs are released from the bone marrow into circulation and begin to migrate to the site of infection to kill vegetative bacilli. 4, vegetative bacilli start producing LT, which intoxicates local PMNs preventing them from killing *B. anthracis* and acts to prevent PMN accumulation. 5, vegetative bacilli start accumulating in the regional draining lymph node. 6, LT produced by vegetative bacilli in the lymph node and initial site of infection starts to accumulate in the serum and bone marrow. 7, bacilli breach containment within the lymph node and accumulate in circulation and other organs.

inoculation is. However, during the course of infection, bacteria are seen growing and producing toxin in the regional draining lymph node for a substantial amount of time before dissemination into the circulatory system occurs. Data in chapter one demonstrates that the lymph node is refractory to germination of bacteria, and spores that do germinate are rapidly cleared. I hypothesise that the lymph node acts to slow down the dissemination of *B. anthracis* during infection, and that contrary to the Trojan horse hypothesis the lymph node is not necessary for dissemination to occur. This could be addressed by experimentally infecting mice where the regional draining lymph node has been removed, or mice which are incapable of producing lymph nodes and determine the mean time to dissemination and death. If the lymph node was necessary for infection to occur, mice would survive infection, if the lymph is inhibitory to infection dissemination would occur faster than normal.

In chapter one, “the point of no return” was defined as the point where enough toxins and bacterial products are in circulation to kill the host, even if all viable bacteria have been eliminated via use of antibiotics. In the future it will be important to distinguish whether the “point of no return” is associated with a stage of infection as I defined in chapter three, or the total cumulative toxin produced regardless of stage of infection. This concept ties into the debate on the role of the draining lymph node during infection. If the lymph node is not necessary for dissemination, then the appearance of vegetative bacilli in the lymph node may not be indicative of a sudden influx of additional toxin, and should not be incorporated as a separate stage of infection. As a result, the stages of infection

would be defined as pre-dissemination and post-dissemination. In the binary definition of the stages of infection, LT levels would be correlated with the total number of bacteria present over time, regardless of the anatomical location of the bacteria. Accordingly, the LF toxin survey reported in chapter three would be reconfigured to report toxin levels based on amount of luminescence present, and not by stage of infection. This distinction has important implications for the treatment of anthrax. If the “point of no return” is associated with a stage of infection, i.e. the mid stage of infection, surgical debridement after infection has progressed to the lymph node would not make a difference in disease outcome and thus other treatment measures should be considered. If the “point of no return” is associated with the amount of toxins present in circulation regardless of stage of infection, then any debridement prior to reaching fatal toxin levels would be helpful. The fundamental difference between these two scenarios is that in one case it is more important to prevent the spread of bacteria, while in the other it is more important to keep toxin production down. These experiments can be performed by treating infected mice with antibiotics at either different stages of infection or different CFU concentrations and then determining differential survival.

When performing BLI infection studies in AJ mice our lab noticed that regardless of the route of infection, *B. anthracis* outgrowth can only be found initially in one location, despite presence of spores in other areas. For example, in inhalational anthrax, at a low concentration of spores, infection always initiates in the NALT. However, when there is a higher concentration of spores, infection will

always initiate in the lung, despite the presence of more spores in the NALT than would be seen in a lower dose infection. Likewise in the subcutaneous model of infection, even if I have injected multiple spots on the same ear only one will show germination and toxin production. Taken together these observations suggest that *B. anthracis* somehow ensures that only one location will undergo germination and growth at a time. Why this would be advantageous is speculative at this time, but it could be that since *B. anthracis* causes very little inflammation initially during infection, multiple infection sites would produce too much global inflammation, thus decreasing chances of successful infection. Alternatively there could be evolutionary implications, where preventing other spores from germinating and causing disease could insure only the bacteria most suited to causing infection will germinate and disseminate. If, in fact, there are factors preventing germination of spores at sites distal from initial germination and bacterial growth, there are major implications for disease treatment. If an anti-germination factor were identified and subsequently purified it could be used to prevent infection in patients who have been exposed to *B. anthracis* until an appropriate course of antibiotics can be prescribed.

Future directions

While the work presented here represents a substantial advancement in the understanding of the dynamics between *B. anthracis* and the PMN immune response, there is great deal left to study. Immediate future directions should determine if circulating LT is capable of preventing phagocytosis of opsonized TKO. If circulating LT can prevent phagocytosis the next focus should be to

determine if other internalization mechanisms are blocked such as pinocytosis, and if the block on phagocytosis is based on disruption of actin filament formation as has been previously suggested (40), or based on a defect in cellular signaling pathways involved in triggering phagocytosis.

Future work should continue to investigate the mechanisms behind LT prevention of PMN killing of bacteria. A subject that was not touched upon here is the possibility that LT may alter PMN granule mobilization. This is important to study because as was mentioned in chapters three and five, human PMNs do not require oxidative burst to kill vegetative bacilli, instead they rely on the antimicrobial peptide α -defensin, which mice do not possess (41, 98). Because of this, in human infections, PMNs may be better able to control *B. anthracis* infection. It is obviously not ethical or practical to conduct circulating LT experiments on human subjects, and the mouse model may be inappropriate to study if LT affects granule mobilization. Future experiments could explore *in vitro* intoxication experiments with both human and mouse PMNs to examine if LT prevents granule fusion to the phagosome and or prevents granule exocytosis. These experiments should determine the appropriate dosing amounts and times by using *in vivo* intoxication of mouse PMN phenotypes as the baseline for what initial *in vitro* experiments should look like. These same doses should then be applied to *in vitro* human PMN experiments. These experiments would be important in order to start to make claims that circulating LT may play a similar role in human infections.

The *in vivo* PMN accumulation assay serves to raise many questions about the nature of LT attenuation of PMN migration to sites of inflammation. As outlined in chapter four there are many steps in PMN chemotaxis to sites of inflammation, and LT could be causing defects in one or all of them. Chapter four demonstrates that PMNs exposed to circulating LT are incapable of migrating across a membrane towards MIP-2. This result does not make the distinction between whether this defect is caused by an inability of PMNs to sense or respond to MIP-2. A variety of chemotactic stimuli should be used to attempt to make this distinction. Another possibility for the decrease in PMN accumulation *in vivo* could be that LT prevents exocytosis of secretory vesicles and tertiary granules which contain elements needed for PMN adhesion to the endothelium and transmigration. LT could also act directly on the endothelium itself. This would not be completely unprecedented, as studies have been published stating that LT causes loss of endothelial layer integrity (91).

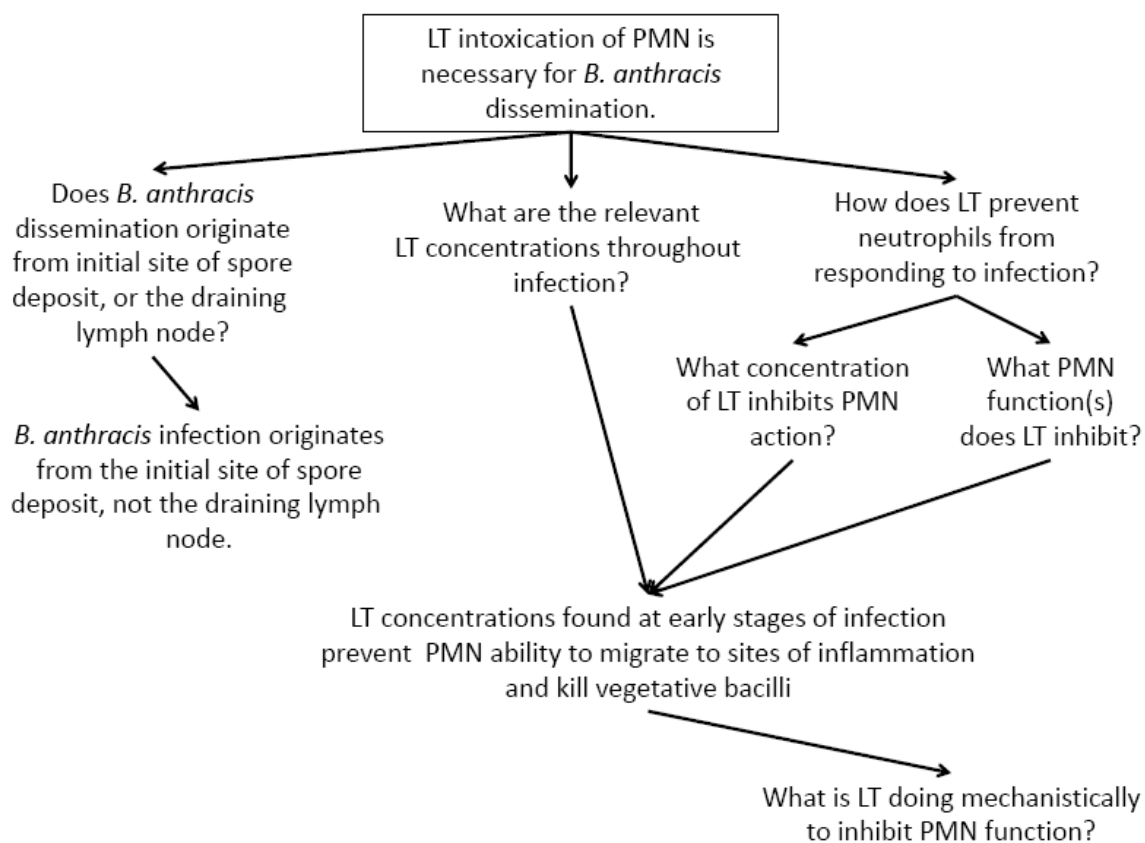
One area that is not explored at all in this work, but will likely prove to be an important field of research is the differential role of local versus systemic toxin. This work demonstrates that circulating LT is capable of acting on PMN reserves within the bone marrow of mice. Some preliminary experiments done in lab suggest that circulating LT does not lead to increased survival of TKO in mice over a 24 hour time period. However TKO injected subcutaneously in conjunction with 20ng of LT does have increased survival compared to TKO in mice where no LT was present after 24 hours (Data not shown). This suggests that local LT may be more important in survival of TKO during the early stages of

infection. This may be because local LT is better able to immediately prevent killing by nearby PMNs, resident macrophages, and dendritic cells, or by attenuating the ability of epithelial cells from producing pro-inflammatory cytokines. While local LT may play a larger role in *B. anthracis* initial survival, systemic LT may have an important role in allowing for quicker dissemination by globally disarming the immune system.

Another immediate future direction involves determining the role of ET during infection. While experiments using defined amounts of ET injected i.p. do not demonstrate any defect in PMNs killing ability, this does not mean that ET does not prevent PMNs from killing TKO. It may be that ET is to acts on the cellular barriers that would otherwise physically prevent dissemination. Many times during my experiments edema is seen only at the site of initial infection, and where it is present much of the muscle tissue has dissolved. This could mean that ET is acting to remove the physical barriers of dissipation within the host. I also demonstrated that EF alone is capable of preventing PMNs accumulation at sites of PMA induced inflammation when injected i.p. This suggests that EF may be capable of reducing the amount of extracellular ATP (a pro-inflammatory signal) by converting it to cAMP, preventing inflammation. Another potential role of ET would be to increase the action of circulating LT. In this case, future experiments should focus on using LT and ET together and test the ability of PMNs to kill and accumulate at sites of inflammation over longer periods.

Perhaps the most important experiments to perform in the future would be to repeat many of the experiments done here using the fully virulent, capsule-producing strain of *B. anthracis*. The primary reason for this is that in addition to secreting toxin components, *B. anthracis* also sheds its poly- γ -d-glutamic acid capsule into circulation. Recent data have demonstrated LT found in serum of rabbits, guinea pigs, and African green monkeys which had been infected with fully virulent *B. anthracis* was associated closely with capsule (42). A later study found that when combined with capsule, LT was better able to act on host cells, and was able to cause death in mice at lower doses than would be seen with LT alone (74). These observations may be due to the ability of capsule to coordinate with PA in order to better trigger the pH-dependent channel formation which is necessary for translocation of LF and EF into the cytosol (79). This may mean that LT concentrations even lower than those utilized in our experiments would be capable of preventing the PMNs response to infection both locally and systemically. The lack of poly- γ -d-glutamic acid capsule in circulation may also have LT-independent activity on PMNs or modulating systemic inflammation, which is a possibility which should be explored.

Figure 6.1: Flow chart summary of dissertation research



**Appendix I: Development of adoptive
transfer *in vivo* PMN accumulation assay**

Introduction

As detailed in chapter four our lab has developed a PMN chemotaxis assay utilizing stop floxed luciferase FVB mice crossed with neutrophil elastase cre mice (NECre luc mice), resulting in hybrid mice where firefly luciferase is selectively expressed in PMNs. These experiments represented a step forward in understanding PMN dynamics in the presence of systemic LT. However, use of the NECre luc mice has significant drawbacks in the study of *B. anthracis* during infection. Principle among these is the fact that both mouse strains used in the cross are not susceptible to BSL2 Sterne strain infection. Because of this, any experiments that follow PMN recruitment to an active site of infection over time would not be possible since both TKO and WT *B. anthracis* infections in hybrid mice would be resolved before substantial toxin levels could be released into circulation.

In order to compare PMN accumulation dynamics during active infection in the BSL2, an *in vivo* PMN imaging technology was developed in Sterne strain susceptible AJ mice and Sterne resistant FVB mice. This technology relies on the adoptive transfer of luminescent PMNs from luc+ mice into non-luminescent mice. Preliminary studies using this technology found that while PMNs accumulate at sites of both PMA and *B. anthracis* induced inflammation, there is no significant difference in accumulation with and without the ability of *B. anthracis* to produce toxins. However, there are several caveats to take into consideration before use of this technology for future experiments. Accordingly, adoptive transfer of PMN *in vivo* accumulation assays have the potential to be a

useful tool in understanding PMN dynamics and could be adapted in the future to answer questions about PMN trafficking during infection.

Results

Generation of luciferase-positive AJ mice

FVB mice in which all cells constitutively express firefly luciferase were first purchased from Xenogen. Because FVB mice are not sensitive to *B. anthracis* Sterne strain infection, it was necessary to breed luciferase expression into Sterne strain susceptible AJ mice. This was accomplished by breeding luc⁺ FVB mice with AJ mice and using speed congenics to generate luciferase positive AJ mice after ten generations of cross breeding.

Adoptive transfer of luminescent PMNs

While luminescent AJ mice were being bred, many proof of concept experiments were performed using FVB mice. In order to determine if adoptively transferred luciferase positive (luc⁺) WBCs could accumulate at sites of PMA induced inflammation in luciferase negative (luc⁻) mice, blood was collected from luminescent female 6-8 week old FVB mice by eye bleed, and WBCs were collected after 3% dextran density sedimentation. As soon as possible 1×10^6 of purified luc⁺ WBC in 100 μ l of PBS was injected via tail vein into luc⁻ age matched FVB mouse. 2.5 μ g of PMA in 5 μ l of DMSO was then spotted onto the left ear of the mouse, and luminescence in the left ear was measured over the course of 3 days using the IVIS 100. An increase in light signal was seen in the inflamed left ear compared to the non-inflamed right ear (Fig. 7.1A), and after quantification of signal several distinct peaks of light were detected (Fig. 7.1B).

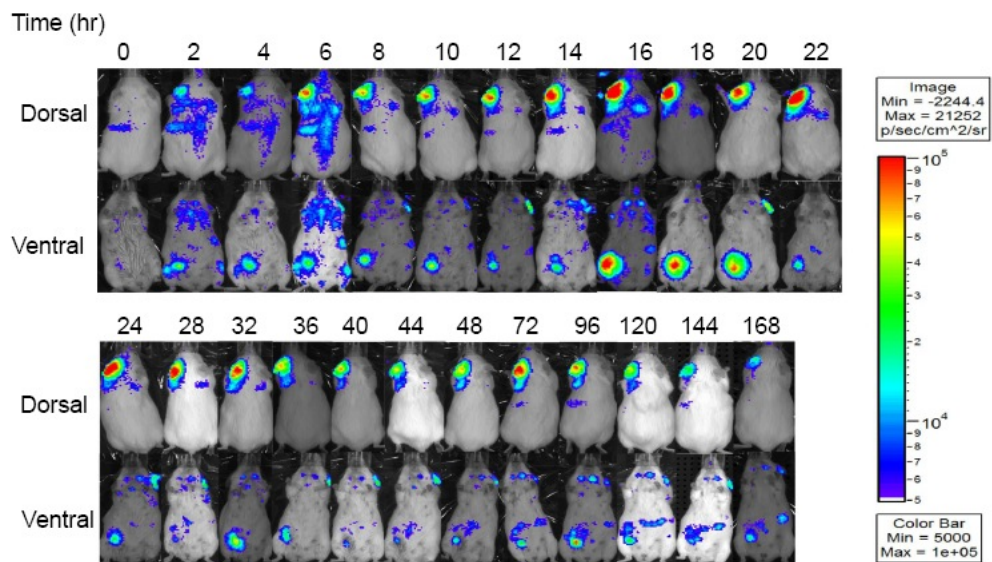
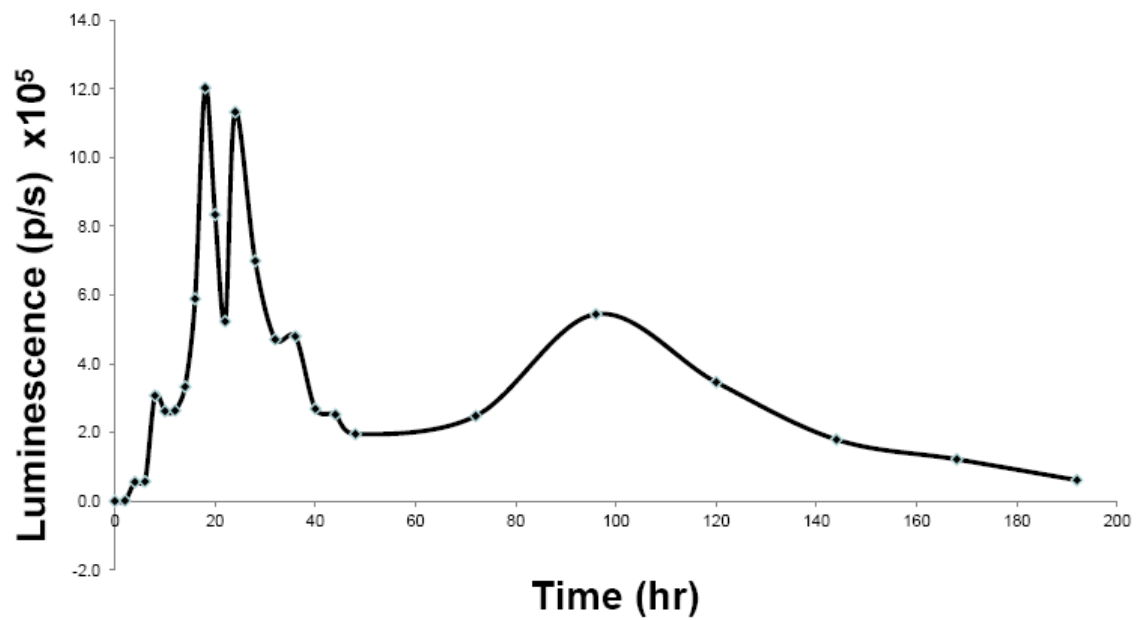
A**B**

Figure 7.1: Adoptively transferred luc+ WBCs accumulate at site of PMA induced inflammation. A single luc- FVB mouse was injected with 1×10^6 luc+ WBCs via tail vein injection and 2.5 μ g of PMA in 5 μ l DMSO was pipetted onto the left ear. (A) Black and white photos of a single FVB mouse over a 168 hour time course overlaid with false-color representation of photon emission intensity as indicated by the scale on the right in p/s/cm-2/sr. (B) Quantification of luminescent signal, representing WBCs, in the left ear of the mouse over the 168 hour time course n=1.

In order to determine if PMN accumulation was inhibited at active sites of *B. anthracis* infection, PMNs were isolated from venous blood of luc+ FVB and AJ mice and injected via tail vein into luc- FVB and AJ mice. Afterwards 1×10^6 WT (Sterne strain) or TKO spores were injected subcutaneously into the left ear of mice and luminescence was monitored in the infected ear every two hours for 24 hours post injection (Fig. 7.2). In both strains of mice, the degree and pattern of PMN accumulation at sites of *B. anthracis* spore injection were highly variable between individual mice, and there were no significant differences in PMN accumulation between WT and TKO injected mice (Fig. 7.2). We hypothesized that the reason luminescence in the ear in response to TKO spore challenge was low and highly variable may be because spores would be relatively immunogenic, and that a more robust and consistent PMN accumulation response could be generated by injecting mice with vegetative TKO (Fig. 7.3). However, AJ mice injected in with vegetative TKO demonstrated no difference in magnitude or consistency of PMN accumulation over time when compared to mice injected with TKO spores (Fig. 7.3).

Quantification of PMNs per luminescence

Since these assays rely on a defined amount of PMNs accumulating at sites of inflammation and not relative amounts, we wanted to know how many of the PMNs injected were at the site of inflammation at any given time. Previous experiments determined that PMNs isolated from both FVB and AJ mice would not produce luminescence *in vitro* despite trying multiple different assay

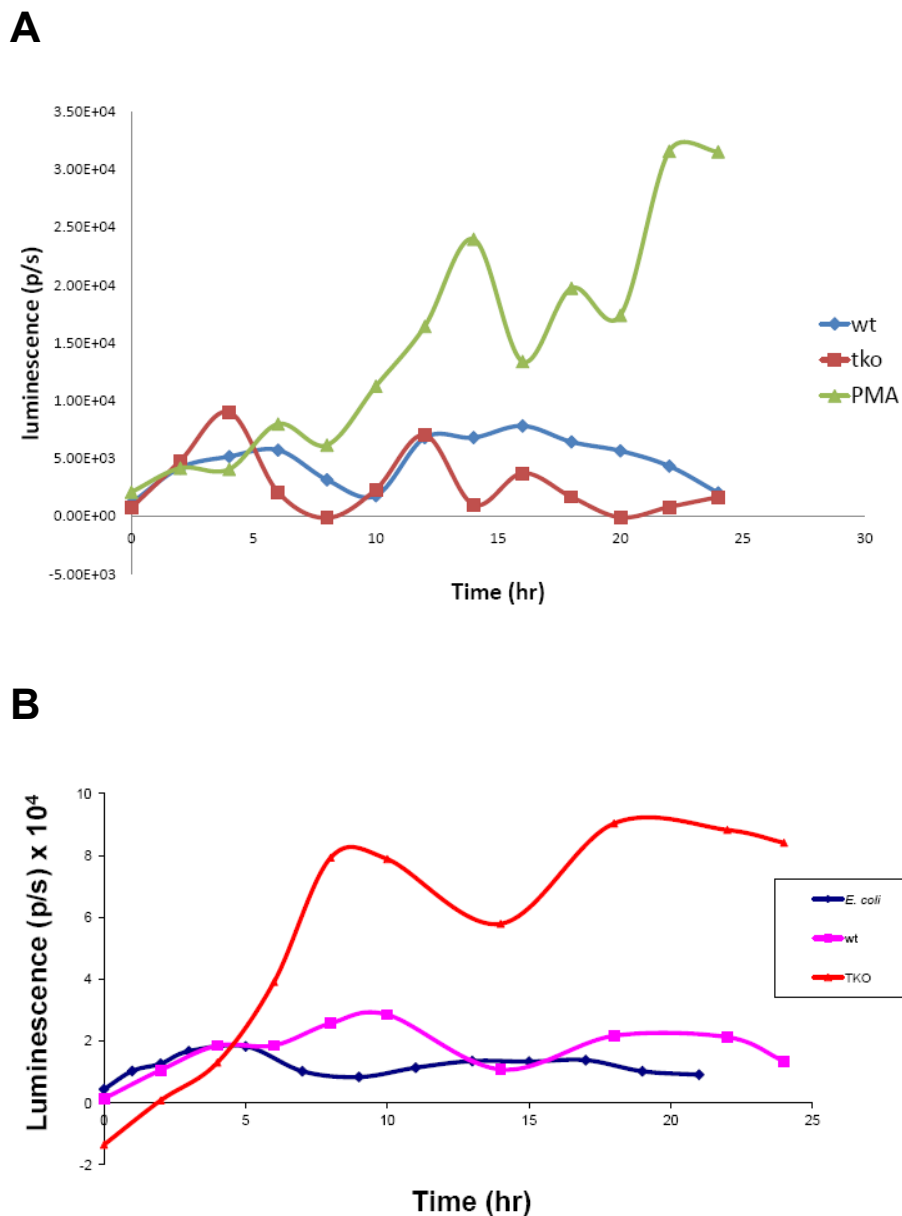


Figure 7.2: PMN accumulation in response to inflammatory stimuli in AJ and FVB mice. Luc- FVB or AJ mice were injected with 5×10^5 luc+ PMNs via tail vein injection. An inflammatory stimulus was then added onto the left ear of mice and luminescence, representing PMNs was then monitored in the left ear over time. Each graph depicts a single representative mouse for each condition. (A) PMN accumulation in the left ear of representative AJ mice in response to

injection of 1×10^6 of purified TKO or WT spores, and 2.5ug of PMA, n=1. (B) PMN accumulation in the left ear representative of FVB mice in response to 1×10^6 of purified TKO or WT spores, and *Escherichia coli* over 24 hours n=1.

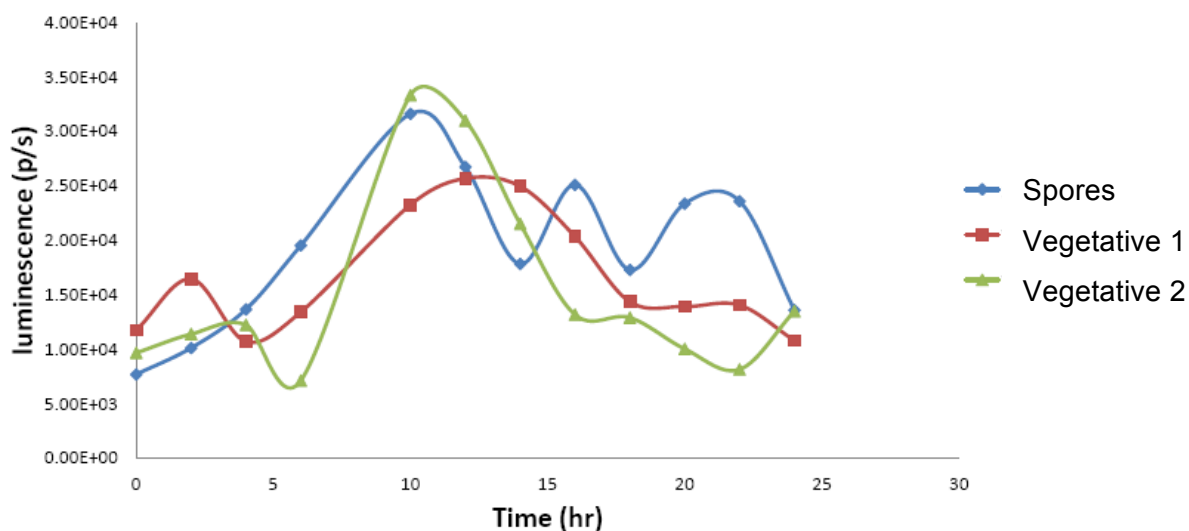
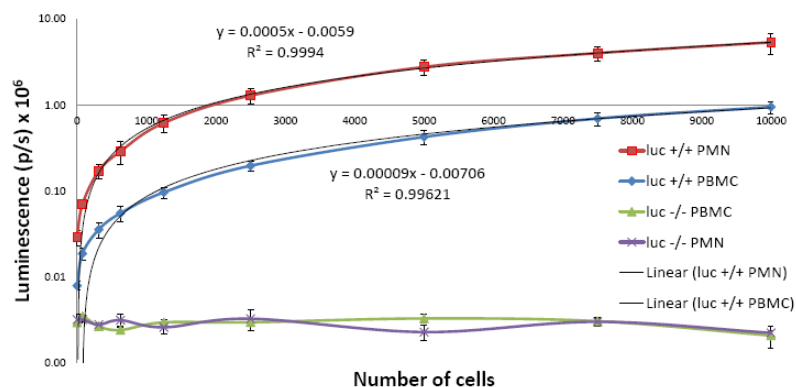


Figure 7.3: PMN migration to TKO spore versus vegetative challenge. Luc-AJ mice were injected with 5×10^5 luc+ PMNs via tail vein injection, then 1×10^6 CFU of either TKO spores or vegetative bacilli was then injected into the left ear. PMN accumulation at sites of inflammation was then monitored and quantified using an IVIS spectrum n=1.

conditions. Considering that this may be due to lack of factors necessary for luminescence production (i.e. ATP or oxygen) within PMNs outside of the host, an *in vitro* lysis-based luciferase assay was used (Promega Oneglow kit). Blood was isolated from luc⁺ AJ and FVB mice, and was fractionated into WBC and PMN fractions by density gradient (Lympholyte Mammal, Cedar Lane Labs) and 3% dextran sedimentation gradient and counted by hemacytometer. To generate a standard curve of luminescence, cells were diluted serially from 1×10^4 to ~ 1 in 50 μ l of PBS and an equal volume of Oneglow reagent was added and allowed to lyse for 5 minutes and read and luminescence was quantified using the IVIS 100 (Fig. 7.4). From this it was found that non-PMN WBCs produce less luminescence on a per cell basis than do PMNs alone, and FVB PMNs produce more luminescence per cell than AJ PMNs do (Fig. 7.4).

Because the *in vitro* assay measures luminescence from lysed PMNs and a large amount of luminescent signal will be lost through the ear, it became necessary to develop a conversion to determine luminescence per PMN in the ear of mice. Luc⁺ PMNs were adoptively transferred into luc⁻ FVB mice and TKO was injected into the left ear and luminescence was monitored over time as was done previously. At hours 3, 5, 20, and 24 after luminescence was read the left ear of mice were removed. The leaves of the ear were then separated so that the inside of the ear was facing towards the camera in the IVIS 100. To determine total luminescent signal 50 μ l of Oneglow was then pipette onto the ear and cells were allowed to lyse for 5 minutes before luminescence was then read again.

A



B

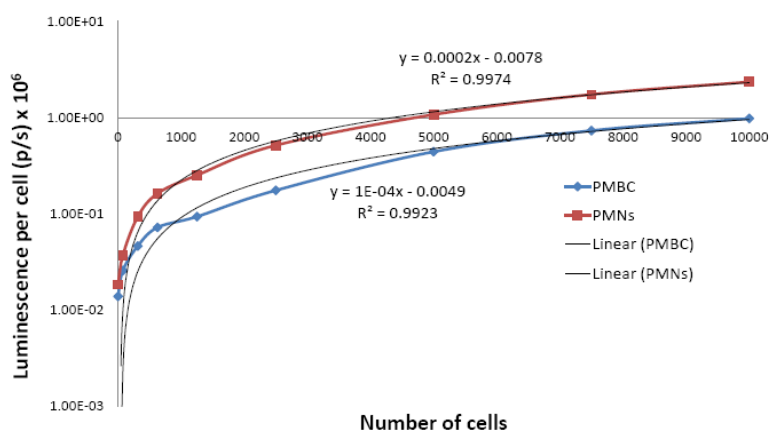


Figure 7.4: Luminescence per PMN and WBC Standard curves. PMNs and WBCs were isolated in 1xPBS after separation by density gradient. Starting at 1×10^4 cells were diluted to ~ 1 cell in 50 μ l PBS in a flat bottom 96well plate. 50 μ l of Promega OneGlow reagent was then added to each well and incubated for 5 minutes at room temperature to allow for lysis then read and quantified using the IVIS 100. (A) Quantification of luminescence per PMN and WBC in luc⁺ and luc⁻ FVB mice n=3. (B) Quantification of luminescence per PMN and WBC in luc⁺ AJ mice n=3.

The percent of total signal from the ear was determined by dividing the luminescence quantified from the whole live mouse by the number determined in the removed ear multiplied by 100. This found that luminescent signal in the ear of live mice represented roughly 10.5% of total signal when treated with Oneglow with a standard error of 1.33%. In order to determine how many PMNs that represented during the course of a PMN accumulation assay, luminescent signal from PMNs was measured in the ear of infected AJ or FVB mice and entered into the following formula:

$$\text{Measured signal (x)} = 0.105 \times \text{total signal (y)}$$

Once total signal was determined by solving for y, total luminescence was then plugged into the luminescence per PMN standard curve equation of the appropriate mouse, as demonstrated in figure 6.5, resulting in determination of the number of PMNs present at the site of inflammation.

Discussion

In summary, we have developed an adoptive transfer-based *in vivo* PMN accumulation assay in mice which are susceptible and non-susceptible to Sterne strain infection. This assay represents significant advantages over *in vitro* PMN migration and accumulation assays, in that it is more representative of the complex environment of PMN accumulation at sites of infection or inflammation than *in vitro* assays. In the context of the Glomski lab research this assay offers a significant advantage over the NEC mice previously used, in that there is the potential to judge PMN dynamics during an active infection in the BSL2. However this assay does have significant drawbacks. PMNs have relatively short half lives

while in circulation, and are terminally differentiated cells (132). Accordingly in order to monitor PMN dynamics reliably past 24 hours from initial injection of PMNs, more PMNs would have to be adoptively transferred. Additionally, injection of PMNs by tail vein itself causes an increase in overall inflammation and it is unclear how this would affect PMNs migration in the context of infection.

Our assays involved tracking PMNs migration to the site of injection of TKO versus Sterne strain spores from initial injection to 48 hours post injection. It is possible the reason no significant differences in PMNs accumulation was seen over this time period is that not enough LT was able to accumulate in circulation in order to start influencing PMNs dynamics as was seen in chapter 3. Future experiments could consider adoptively transferring PMNs 24 or 48 hours post injection with Sterne strain as compared with TKO to look at potential defects in PMNs migration. This would allow for additional time for toxins to accumulate in circulation and bone marrow reserves, and possibly acting on the cellular epithelium. Another important experiment to consider would be to adoptively transfer luc⁺ PMNs from mice which have been intoxicated by LT, and measuring PMNs accumulation to PMA. This experiment would be able to test if the LT induced defect in PMNs accumulation *in vivo* is due to PMNs being intoxicated, or if something else is responsible (i.e. the cellular endothelium).

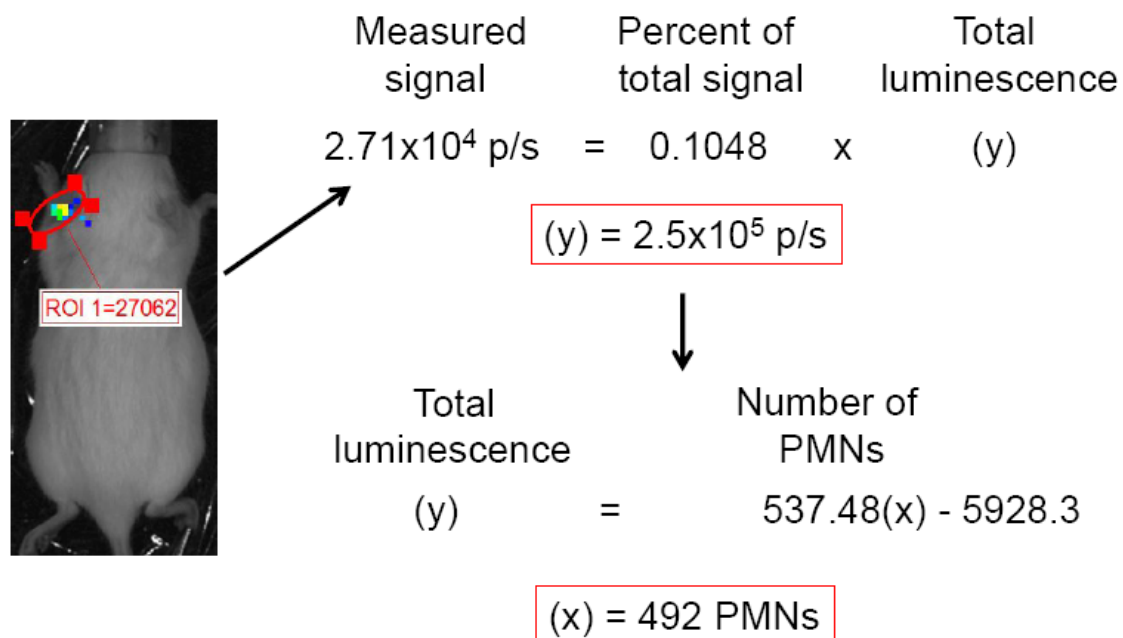


Figure 7.5: Quantification of PMNs at site of inflammation *in vivo*. Luc – FVB mouse was injected i.v. with 1×10^5 luc+ PMNs, and then with 1×10^6 TKO spores subcutaneously in the left ear. At 24 hours the mouse was injected with luciferin and imaged using the IVIS 100. After imaging luminescence was quantified and number of PMNs was determined by multiplying measured luminescence by percent total signal to produce total luminescence. The value of total luminescence was then plugged into the standard curve for luminescence/PMNs and number of PMNs was determined.

**Appendix II: Establishment of a luminol
chemiluminescence assay to access the
effects of LT on murine PMNs oxidative burst**

Introduction

Luminol assays were used in chapter 5 to demonstrate that circulating LT is capable of preventing cellular receptor-based, but not PMA-based activation of NADPH oxidase complex. The following data demonstrate how the conditions used for the luminol assays in chapter 5 were determined, and highlight some interesting observations that arose along the way. These data demonstrate that the presence of heat inactivated mouse serum plays an inhibitory role in PMA induced oxidative burst, but promotes TKO induced oxidative burst. It was also found that the presence of Ca and Mg cations within HBSS is sufficient to produce a robust oxidative burst when PMNs are stimulated with both TKO and PMA. However, the presence of cations also causes low-level activation of PMNs in the assay. While these data do not play into the major part of this dissertation, they may be of interest to anyone who wishes to follow up my work in lab, and may provide insights into the regulation of the NADPH oxidase complex.

Results

Presence of heat-inactivated serum promotes TKO induced oxidative burst

Because previous assays required 10% heat inactivated serum in HBSS for PMNs to kill vegetative TKO, initial luminol assays included serum. PMNs were isolated from C57Bl/6 mice and plated at a concentration of 1×10^5 PMNs into a 96 well plate. PMNs were then stimulated with TKO at an MOI of 1:1 and luminescence was measured using a plate reader. As variable concentrations of heat inactivated mouse serum was used in the HBSS, ranging from 0-10% and ability of PMNs to produce oxidative burst was measured over the course of an

hour. It was found that as serum concentration increased so did the amount of oxidative burst produced, up to 1% serum, where maximum luminescence was observed (Fig. 8.1). At a concentration of 10% a peak of luminescence was observed with signal quickly trailing off (Fig. 8.1). These data demonstrate that the presence of heat-inactivated serum is important for PMNs to produce an oxidative burst in response to TKO.

Presence of heat inactivated serum inhibits PMA induced oxidative burst

While performing the serum gradient experiments to determine the degree of PMNs production of oxidative burst after stimulation by TKO, PMNs were also activated by 10ng of PMA. Contrary to the results seen for TKO stimulated PMNs, when stimulated by PMA the less serum present the higher the response, where a concentration of 0.1% serum yielded the same response as no serum controls (Fig. 8.2). These results made future experiments complicated because a balance of serum concentration would need to be determined for optimal oxidative burst production after induction by PMA and TKO.

Mg and Ca activate PMNs oxidative burst

Some NADPH oxidative burst studies in the literature will use HBSS with the addition of Ca and Mg cations, which is sufficient for PMNs activation. In order to determine if this would be a viable alternative to using HBSS with serum, C57Bl/6 PMNs were added to a 96 well plate as before and PMA and TKO were added and compared to no stimulus controls. Whereas all no-stimuli controls for HBSS plus serum showed no endogenous levels of activation (Data not shown), HBSS plus cations controls had a high level of activation, although compared to

stimulated PMNs the ROS production dropped off quickly (Fig. 8.3). However, HBSS plus cation samples had an equivalent level oxidative burst between PMA and TKO induced PMNs (Fig. 8.3).

Discussion and future directions

These results suggest that there are some interesting avenues remaining to be explored with PMNs regulation of NADPH oxidative burst. There are many questions that these data bring up that were not addressed during the course of this project. The first thing that should be examined is the possibility that serum is physically preventing PMA from transfusing into the PMNs, which is why no oxidative burst is recorded in those samples. The second question to ask is why receptor-mediated oxidative burst requires serum while PKC-mediated does not. Finally why does the presence of cations cause PMNs to produce oxidative burst without the presence of a stimulus while serum does not? Future NADPH oxidative burst luminol assays performed using mouse PMNs should consider these data when designing experiments and when interpreting data.

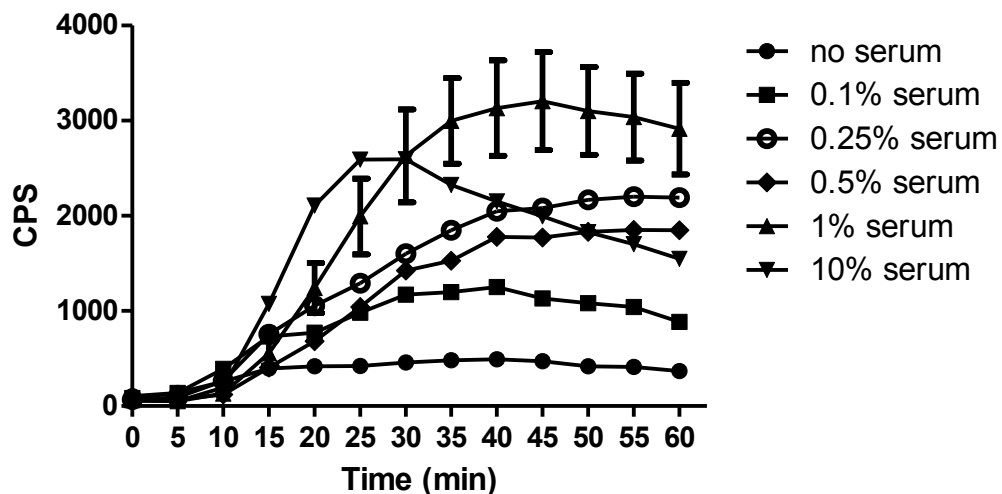


Figure 8.1: Presence of heat-inactivated serum is necessary for TKO induced oxidative burst. PMNs from C57Bl/6 mice were isolated and activated by TKO in the presence of luminol, with varying concentrations of heat inactivated C57Bl/6 serum. Degree of oxidative burst was determined by measurement of chemiluminescence. An increase in oxidative burst stimulated by TKO was associated with an increase of heat inactivated serum.

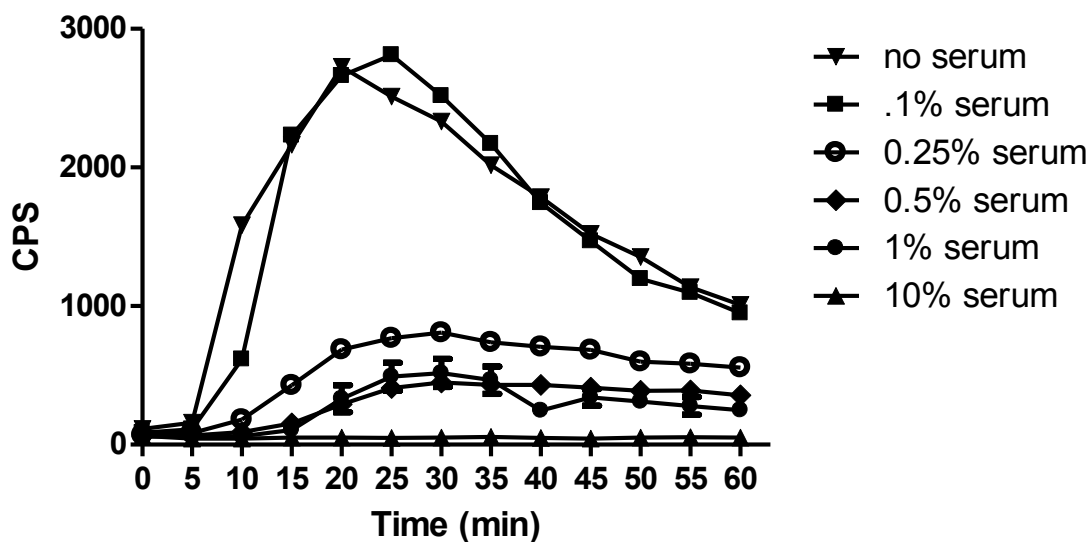


Figure 8.2: Presence of heat-inactivated serum inhibits PMA-induced oxidative burst. PMNs from C57Bl/6 mice were isolated and activated by PMA in the presence of luminol, with varying concentrations of heat inactivated C57Bl/6 serum. Degree of oxidative burst was determined by measurement of chemiluminescence. A decrease in oxidative burst stimulated by PMA was associated with an increase of heat inactivated serum.

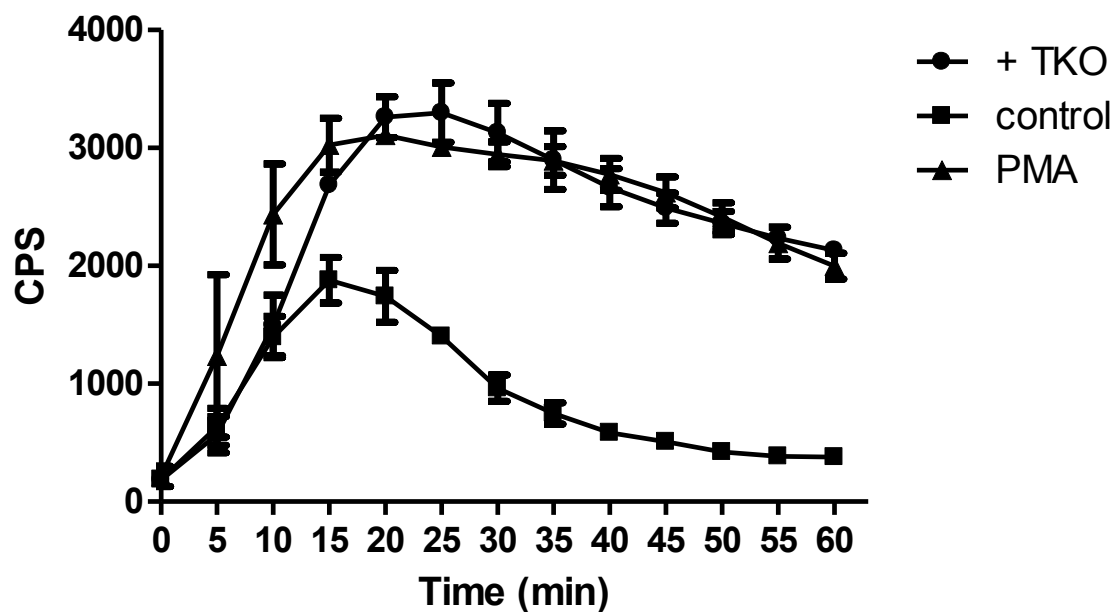


Figure 8.3: HBSS +Ca +Mg causes oxidative burst in control unstimulated PMNs. PMNs from C57Bl/6 mice were isolated and activated by TKO or PMA in the presence of luminol, in HBSS containing Ca and Mg. Degree of oxidative burst was then determined by measurement of chemiluminescence. Control PMNs which had not been stimulated by either PMA or TKO exhibited ROS production.

References

1. **Abadie, V., E. Badell, P. Douillard, D. Ensergueix, P. J. Leenen, M. Tanguy, L. Fiette, S. Saeland, B. Gicquel, and N. Winter.** 2005. Neutrophils rapidly migrate via lymphatics after Mycobacterium bovis BCG intradermal vaccination and shuttle live bacilli to the draining lymph nodes. *Blood* **106**:1843-1850.
2. **Abramova, F. A., L. M. Grinberg, O. V. Yampolskaya, and D. H. Walker.** 1993. Pathology of inhalational anthrax in 42 cases from the Sverdlovsk outbreak of 1979. *Proc Natl Acad Sci U S A* **90**:2291-2294.
3. **Agrawal, A., J. Lingappa, S. H. Leppla, S. Agrawal, A. Jabbar, C. Quinn, and B. Pulendran.** 2003. Impairment of dendritic cells and adaptive immunity by anthrax lethal toxin. *Nature* **424**:329-334.
4. **Albrink, W. S., and R. J. Goodlow.** 1959. Experimental inhalation anthrax in the chimpanzee. *Am J Pathol* **35**:1055-1065.
5. **Barth, H., K. Aktories, M. R. Popoff, and B. G. Stiles.** 2004. Binary bacterial toxins: biochemistry, biology, and applications of common Clostridium and Bacillus proteins. *Microbiol Mol Biol Rev* **68**:373-402, table of contents.
6. **Beatty, M. E., D. A. Ashford, P. M. Griffin, R. V. Tauxe, and J. Sobel.** 2003. Gastrointestinal anthrax: review of the literature. *Arch Intern Med* **163**:2527-2531.
7. **Beaumont, G.** 2010. Anthrax in a Scottish intravenous drug user. *J Forensic Leg Med* **17**:443-445.
8. **Belkaid, Y., S. Mendez, R. Lira, N. Kadambi, G. Milon, and D. Sacks.** 2000. A natural model of *Leishmania major* infection reveals a prolonged "silent" phase of parasite amplification in the skin before the onset of lesion formation and immunity. *J Immunol* **165**:969-977.
9. **Bischof, T. S., B. L. Hahn, and P. G. Sohnle.** 2007. Experimental cutaneous Bacillus anthracis infections in hairless HRS/J mice. *Int J Exp Pathol* **88**:75-84.
10. **Borregaard, N., and J. B. Cowland.** 1997. Granules of the human neutrophilic polymorphonuclear leukocyte. *Blood* **89**:3503-3521.
11. **Borregaard, N., O. E. Sorensen, and K. Theilgaard-Monch.** 2007. Neutrophil granules: a library of innate immunity proteins. *Trends Immunol* **28**:340-345.
12. **Boyer, A. E., C. P. Quinn, A. R. Woolfitt, J. L. Pirkle, L. G. McWilliams, K. L. Stamey, D. A. Bagarozzi, J. C. Hart, Jr., and J. R. Barr.** 2007. Detection and quantification of anthrax lethal factor in serum by mass spectrometry. *Anal Chem* **79**:8463-8470.
13. **Brachman, P. S.** 1980. Inhalation anthrax. *Ann N Y Acad Sci* **353**:83-93.
14. **Brittingham, K. C., G. Ruthel, R. G. Panchal, C. L. Fuller, W. J. Ribot, T. A. Hoover, H. A. Young, A. O. Anderson, and S. Bavari.** 2005. Dendritic cells endocytose Bacillus anthracis spores: implications for anthrax pathogenesis. *J Immunol* **174**:5545-5552.
15. **Brookmeyer, R., and N. Blades.** 2002. Prevention of inhalational anthrax in the U.S. outbreak. *Science* **295**:1861.

16. **Candela, T., and A. Fouet.** 2005. Bacillus anthracis CapD, belonging to the gamma-glutamyltranspeptidase family, is required for the covalent anchoring of capsule to peptidoglycan. *Mol Microbiol* **57**:717-726.
17. **Carrera, M., R. O. Zandomeni, J. Fitzgibbon, and J. L. Sagripanti.** 2007. Difference between the spore sizes of Bacillus anthracis and other Bacillus species. *J Appl Microbiol* **102**:303-312.
18. **Chand, H. S., M. Drysdale, J. Lovchik, T. M. Koehler, M. F. Lipscomb, and C. R. Lyons.** 2009. Discriminating virulence mechanisms among Bacillus anthracis strains by using a murine subcutaneous infection model. *Infect Immun* **77**:429-435.
19. **Chou, P. J., C. A. Newton, I. Perkins, H. Friedman, and T. W. Klein.** 2008. Suppression of dendritic cell activation by anthrax lethal toxin and edema toxin depends on multiple factors including cell source, stimulus used, and function tested. *DNA Cell Biol* **27**:637-648.
20. **Chtanova, T., M. Schaeffer, S. J. Han, G. G. van Dooren, M. Nollmann, P. Herzmark, S. W. Chan, H. Satija, K. Camfield, H. Aaron, B. Striepen, and E. A. Robey.** 2008. Dynamics of neutrophil migration in lymph nodes during infection. *Immunity* **29**:487-496.
21. **Chung, M. C., T. G. Popova, B. A. Millis, D. V. Mukherjee, W. Zhou, L. A. Liotta, E. F. Petricoin, V. Chandhoke, C. Bailey, and S. G. Popov.** 2006. Secreted neutral metalloproteases of Bacillus anthracis as candidate pathogenic factors. *J Biol Chem* **281**:31408-31418.
22. **Cicchetti, G., P. G. Allen, and M. Glogauer.** 2002. Chemotactic signaling pathways in neutrophils: from receptor to actin assembly. *Crit Rev Oral Biol Med* **13**:220-228.
23. **Cleret, A., A. Quesnel-Hellmann, A. Vallon-Eberhard, B. Verrier, S. Jung, D. Vidal, J. Mathieu, and J. N. Tournier.** 2007. Lung dendritic cells rapidly mediate anthrax spore entry through the pulmonary route. *J Immunol* **178**:7994-8001.
24. **Collier, R. J., and J. A. Young.** 2003. Anthrax toxin. *Annu Rev Cell Dev Biol* **19**:45-70.
25. **Colotta, F., F. Re, N. Polentarutti, S. Sozzani, and A. Mantovani.** 1992. Modulation of granulocyte survival and programmed cell death by cytokines and bacterial products. *Blood* **80**:2012-2020.
26. **Cossart, P., and P. J. Sansonetti.** 2004. Bacterial invasion: the paradigms of enteroinvasive pathogens. *Science* **304**:242-248.
27. **Cote, C. K., J. Bozue, N. Twenhafel, and S. L. Welkos.** 2009. Effects of altering the germination potential of Bacillus anthracis spores by exogenous means in a mouse model. *J Med Microbiol* **58**:816-825.
28. **Cote, C. K., K. M. Rea, S. L. Norris, N. van Rooijen, and S. L. Welkos.** 2004. The use of a model of in vivo macrophage depletion to study the role of macrophages during infection with Bacillus anthracis spores. *Microb Pathog* **37**:169-175.
29. **Cote, C. K., N. Van Rooijen, and S. L. Welkos.** 2006. Roles of macrophages and neutrophils in the early host response to Bacillus anthracis spores in a mouse model of infection. *Infect Immun* **74**:469-480.

30. **Crawford, M. A., C. V. Aylott, R. W. Bourdeau, and G. M. Bokoch.** 2006. Bacillus anthracis toxins inhibit human neutrophil NADPH oxidase activity. *J Immunol* **176**:7557-7565.
31. **Cybulski, R. J., Jr., P. Sanz, F. Alem, S. Stibitz, R. L. Bull, and A. D. O'Brien.** 2009. Four superoxide dismutases contribute to Bacillus anthracis virulence and provide spores with redundant protection from oxidative stress. *Infect Immun* **77**:274-285.
32. **Day, R. B., and D. C. Link.** 2012. Regulation of neutrophil trafficking from the bone marrow. *Cell Mol Life Sci* **69**:1415-1423.
33. **Dewas, C., M. Fay, M. A. Gougerot-Pocidallo, and J. El-Benna.** 2000. The mitogen-activated protein kinase extracellular signal-regulated kinase 1/2 pathway is involved in formyl-methionyl-leucyl-phenylalanine-induced p47phox phosphorylation in human neutrophils. *J Immunol* **165**:5238-5244.
34. **Dixon, T. C., A. A. Fadl, T. M. Koehler, J. A. Swanson, and P. C. Hanna.** 2000. Early Bacillus anthracis-macrophage interactions: intracellular survival and escape. *Cell Microbiol* **2**:453-463.
35. **Downey, G. P., J. R. Butler, H. Tapper, L. Fialkow, A. R. Saltiel, B. B. Rubin, and S. Grinstein.** 1998. Importance of MEK in neutrophil microbicidal responsiveness. *J Immunol* **160**:434-443.
36. **Druett, H. A., D. W. Henderson, L. Packman, and S. Peacock.** 1953. Studies on respiratory infection. I. The influence of particle size on respiratory infection with anthrax spores. *J Hyg (Lond)* **51**:359-371.
37. **Duesbery, N., V. Woude, C. Webb, and K. Klimpel.** 1998. Proteolytic inactivation of MAP-kinase-kinase by anthrax lethal factor. *Science* **280**:734-737.
38. **Duesbery, N. S., C. P. Webb, S. H. Leppla, V. M. Gordon, K. R. Klimpel, T. D. Copeland, N. G. Ahn, M. K. Oskarsson, K. Fukasawa, K. D. Paull, and G. F. Vande Woude.** 1998. Proteolytic inactivation of MAP-kinase-kinase by anthrax lethal factor. *Science* **280**:734-737.
39. **Dumetz, F., G. Jouvion, H. Khun, I. J. Glomski, J. P. Corre, C. Rougeaux, W. J. Tang, M. Mock, M. Huerre, and P. L. Goossens.** 2011. Noninvasive imaging technologies reveal edema toxin as a key virulence factor in anthrax. *Am J Pathol* **178**:2523-2535.
40. **During, R. L., W. Li, B. Hao, J. M. Koenig, D. S. Stephens, C. P. Quinn, and F. S. Southwick.** 2005. Anthrax lethal toxin paralyzes neutrophil actin-based motility. *J Infect Dis* **192**:837-845.
41. **Eisenhauer, P. B., and R. I. Lehrer.** 1992. Mouse neutrophils lack defensins. *Infect Immun* **60**:3446-3447.
42. **Ezzell, J. W., T. G. Abshire, R. Panchal, D. Chabot, S. Bavari, E. K. Leffel, B. Purcell, A. M. Friedlander, and W. J. Ribot.** 2009. Association of Bacillus anthracis capsule with lethal toxin during experimental infection. *Infect Immun* **77**:749-755.
43. **Fang, F. C.** 2004. Antimicrobial reactive oxygen and nitrogen species: concepts and controversies. *Nat Rev Microbiol* **2**:820-832.
44. **Fiole, D., J. N. Tournier, A. Cleret, J. Mathieu, and A. Quesnel-Hellmann.** 2009. B. anthracis edema toxin alters migration of airway dendritic cells. Abstract submitted to the 2009 ASM Bacillus-ACT Symposium.

45. **Firoved, A. M., G. F. Miller, M. Moayeri, R. Kakkar, Y. Shen, J. F. Wiggins, E. M. McNally, W. J. Tang, and S. H. Leppla.** 2005. Bacillus anthracis edema toxin causes extensive tissue lesions and rapid lethality in mice. *Am J Pathol* **167**:1309-1320.
46. **Fontes, R. A., Jr., C. M. Ogilvie, and T. Mclau.** 2000. Necrotizing soft-tissue infections. *J Am Acad Orthop Surg* **8**:151-158.
47. **Fraenkel, E.** 1924. Uber Inhalationsmilzbrand. *Virchows Arch. Pathol. Anat. Physiol.* **254**:363-378.
48. **Friedlander, A. M.** 1997. Chapter 22: Anthrax, p. 467 - 478. *In* M. Brigadier General Russ Zajtchuk, U.S. Army (ed.), *Medical Aspects of Chemical and Biological Warfare*. Office of The Surgeon General, Borden Institute, Walter Reed Army Medical Center, Washington D.C.
49. **Friedlander, A. M., S. L. Welkos, M. L. Pitt, J. W. Ezzell, P. L. Worsham, K. J. Rose, B. E. Ivins, J. R. Lowe, G. B. Howe, P. Mikesell, and et al.** 1993. Postexposure prophylaxis against experimental inhalation anthrax. *J Infect Dis* **167**:1239-1243.
50. **Fritz, D. L., N. K. Jaax, W. B. Lawrence, K. J. Davis, M. L. Pitt, J. W. Ezzell, and A. M. Friedlander.** 1995. Pathology of experimental inhalation anthrax in the rhesus monkey. *Lab Invest* **73**:691-702.
51. **Gerhardt, P.** 1967. Cytology of Bacillus anthracis. *Fed Proc* **26**:1504-1517.
52. **Glomski, I. J.** 2011. *Bacillus anthracis* Dissemination through Hosts, p. 227-249. *In* N. H. Bergman (ed.), *Bacillus anthracis* and Anthrax. John Wiley & Sons, Inc., Hoboken, NJ.
53. **Glomski, I. J., J. P. Corre, M. Mock, and P. L. Goossens.** 2007. Noncapsulated toxinogenic Bacillus anthracis presents a specific growth and dissemination pattern in naive and protective antigen-immune mice. *Infect Immun* **75**:4754-4761.
54. **Glomski, I. J., F. Dumetz, G. Jouvion, M. R. Huerre, M. Mock, and P. L. Goossens.** 2008. Inhaled non-capsulated Bacillus anthracis in A/J mice: nasopharynx and alveolar space as dual portals of entry, delayed dissemination, and specific organ targeting. *Microbes Infect* **10**:1398-1404.
55. **Glomski, I. J., J. H. Fritz, S. J. Keppler, V. Balloy, M. Chignard, M. Mock, and P. L. Goossens.** 2007. Murine splenocytes produce inflammatory cytokines in a MyD88-dependent response to Bacillus anthracis spores. *Cell Microbiol* **9**:502-513.
56. **Glomski, I. J., A. Piris-Gimenez, M. Huerre, M. Mock, and P. L. Goossens.** 2007. Primary involvement of pharynx and peyer's patch in inhalational and intestinal anthrax. *PLoS Pathog* **3**:e76.
57. **Goossens, P. L.** 2009. Animal models of human anthrax: the Quest for the Holy Grail. *Mol Aspects Med* **30**:467-480.
58. **Greenfield, W. S.** 1882. Supplementary report on woolsorters disease in the Bradford district. Rept. Med. Off. Local Govt. Board, London.
59. **Grinberg, L. M., F. A. Abramova, O. V. Yampolskaya, D. H. Walker, and J. H. Smith.** 2001. Quantitative pathology of inhalational anthrax I: quantitative microscopic findings. *Mod Pathol* **14**:482-495.

60. **Guidi-Rontani, C.** 2002. The alveolar macrophage: the Trojan horse of *Bacillus anthracis*. *Trends Microbiol* **10**:405-409.
61. **Guidi-Rontani, C., M. Levy, H. Ohayon, and M. Mock.** 2001. Fate of germinated *Bacillus anthracis* spores in primary murine macrophages. *Mol Microbiol* **42**:931-938.
62. **Guidi-Rontani, C., M. Weber-Levy, E. Labruyere, and M. Mock.** 1999. Germination of *Bacillus anthracis* spores within alveolar macrophages. *Mol Microbiol* **31**:9-17.
63. **Hager, M., J. B. Cowland, and N. Borregaard.** 2010. Neutrophil granules in health and disease. *J Intern Med* **268**:25-34.
64. **Hanna, P. C., B. A. Kruskal, R. A. Ezekowitz, B. R. Bloom, and R. J. Collier.** 1994. Role of macrophage oxidative burst in the action of anthrax lethal toxin. *Mol Med* **1**:7-18.
65. **Harper, G. J., and J. D. Morton.** 1953. The respiratory retention of bacterial aerosols: experiments with radioactive spores. *J Hyg (Lond)* **51**:372-385.
66. **Henderson, D. W., S. Peacock, and F. C. Belton.** 1956. Observations on the prophylaxis of experimental pulmonary anthrax in the monkey. *J Hyg (Lond)* **54**:28-36.
67. **Hirsh, M. I., I. Manov, V. Cohen-Kaplan, and T. C. Iancu.** 2007. Ultrastructural features of lymphocyte suppression induced by anthrax lethal toxin and treated with chloroquine. *Lab Invest* **87**:182-188.
68. **Hu, H., J. Emerson, and A. I. Aronson.** 2007. Factors involved in the germination and inactivation of *Bacillus anthracis* spores in murine primary macrophages. *FEMS Microbiol Lett* **272**:245-250.
69. **Hu, H., Q. Sa, T. M. Koehler, A. I. Aronson, and D. Zhou.** 2006. Inactivation of *Bacillus anthracis* spores in murine primary macrophages. *Cell Microbiol* **8**:1634-1642.
70. **Inglesby, T. V., T. O'Toole, D. A. Henderson, J. G. Bartlett, M. S. Ascher, E. Eitzen, A. M. Friedlander, J. Gerberding, J. Hauer, J. Hughes, J. McDade, M. T. Osterholm, G. Parker, T. M. Perl, P. K. Russell, and K. Tonat.** 2002. Anthrax as a biological weapon, 2002: updated recommendations for management. *JAMA* **287**:2236-2252.
71. **Ivanova, N., A. Sorokin, I. Anderson, N. Galleron, B. Candelon, V. Kapatral, A. Bhattacharyya, G. Reznik, N. Mikhailova, A. Lapidus, L. Chu, M. Mazur, E. Goltsman, N. Larsen, M. D'Souza, T. Walunas, Y. Grechkin, G. Pusch, R. Haselkorn, M. Fonstein, S. D. Ehrlich, R. Overbeek, and N. Kyrpides.** 2003. Genome sequence of *Bacillus cereus* and comparative analysis with *Bacillus anthracis*. *Nature* **423**:87-91.
72. **Jallali, N., S. Hettiaratchy, A. C. Gordon, and A. Jain.** The surgical management of injectional anthrax. *J Plast Reconstr Aesthet Surg* **64**:276-277.
73. **Janes, B. K., and S. Stibitz.** 2006. Routine markerless gene replacement in *Bacillus anthracis*. *Infect Immun* **74**:1949-1953.
74. **Jang, J., M. Cho, J. H. Chun, M. H. Cho, J. Park, H. B. Oh, C. K. Yoo, and G. E. Rhie.** 2011. The poly-gamma-D-glutamic acid capsule of *Bacillus anthracis* enhances lethal toxin activity. *Infect Immun* **79**:3846-3854.

75. **Jernigan, D. B., P. L. Raghunathan, B. P. Bell, R. Brechner, E. A. Bresnitz, J. C. Butler, M. Cetron, M. Cohen, T. Doyle, M. Fischer, C. Greene, K. S. Griffith, J. Guarner, J. L. Hadler, J. A. Hayslett, R. Meyer, L. R. Petersen, M. Phillips, R. Pinner, T. Popovic, C. P. Quinn, J. Reefhuis, D. Reissman, N. Rosenstein, A. Schuchat, W. J. Shieh, L. Siegal, D. L. Swerdlow, F. C. Tenover, M. Traeger, J. W. Ward, I. Weisfuse, S. Wiersma, K. Yeskey, S. Zaki, D. A. Ashford, B. A. Perkins, S. Ostroff, J. Hughes, D. Fleming, J. P. Koplan, and J. L. Gerberding.** 2002. Investigation of bioterrorism-related anthrax, United States, 2001: epidemiologic findings. *Emerg Infect Dis* **8**:1019-1028.
76. **Jog, N. R., M. J. Rane, G. Lominadze, G. C. Luerman, R. A. Ward, and K. R. McLeish.** 2007. The actin cytoskeleton regulates exocytosis of all neutrophil granule subsets. *Am J Physiol Cell Physiol* **292**:C1690-1700.
77. **Kang, T. J., M. J. Fenton, M. A. Weiner, S. Hibbs, S. Basu, L. Baillie, and A. S. Cross.** 2005. Murine macrophages kill the vegetative form of *Bacillus anthracis*. *Infect Immun* **73**:7495-7501.
78. **Kim, C., S. Wilcox-Adelman, Y. Sano, W. J. Tang, R. J. Collier, and J. M. Park.** 2008. Antiinflammatory cAMP signaling and cell migration genes co-opted by the anthrax bacillus. *Proc Natl Acad Sci U S A* **105**:6150-6155.
79. **Kintzer, A. F., Tang, II, A. K. Schawel, M. J. Brown, and B. A. Krantz.** 2012. Anthrax toxin protective antigen integrates poly-gamma-D-glutamate and pH signals to sense the optimal environment for channel formation. *Proc Natl Acad Sci U S A* **109**:18378-18383.
80. **Kintzer, A. F., K. L. Thoren, H. J. Sterling, K. C. Dong, G. K. Feld, Tang, II, T. T. Zhang, E. R. Williams, J. M. Berger, and B. A. Krantz.** 2009. The protective antigen component of anthrax toxin forms functional octameric complexes. *J Mol Biol* **392**:614-629.
81. **Koch, R.** 1878. Die Aetiologie der Milzbrand-Krankheit bergundet auf die Entwicklungsgeschichte des *Bacillus anthracis*. *Beitrage zur Biologie der Pflazen* **2**:277-311.
82. **Kolaczowska, E., and P. Kubes.** 2013. Neutrophil recruitment and function in health and inflammation. *Nat Rev Immunol* **13**:159-175.
83. **Leppia, S. H.** 1982. Anthrax toxin edema factor: a bacterial adenylate cyclase that increases cyclic AMP concentrations of eukaryotic cells. *Proc Natl Acad Sci U S A* **79**:3162-3166.
84. **Levchenko, A., and P. A. Iglesias.** 2002. Models of eukaryotic gradient sensing: application to chemotaxis of amoebae and neutrophils. *Biophys J* **82**:50-63.
85. **Ley, K., C. Laudanna, M. I. Cybulsky, and S. Nourshargh.** 2007. Getting to the site of inflammation: the leukocyte adhesion cascade updated. *Nat Rev Immunol* **7**:678-689.
86. **Lin, F., C. M. Nguyen, S. J. Wang, W. Saadi, S. P. Gross, and N. L. Jeon.** 2004. Effective neutrophil chemotaxis is strongly influenced by mean IL-8 concentration. *Biochem Biophys Res Commun* **319**:576-581.
87. **Lincoln, R. E., D. R. Hodges, F. Klein, B. G. Mahlandt, W. I. Jones, Jr., B. W. Haines, M. A. Rhian, and J. S. Walker.** 1965. Role of the lymphatics in the pathogenesis of anthrax. *J Infect Dis* **115**:481-494.

88. **Liu, S., S. Miller-Randolph, D. Crown, M. Moayeri, I. Sastalla, S. Okugawa, and S. H. Leppla.** 2010. Anthrax toxin targeting of myeloid cells through the CMG2 receptor is essential for establishment of *Bacillus anthracis* infections in mice. *Cell Host Microbe* **8**:455-462.
89. **Loving, C. L., M. Kennett, G. M. Lee, V. K. Grippe, and T. J. Merkel.** 2007. Murine aerosol challenge model of anthrax. *Infect Immun* **75**:2689-2698.
90. **Loving, C. L., T. Khurana, M. Osorio, G. M. Lee, V. K. Kelly, S. Stibitz, and T. J. Merkel.** 2009. Role of anthrax toxins in dissemination, disease progression, and induction of protective adaptive immunity in the mouse aerosol challenge model. *Infect Immun* **77**:255-265.
91. **Lowe, D. E., and I. J. Glomski.** 2012. Cellular and physiological effects of anthrax exotoxin and its relevance to disease. *Front Cell Infect Microbiol* **2**:76.
92. **Lyons, C. R., J. Lovchik, J. Hutt, M. F. Lipscomb, E. Wang, S. Heninger, L. Berliba, and K. Garrison.** 2004. Murine model of pulmonary anthrax: kinetics of dissemination, histopathology, and mouse strain susceptibility. *Infect Immun* **72**:4801-4809.
93. **Makino, S., I. Uchida, N. Terakado, C. Sasakawa, and M. Yoshikawa.** 1989. Molecular characterization and protein analysis of the cap region, which is essential for encapsulation in *Bacillus anthracis*. *J Bacteriol* **171**:722-730.
94. **Makino, S., M. Watarai, H. I. Cheun, T. Shirahata, and I. Uchida.** 2002. Effect of the lower molecular capsule released from the cell surface of *Bacillus anthracis* on the pathogenesis of anthrax. *J Infect Dis* **186**:227-233.
95. **Maldonado-Arocho, F. J., and K. A. Bradley.** 2009. Anthrax edema toxin induces maturation of dendritic cells and enhances chemotaxis towards macrophage inflammatory protein 3beta. *Infect Immun* **77**:2036-2042.
96. **Manchee, R. J., M. G. Broster, A. J. Stagg, and S. E. Hibbs.** 1994. Formaldehyde Solution Effectively Inactivates Spores of *Bacillus anthracis* on the Scottish Island of Gruinard. *Appl Environ Microbiol* **60**:4167-4171.
97. **Mauer, A. M., J. W. Athens, H. Ashenbrucker, G. E. Cartwright, and M. M. Wintrobe.** 1960. Leukokinetic Studies. Ii. A Method for Labeling Granulocytes in Vitro with Radioactive Diisopropylfluorophosphate (Dfp). *J Clin Invest* **39**:1481-1486.
98. **Mayer-Scholl, A., R. Hurwitz, V. Brinkmann, M. Schmid, P. Jungblut, Y. Weinrauch, and A. Zychlinsky.** 2005. Human neutrophils kill *Bacillus anthracis*. *PLoS Pathog* **1**:e23.
99. **Mayer, T. A., A. Morrison, S. Bersoff-Matcha, G. Druckenbrod, C. Murphy, J. Howell, D. Hanfling, R. Cates, D. Pauze, and J. Earls.** 2003. Inhalational anthrax due to bioterrorism: would current Centers for Disease Control and Prevention guidelines have identified the 11 patients with inhalational anthrax from October through November 2001? *Clin Infect Dis* **36**:1275-1283.
100. **McGovern, T. W., and S. A. Norton.** 2002. Recognition and management of anthrax. *N Engl J Med* **346**:943-945; author reply 943-945.
101. **Meselson, M., J. Guillemin, M. Hugh-Jones, A. Langmuir, I. Popova, A. Shelokov, and O. Yampolskaya.** 1994. The Sverdlovsk anthrax outbreak of 1979. *Science* **266**:1202-1208.

102. **Moayeri, M., D. Crown, Z. L. Newman, S. Okugawa, M. Eckhaus, C. Cataisson, S. Liu, I. Sastalla, and S. H. Leppla.** 2010. Inflammasome sensor Nlrp1b-dependent resistance to anthrax is mediated by caspase-1, IL-1 signaling and neutrophil recruitment. *PLoS Pathog* **6**:e1001222.
103. **Moayeri, M., D. Haines, H. A. Young, and S. H. Leppla.** 2003. *Bacillus anthracis* lethal toxin induces TNF-alpha-independent hypoxia-mediated toxicity in mice. *J Clin Invest* **112**:670-682.
104. **Mock, M., and A. Fouet.** 2001. Anthrax. *Annu Rev Microbiol* **55**:647-671.
105. **Nordenfelt, P., and H. Tapper.** 2011. Phagosome dynamics during phagocytosis by neutrophils. *J Leukoc Biol* **90**:271-284.
106. **O'Brien, J., A. Friedlander, T. Dreier, J. Ezzell, and S. Leppla.** 1985. Effects of anthrax toxin components on human neutrophils. *Infect Immun* **47**:306-310.
107. **Otto, M.** 2012. MRSA virulence and spread. *Cell Microbiol* **14**:1513-1521.
108. **Paccani, S. R., and C. T. Baldari.** 2011. T cell targeting by anthrax toxins: two faces of the same coin. *Toxins (Basel)* **3**:660-671.
109. **Passalacqua, K. D., and N. H. Bergman.** 2006. *Bacillus anthracis*: interactions with the host and establishment of inhalational anthrax. *Future Microbiol* **1**:397-415.
110. **Pezard, C., P. Berche, and M. Mock.** 1991. Contribution of individual toxin components to virulence of *Bacillus anthracis*. *Infect Immun* **59**:3472-3477.
111. **Phillipson, M., and P. Kubes.** 2011. The neutrophil in vascular inflammation. *Nat Med* **17**:1381-1390.
112. **Pollock, J. D., D. A. Williams, M. A. Gifford, L. L. Li, X. Du, J. Fisherman, S. H. Orkin, C. M. Doerschuk, and M. C. Dinauer.** 1995. Mouse model of X-linked chronic granulomatous disease, an inherited defect in phagocyte superoxide production. *Nat Genet* **9**:202-209.
113. **Popov, S. G., T. G. Popova, S. Hopkins, R. S. Weinstein, R. MacAfee, K. J. Fryxell, V. Chandhoke, C. Bailey, and K. Alibek.** 2005. Effective antiprotease-antibiotic treatment of experimental anthrax. *BMC Infect Dis* **5**:25.
114. **Preshaw, P. M., R. E. Schifferle, and J. D. Walters.** 1999. *Porphyromonas gingivalis* lipopolysaccharide delays human polymorphonuclear leukocyte apoptosis in vitro. *J Periodontal Res* **34**:197-202.
115. **Ramsay, C. N., A. Stirling, J. Smith, G. Hawkins, T. Brooks, J. Hood, G. Penrice, L. M. Browning, and S. Ahmed.** 2010. An outbreak of infection with *Bacillus anthracis* in injecting drug users in Scotland. *Euro Surveill* **15**.
116. **Ribot, W. J., R. G. Panchal, K. C. Brittingham, G. Ruthel, T. A. Kenny, D. Lane, B. Curry, T. A. Hoover, A. M. Friedlander, and S. Bavari.** 2006. Anthrax lethal toxin impairs innate immune functions of alveolar macrophages and facilitates *Bacillus anthracis* survival. *Infect Immun* **74**:5029-5034.
117. **Richter, S., V. J. Anderson, G. Garufi, L. Lu, J. M. Budzik, A. Joachimiak, C. He, O. Schneewind, and D. Missiakas.** 2009. Capsule anchoring in *Bacillus anthracis* occurs by a transpeptidation reaction that is inhibited by capsidin. *Mol Microbiol* **71**:404-420.
118. **Ringertz, S. H., E. A. Hoiby, M. Jensenius, J. Maehlen, D. A. Caugant, A. Myklebust, and K. Fossum.** 2000. Injectional anthrax in a heroin skin-popper. *Lancet* **356**:1574-1575.

119. **Ross, J. M.** 1957. The pathogenesis of anthrax following the administration of spores by the respiratory route *Journal of pathology and bacteriology* **73**:9.
120. **Rossi Paccani, S., F. Tonello, L. Patrussi, N. Capitani, M. Simonato, C. Montecucco, and C. T. Baldari.** 2007. Anthrax toxins inhibit immune cell chemotaxis by perturbing chemokine receptor signalling. *Cell Microbiol* **9**:924-929.
121. **Russell, B. H., Q. Liu, S. A. Jenkins, M. J. Tuvim, B. F. Dickey, and Y. Xu.** 2008. In vivo demonstration and quantification of intracellular *Bacillus anthracis* in lung epithelial cells. *Infect Immun* **76**:3975-3983.
122. **Russell, B. H., R. Vasan, D. R. Keene, and Y. Xu.** 2007. *Bacillus anthracis* internalization by human fibroblasts and epithelial cells. *Cell Microbiol* **9**:1262-1274.
123. **Ruthel, G., W. J. Ribot, S. Bavari, and T. A. Hoover.** 2004. Time-lapse confocal imaging of development of *Bacillus anthracis* in macrophages. *J Infect Dis* **189**:1313-1316.
124. **Saadia, R., and M. Schein.** 2000. Debridement of gunshot wounds: semantics and surgery. *World J Surg* **24**:1146-1149.
125. **Safran, M., W. Y. Kim, A. L. Kung, J. W. Horner, R. A. DePinho, and W. G. Kaelin, Jr.** 2003. Mouse reporter strain for noninvasive bioluminescent imaging of cells that have undergone Cre-mediated recombination. *Mol Imaging* **2**:297-302.
126. **Sanz, P., L. D. Teel, F. Alem, H. M. Carvalho, S. C. Darnell, and A. D. O'Brien.** 2008. Detection of *Bacillus anthracis* spore germination in vivo by bioluminescence imaging. *Infect Immun* **76**:1036-1047.
127. **Schneerson, R., J. Kubler-Kielb, T. Y. Liu, Z. D. Dai, S. H. Leppla, A. Yergey, P. Backlund, J. Shiloach, F. Majadly, and J. B. Robbins.** 2003. Poly(γ -D-glutamic acid) protein conjugates induce IgG antibodies in mice to the capsule of *Bacillus anthracis*: a potential addition to the anthrax vaccine. *Proc Natl Acad Sci U S A* **100**:8945-8950.
128. **Sirard, J. C., M. Mock, and A. Fouet.** 1994. The three *Bacillus anthracis* toxin genes are coordinately regulated by bicarbonate and temperature. *J Bacteriol* **176**:5188-5192.
129. **Spencer, R. C.** 2003. *Bacillus anthracis*. *J Clin Pathol* **56**:182-187.
130. **Stevens, D. L., M. J. Aldape, and A. E. Bryant.** 2012. Life-threatening clostridial infections. *Anaerobe* **18**:254-259.
131. **Strieter, R. M., S. H. Phan, H. J. Showell, D. G. Remick, J. P. Lynch, M. Genord, C. Raiford, M. Eskandari, R. M. Marks, and S. L. Kunkel.** 1989. Monokine-induced neutrophil chemotactic factor gene expression in human fibroblasts. *J Biol Chem* **264**:10621-10626.
132. **Summers, C., S. M. Rankin, A. M. Condliffe, N. Singh, A. M. Peters, and E. R. Chilvers.** 2010. Neutrophil kinetics in health and disease. *Trends Immunol* **31**:318-324.
133. **Swartz, M. N.** 2001. Recognition and management of anthrax--an update. *N Engl J Med* **345**:1621-1626.

134. **Szarowicz, S. E., R. L. During, W. Li, C. P. Quinn, W. J. Tang, and F. S. Southwick.** 2009. Bacillus anthracis edema toxin impairs neutrophil actin-based motility. *Infect Immun* **77**:2455-2464.
135. **Tacke, F., and G. J. Randolph.** 2006. Migratory fate and differentiation of blood monocyte subsets. *Immunobiology* **211**:609-618.
136. **Tessier, J., C. Green, D. Padgett, W. Zhao, L. Schwartz, M. Hughes, and E. Hewlett.** 2007. Contributions of histamine, prostanoids, and neurokinins to edema elicited by edema toxin from Bacillus anthracis. *Infect Immun* **75**:1895-1903.
137. **Tkalcevic, J., M. Novelli, M. Phylactides, J. P. Iredale, A. W. Segal, and J. Roes.** 2000. Impaired immunity and enhanced resistance to endotoxin in the absence of neutrophil elastase and cathepsin G. *Immunity* **12**:201-210.
138. **Tournier, J. N., A. Quesnel-Hellmann, A. Cleret, and D. R. Vidal.** 2007. Contribution of toxins to the pathogenesis of inhalational anthrax. *Cell Microbiol* **9**:555-565.
139. **Tournier, J. N., A. Quesnel-Hellmann, J. Mathieu, C. Montecucco, W. J. Tang, M. Mock, D. R. Vidal, and P. L. Goossens.** 2005. Anthrax edema toxin cooperates with lethal toxin to impair cytokine secretion during infection of dendritic cells. *J Immunol* **174**:4934-4941.
140. **Tu, W. Y., S. Pohl, K. Gizynski, and C. R. Harwood.** 2012. The iron-binding protein Dps2 confers peroxide stress resistance on Bacillus anthracis. *J Bacteriol* **194**:925-931.
141. **Turnbull, P. C.** 1999. Definitive identification of Bacillus anthracis--a review. *J Appl Microbiol* **87**:237-240.
142. **Van den Broeck, W., A. Derore, and P. Simoens.** 2006. Anatomy and nomenclature of murine lymph nodes: Descriptive study and nomenclatory standardization in BALB/cAnNCrI mice. *J Immunol Methods* **312**:12-19.
143. **van Sorge, N. M., C. M. Ebrahimi, S. M. McGillivray, D. Quach, M. Sabet, D. G. Guiney, and K. S. Doran.** 2008. Anthrax toxins inhibit neutrophil signaling pathways in brain endothelium and contribute to the pathogenesis of meningitis. *PLoS ONE* **3**:e2964.
144. **Wade, B. H., G. G. Wright, E. L. Hewlett, S. H. Leppla, and G. L. Mandell.** 1985. Anthrax toxin components stimulate chemotaxis of human polymorphonuclear neutrophils. *Proc Soc Exp Biol Med* **179**:159-162.
145. **Walsh, J. J., N. Pesik, C. P. Quinn, V. Urdaneta, C. A. Dykewicz, A. E. Boyer, J. Guarner, P. Wilkins, K. J. Norville, J. R. Barr, S. R. Zaki, J. B. Patel, S. P. Reagan, J. L. Pirkle, T. A. Treadwell, N. R. Messonnier, L. D. Rotz, R. F. Meyer, and D. S. Stephens.** 2007. A case of naturally acquired inhalation anthrax: clinical care and analyses of anti-protective antigen immunoglobulin G and lethal factor. *Clin Infect Dis* **44**:968-971.
146. **Warfel, J. M., A. D. Steele, and F. D'Agnillo.** 2005. Anthrax lethal toxin induces endothelial barrier dysfunction. *Am J Pathol* **166**:1871-1881.
147. **Watson, F., J. Robinson, and S. W. Edwards.** 1991. Protein kinase C-dependent and -independent activation of the NADPH oxidase of human neutrophils. *J Biol Chem* **266**:7432-7439.

148. **Watts, C. J., B. L. Hahn, and P. G. Sohnle.** 2009. Resistance of athymic nude mice to experimental cutaneous *Bacillus anthracis* infection. *J Infect Dis* **199**:673-679.
149. **Weiner, Z. P., A. E. Boyer, M. Gallegos-Candela, A. N. Cardani, J. R. Barr, and I. J. Glomski.** 2012. Debridement increases survival in a mouse model of subcutaneous anthrax. *PLoS One* **7**:e30201.
150. **Weiner, Z. P., and I. J. Glomski.** 2012. Updating perspectives on the initiation of *Bacillus anthracis* growth and dissemination through its host. *Infect Immun* **80**:1626-1633.
151. **Welkos, S. L., R. W. Trotter, D. M. Becker, and G. O. Nelson.** 1989. Resistance to the Sterne strain of *B. anthracis*: phagocytic cell responses of resistant and susceptible mice. *Microb Pathog* **7**:15-35.
152. **Welkos, S. L., N. J. Vietri, and P. H. Gibbs.** 1993. Non-toxigenic derivatives of the Ames strain of *Bacillus anthracis* are fully virulent for mice: role of plasmid pX02 and chromosome in strain-dependent virulence. *Microb Pathog* **14**:381-388.
153. **WHO.** 2008. Anthrax in Humans and Animals. World Health Organization.
154. **Wright, G. G., and G. L. Mandell.** 1986. Anthrax toxin blocks priming of neutrophils by lipopolysaccharide and by muramyl dipeptide. *J Exp Med* **164**:1700-1709.
155. **Wu, W., H. Mehta, K. Chakrabarty, J. L. Booth, E. S. Duggan, K. B. Patel, J. D. Ballard, K. M. Coggeshall, and J. P. Metcalf.** 2009. Resistance of human alveolar macrophages to *Bacillus anthracis* lethal toxin. *J Immunol* **183**:5799-5806.
156. **Xu, L., H. Fang, and D. M. Frucht.** 2008. Anthrax lethal toxin increases superoxide production in murine neutrophils via differential effects on MAPK signaling pathways. *J Immunol* **180**:4139-4147.
157. **Yang, J., S. S. Woo, Y. H. Ryu, C. H. Yun, M. H. Cho, G. E. Rhie, B. S. Kim, H. B. Oh, and S. H. Han.** 2009. *Bacillus anthracis* lethal toxin attenuates lipoteichoic acid-induced maturation and activation of dendritic cells through a unique mechanism. *Mol Immunol* **46**:3261-3268.
158. **Young, G. A., Jr., M. R. Zelle, and R. E. Lincoln.** 1946. Respiratory pathogenicity of *Bacillus anthracis* spores; methods of study and observations on pathogenesis. *J Infect Dis* **79**:233-246.